LBL-21232
UC-94c

Lawrence Berkeley Laboratory
UNIVERSITY OF CALIFORNIA

APPLIED SCIENCE DIVISION

RESEARCH ON MATERIALS RELATED
TO THE SODIUM HEAT ENGINE: FINAL REPORT

T.K. Hunt

March 1986

APPLIED SCIENCE DIVISION

Prepared for the U.S. Department of Energy under Contract DE-AC03-76SF00098

DISCLAIMER

LBL-21232

RESEARCH ON MATERIALS RELATED TO THE SODIUM HEAT ENGINE

Final Report

March 1986

by

Thomas K. Hunt

Ford Motor Company
P.O. Box 2053
Dearborn, Michigan 48121

for

Technology Base Research Project
Lawrence Berkeley Laboratory
University of California
Berkeley, California 94720

This work was supported by the Assistant Secretary for Conservation and Renewable Energy, Office of Energy Storage and Distribution of the U.S. Department of Energy under Contract No. DE-AC03-76SF00098, Subcontract No. 4521610 with the Lawrence Berkeley Laboratory.

TABLE OF CONTENTS

A. INTRODUCTION

This report covers all work performed by the Ford Motor Company under Subcontract 4521610 titled 'Research on Materials Relating to the Sodium Heat Engine' and the first and second amendments thereto between the Ford Motor Company and the Regents of the University of California.

The research was undertaken to achieve an understanding of the problem of electrode stability as related to the performance of Sodium Heat Engine systems and the detailed manner in which the high power electrode-electrolyte system functions.

This final report contains discussions of all aspects of the contract work performed in pursuit of these goals.

B. SUMMARY

The Sodium Heat Engine (SHE) is a direct thermal to electrical energy conversion device using sodium beta''-alumina solid electrolyte (BASE) as an ion selective membrane and operating on the basic principle of a thermally regenerative concentration cell. SHE cells have demonstrated high output power densities and should be capable of high efficiency even in units of relatively small output power.

The work performed under this subcontract was directed toward gaining an understanding of the problem of electrode stability as related to the Sodium Heat Engine and of the detailed manner in which this high power electrode-electrolyte system functions. Substantial progress toward this objective was made and is reported under specialized headings in following sections of this report.

As a gauge of progress toward the overall project goals, a set of Technical Milestones was adopted at the outset. They were as follows:

1. Identification of promising electrode preparations and their ranking with respect to performance and durability using demountable test cell (DTC) tests for screening.

2. A finding on the possible decomposition of BASE by sodium by searching for products related to a chemical reaction of BASE with sodium at the negative electrode.

3. The testing for stability of sputtered alloy films containing active metal oxides to stabilize the film grain boundaries.

4. The testing of performance and stability of flame-sprayed electrodes of beta''-alumina and refractory metals.

The first, second and fourth of these milestones were passed and the third was altered somewhat as the result of the achievement of a markedly improved understanding of the electrode-electrolyte process in the high power molybdenum SHE electrodes. A variety of electrode materials was tested for performance and durability on the scale of hundreds of hours using DTC equipment. Sputtered titanium nitride electrodes appear to have the potential for long life at temperatures of 800 to 900°C at performance levels of approximately 0.4 W/cm^2. Liquid metal electrodes of tin and tin-zirconium alloys were tested at several temperatures and show excellent performance potential as well as endurance which appears to be limited only by loss of electrode material due to evaporation. In certain circumstances where SHE operation at temperatures in the 650 - 700°C range may be desirable for other reasons, these liquid metal electrodes may provide important options.

Previous studies of the stability of BASE materials were extended to include investigations of the surfaces of the ceramic material in contact with both the sodium negative electrode and the positive permeable electrode materials. No evidence of BASE decomposition or degradation was found which would suggest any limitation for the durability of this material in SHE applications.

It was discovered that beta''-alumina powders can be flame-sprayed onto the surface of conventionally formed BASE tubes as a porous layer while retaining the proper beta'' crystal structure. It has also proved possible to impregnate such flame-sprayed porous layers with molybdenum metal deposited from solution and by this means to produce a mixed conductor electrode material which can provide both electronic conduction and a distributed, ionically conducting surface. Additional experiments have shown that co-deposition of the beta''-alumina and molybdenum metal powders using the flame-spray apparatus can provide a mixed conductor coating in a single step. The performance and high power endurance of electrodes formed in this way appears to depend strongly on the details of their deposition but has not yet reached the levels established for BASE/molybdenum cermet electrodes produced by more conventional ceramics methods.

C. ELECTRODE PERMEABILITY STUDIES

High permeability of the positive SHE electrode to neutral sodium atoms is required in order to avoid a serious reduction of output voltage and consequent loss of power density in SHE cells. Investigations of the sodium permeation process have been conducted using the current-interrupt method.[1,2] In these experiments, a steady state current is drawn from a SHE electrode for a time and then abruptly interrupted. The voltage across the cell is then monitored as a function of time using a fast recording oscilloscope. The response generally consists of two distinguishable parts. The first or fast response is an increase in the voltage measured across the cell which corresponds quite accurately to the voltage drop across the electrolyte and electrode. This voltage corresponds to the test current times the electrolyte resistance. The second or slow portion of the response to current interruption is a gradual increase in voltage consistent with a reduction in the concentration of sodium at the electrode electrolyte interface as the sodium diffuses through the electrode and evaporates from its outer surface. When the performance of SHE electrodes degrades over time at high temperatures, the major change in the response of the electrodes to the interruption of a test current is observed to occur in the slow or concentration dependent portion of the voltage drop induced during current flow. This is the response one would expect following a reduction of sodium permeability in the electrode and a consequent decrease in the rate of transport of sodium away from the electrode-electrolyte interface.

Experiments performed during this contract period have indicated that the excellent initial performance of molybdenum electrodes in SHE cells can be largely accounted for by the presence of sodium molybdate or other sodium-molybdenum-oxygen compounds at the electrode-electrolyte interface, and in the body of the electrode film at grain boundaries or on the interior surfaces of pores. Degradation is now seen as a result of the loss of these compounds due to decomposition or evaporation at high operating temperatures and the consequent reduction of the sodium transport conductance to a level corresponding to physical diffusion through pores in the film. It was therefore deemed to be useful to investigate the physical porosity of typical sputtered molybdenum films in order to better assess the possibilities for improving the final state electrode permeability. Experiments were designed to investigate the permeability of electrode films using a conceptually simple gas permeation method.

The initial intention was to use porous pre-vycor as a substrate for the deposition of electrode-like films, with the expectation that the films would form a continuous layer bridging the pores (approximately 100 A in diameter). The porour vycor substrate would then provide a low 'impedance' to gas flow in series with the film under test. Unfortunately, the practical handling of the vycor samples proved to be more difficult than expected and its use was deferred. The use of thin polymer films as substrates offers simpler handling and susequent tests were therefore made using a fixture that was constructed to allow clamping a thin polymer membrane between two test chambers. The test gas could then be introduced on one side of the membrane at a known pressure and the rate of diffusion across the membrane measured by examination of the other side using either a mass spectrometer/residual gas analyzer or for time averaging of the response, a simple mechanical pressure gauge. Mylar membranes having thicknesses from 0.001 to 0.009 inches were used as substrates. Because the electrode films are thin (1-4 micrometers), only the thinner polymer

membranes can have their background conductance large enough that the reduction expected from a sputter deposited thin film on the polymer membrane would be readily measurable. Further difficulties arose at this stage and vacuum sealing of the polymer film edges proved to be very difficult at the low leak rates required for these tests. For the 0.001-inch mylar films, consistent basal leak rates were finally obtained, but adequate sealing of their edges was extremely difficult to verify. Sealing of such thin films using O-ring joints did not appear to be effective and with the particular choices of polymer film materials available at the time, adhesives also were difficult to use.

Because of the difficulties encountered with sealing these polymer films to the chamber and in obtaining good verification, this investigation was set aside until the need for the answers it might provide becomes more urgent.

References

1. T.K. Hunt, N. Weber and T. Cole, Solid State Ionics, 5 263 (1981)

2. A.K. Detwiler III, Doctoral thesis - University of Houston, (1983).

D. ELECTRODE COMPOSITION STUDIES

A large number of different electrode materials were studied during the contract period. In this section we report the details of the experimental observations on the performance of various electrode compositions and discuss some of the conclusions which can be suitably drawn from these results.

SHE electrodes are required not only to carry the electrons from the load to the interface with the BASE where they can recombine with the sodium ions, but also to allow free movement of the neutral sodium atoms to the vacuum space so that they may pass directly to the condenser. The earliest experiments on the SHE system employed a variety of electrode materials, including a number of the noble metals and carbon. In early experiments, the latter electrode materials exhibited a number of serious deficiencies. Carbon has the serious chemical complication that it can scavenge oxygen from the beta-alumina thereby releasing sodium and converting the beta-alumina to an insulating form unsuitable for the SHE system. The noble metals all tend to form solutions or compounds with sodium, and in addition tend, with the exception of platinum, to have vapor pressures sufficiently high at SHE operating temperatures to result in loss of the electrode material due to evaporation in times too short for most practical SHE uses. A number of the refractory metals such as molybdenum, tungsten and niobium have been tested with more interesting results.

A series of early electrode studies focussed on molybdenum films. Initially, samples were deposited by chemical vapor deposition (CVD) from the molybdenum hexacarbonyl, $Mo(CO)_6$[1]. Subsequently, sputtering was introduced for the deposition of metal film electrodes. Sputtering offers a much wider range of compositional options than CVD and it has become the application method of choice for metal electrode materials. Details of our studies of the molybdenum electrode, its performance, durability and operating mechanisms are given in the following section.

PROPERTIES OF MOLYBDENUM ELECTRODES

There have been many tests of molybdenum film electrodes on beta''-alumina in vacuo at elevated temperatures.[2,3,4] This electrode-electrolyte combination has been studied for application in the SHE experimental thermoelectric converter. Candidate electrodes for the SHE are required to have minimum levels of sheet conductivity and permeability to neutral sodium. Molybdenum SHE electrodes have been prepared by chemical vapor deposition, sputtering and flame spraying. The beta''-alumina electrolyte is typically a thin walled tube. Tests are made with patch electrodes one square centimeter in area deposited on the outer surface of an electrolyte tube suspended in an evacuated chamber. To obviate the need for seals compatible with hot sodium, the lower two thirds of the tube constitutes a hot sodium reservoir and sodium is not generally recirculated. To conserve sodium, electrode current is drawn intermittently and between tests the cell stands at open circuit. Evacuation of the chamber surrounding the tube is accomplished with a trapped mechanical pump and sorption and 'VacIon' pumps. Occasionally the residual gas in the vacuum space is monitored using a mass spectrometer. The total pressure is usually greater than 10^{-7} torr, and prior to the passage of current and accumulation of sodium, is composed mostly of water vapor. We and others have observed that beta''-alumina tends to absorb water from ambient air and evolve it upon heating in vacuum.

Electrodes are usually tested at temperature intervals of 100°C between 500 and 900°C. Most of the extended time tests are performed at 800 and 900°C. With some exceptions the power output of molybdenum film electrodes degrades with time above 800°C as shown in Figures D1 and D2. An initial power of 0.6 to 1.0 watts/cm^2, for example, decays to 0.1 to 0.3 W/cm^2 in a few hours at 900°C and in a few tens of hours at 800°C. The initial specific power can, remarkably, often approach the theoretical limit imposed by the bulk resistance of the electrolyte. Electrodes whose behavior did not follow this pattern always gave comparatively low initial power. These included a Mo electrode prepared in situ on the electrolyte tube by electrochemical reduction of $MoCl_5$ by sodium, and a carbonyl CVD electrode back-biased 3.0 volts and heated in hydrogen before evacuating at high temperature.

Except for optical microscope observation, electrodes were not routinely scrutinized by modern surface techniques because of the problems presented by the sheer bulk of the electrolyte tube and associated plumbing. By ordinary XRD, only molybdenum metal is observed. From a qualitative test, we find that the degraded CVD electrodes adhere less well than fresh electrodes. A brownish stain is frequently observed under and at the periphery of electrodes after testing. In a procedure discovered by accident and confirmed repeatedly, a high-temperature controlled oxidation revives degraded electrodes dramatically. The restoration is, however, not permanent.

Many electrodes show a 'training' behavior particularly after oxygen treatment, characterized by an output from the electrode that changes with time (usually upward) under constant load. When degraded electrodes are removed from the electrolyte tube by grit blasting and replaced with fresh electrodes, cell performance returns to its high initial level. This result, obtained many times, proves that the locus of the impedance increase is not in the bulk of the electrolyte or at the liquid sodium/electrolyte interface.

Current-interrupt experiments have been performed on electrodes before and after the step-wise impedance increase.[5] These studies have been interpreted as revealing that the impedance increase stems almost completely from a decrease in the permeability of the electrode to neutral sodium and not from an increase in charge transfer 'resistance'. This conclusion depends on the reliability of a particular model for the equivalent electrical circuit of a real cell. In apparent contradiction to this conclusion are some results from experiments with a single loop of wire 'electrode' around an electrolyte tube. These wire electrodes also show an increase of impedance with time above 800°C but at a slower rate than the film electrodes. It is quite possible that the processes responsible for the impedance increases in film and wires or cat's whisker electrodes are completely different from those in thin films. It is well-established that treatment with oxygen has a profound effect on the performance of molybdenum electrodes, and it has been suspected that oxygen plays a role in electrode behavior even when it is not deliberately introduced. It has been proposed, for example, that the surprisingly good permeability of fresh film electrodes is the result of a small but significant area fraction of sodium molybdenum bronze at grain boundaries in the metal. Clues to electrode behavior are possibly found in the literature of the sodium-oxygen-molybenum ternary system. Of special interest is the possible occurence in the

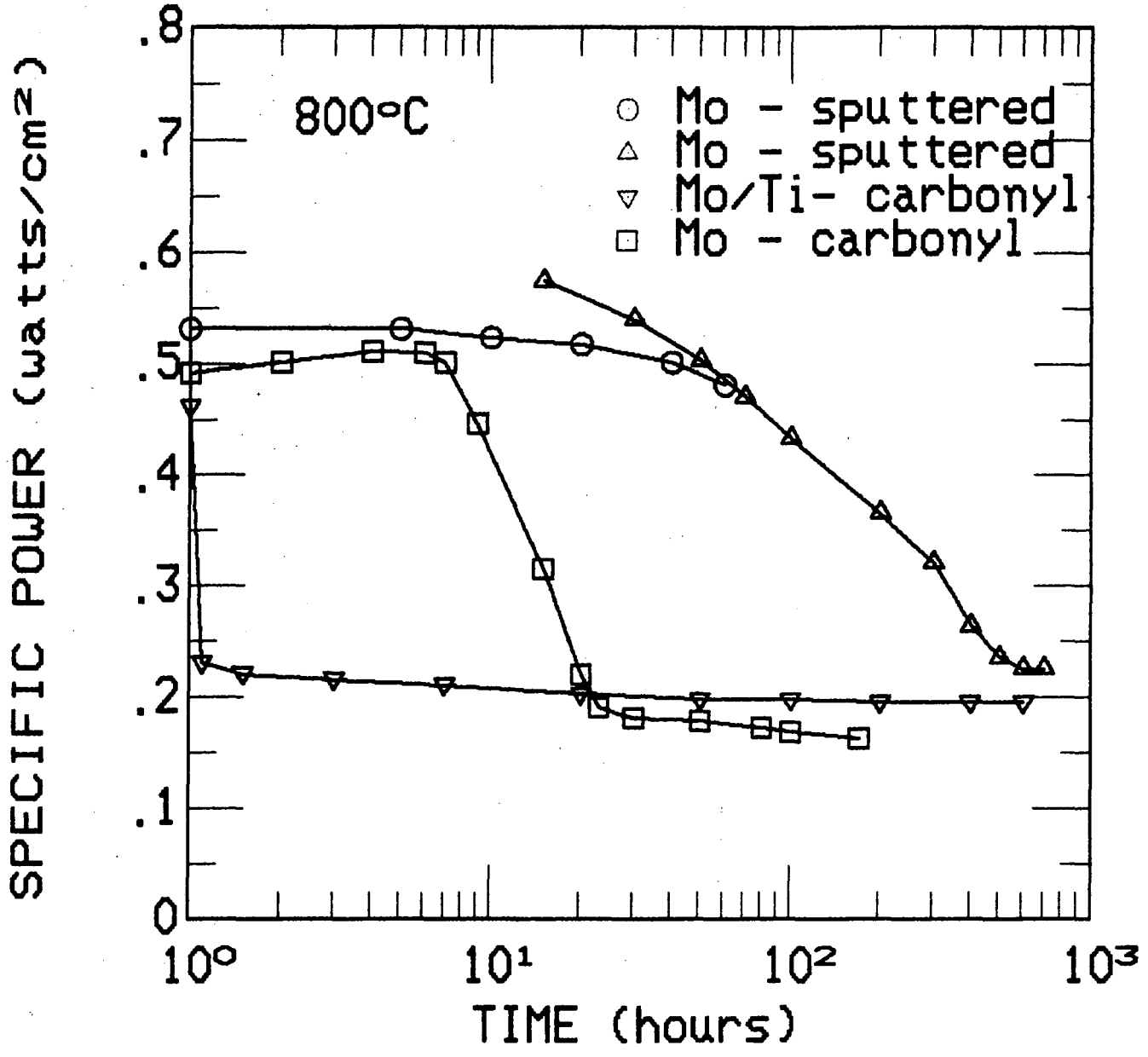

D1. Molybdenum Electrode Power vs. Time at 800°C

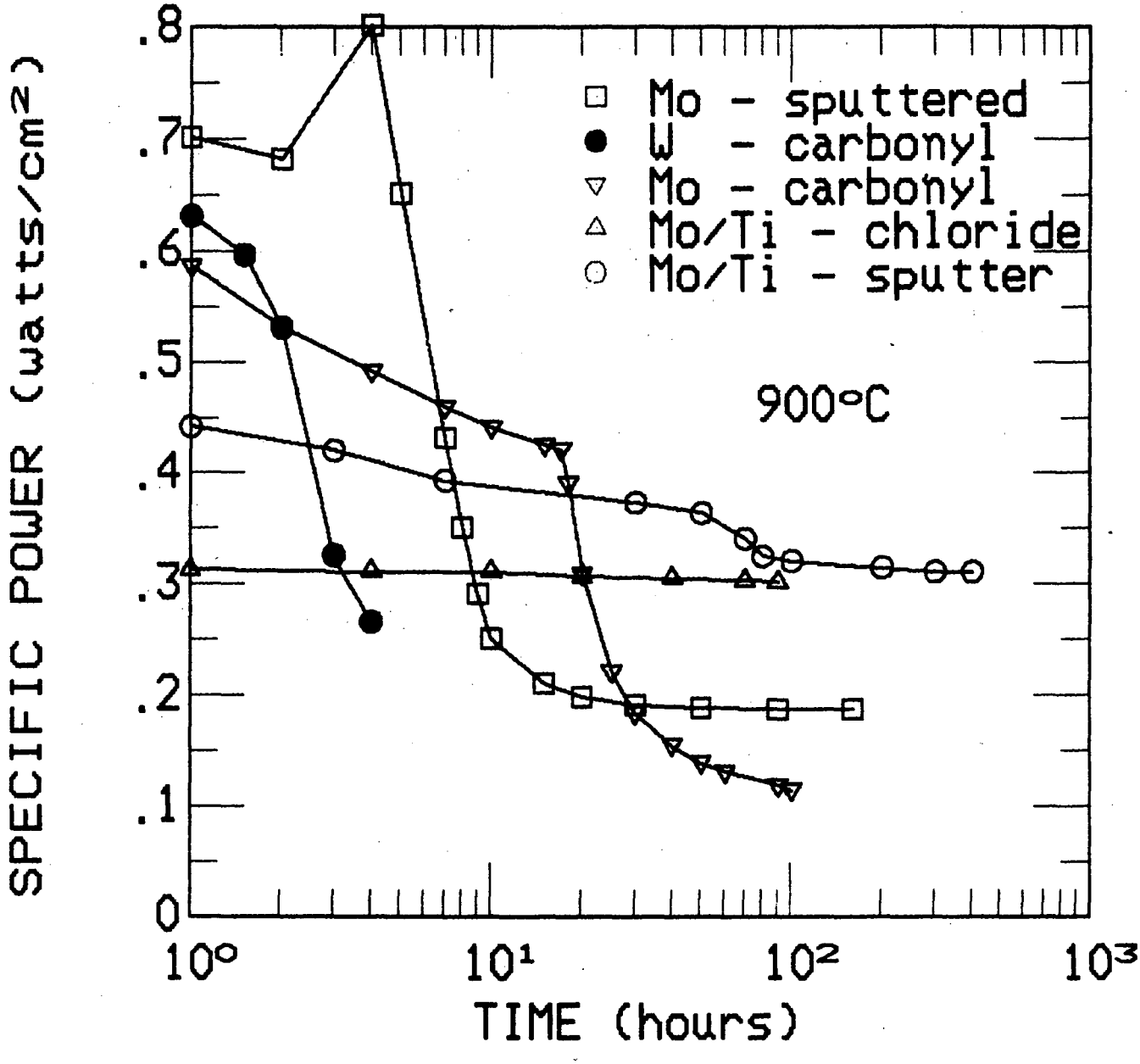

D2. Molybdenum Electrode Power vs. Time at 900°C.

electrodes of phases having unusually high electronic or ionic conductivity such as sodium bronzes and molten salts. Under the headings of reasonably well identified compounds, this literature is briefly reviewed.

$\underline{Na_2MoO_4}$

The properties of sodium molybdate have been extensively listed.[6] Of special significance to the present study are the melting point (686°C) and the vapor pressure at elevated temperatures[7]. The latter property is described by the equation,

$\ln P \text{ (mm Hg)} = -33{,}390/T^{\circ}K + 22.18.$

The evaporation was found to proceed as

$Na_2MoO_4(s,l) \rightarrow Na_2MoO_4\ (g)$

Also relevant is a study[8] of the frictional behavior of molybdenum surfaces in a molten sodium environment. In this work, a MoO_3 film was found by electron diffraction on a fresh molybdenum surface. This film was converted to MoO_2 by heating in vacuum and the MoO_2 was in turn converted to Na_2MoO_4 when exposed to sodium vapor (temperature not specified but below 600°C). It was stated that Na_2MoO_4 formed whenever sodium was present and regardless of the surface condition of the molybdenum.

$\underline{Na_xMoO_3}$

Isotypic with known cubic tungsten bronze with x in the range 0.90 -0.97. This compound was prepared[9] from reaction of Na_2MoO_4, MoO_3 and Mo <u>at high pressure only</u> (65 kilobars) at temperatures between 500 and 1000°C. This compound has an electrical resistivity typical of metallic conduction (10^{-4} ohm-cm at 400°C).

$\underline{Na_xMo_6O_{17}}$

First reported[10] sodium molybdenum bronze - crystals grown by electrolytic reduction of Na_2MoO_4-MoO_3 melts. Not formed above 550°C. At higher temperature MoO_2 is formed by this method - Resistivity 2.6 x 10^{-1} ohm-cm at 60°C - has a distorted perovskite structure[11] - later prepared by the reaction,

$(1-y)Na_2MoO_4 + (8+2y)MoO_3 + (3-y)MoO_2 \rightarrow 2Na_{(1-y)}Mo_6O_{17}$

above 580°C, $Na_{1.6}Mo_6O_{17}$ decomposes under an inert atmosphere with the formation of Mo_4O_{11}, MoO_2 and <u>molten molybdate</u>.

$\underline{NaMoO_2}$

Formed by reaction of sodium vapor at 10^{-2} torr on MoO_2 at 400°C [12], this compound is isostructural with rhombohedral alpha $NaFeO_2$. Under vacuum at 550°C, it decomposes according to the equation,

$3\ NaMoO_2 \rightarrow Na_2Mo_3O_6 + Na$

A sample made from pressed powder of $NaMoO_2$ was found to be a semiconductor with a small activation energy.

$\underline{Na_2Mo_3O_6}$ or $\underline{Na_{.66}MoO_2}$

This compound is a sodium molybdite formed[13] by the reaction of Na_2O or Na_2CO_3 on MoO_2 at 800°C under secondary vacuum - also prepared by the reduction of Na_2O-$3MoO_3$ in hydrogen.

$$2Na_2O + 4\ MoO_2 \xrightarrow{800^\circ C} Na_2Mo_3O_6 + Na_2MoO_4$$

$$Na_2O\text{-}3MoO_3 \xrightarrow[750^\circ C]{H_2} Na_2Mo_3O_6 + MoO_2 + Na_2MoO_4 + H_2O$$

Also reported[6] as the product in the reaction,

$$Na_2MoO_4 + MoO_2 + Mo \xrightarrow{800^\circ C} 3\ Na_{.66}MoO_2.$$

At 800°C, the reaction,

$$Na_2O + 3/2\ MoO_3 + 1/2\ MoO_2 + Mo \xrightarrow{800^\circ C} Na_2Mo_3O_{6.5}$$

is described[13] as one from which it is difficult to obtain the molybdite because 'the reduction by molybdenum is very slow and the molybdate has time to sublime' in secondary vaccum at 800°C. At temperatures between 950 and 1000°C in high vacuum, $Na_2Mo_3O_6$ decomposed[13] into Na_2MoO_4 and MoO_2,

$$Na_2Mo_3O_{6.5} \xrightarrow{950\text{-}1000^\circ C} .25\ Na_2MoO_4 \uparrow + 2.75\ MoO_2 + 1.5\ Na \uparrow.$$

$\underline{Na_3MoO_4}$

The compound Na_3MoO_4 is a brown-black salt formed[12] by vapor of sodium at 10^{-2} torr on Na_2MoO_4 at 400°C. The powder x-ray pattern is complex and the compound was not isostructural with any compound Na_3XO_4. Na_3MoO_4 decomposes at 550°C under vacuum by the reversed preparation reaction,

$$Na_3MoO_4 \longrightarrow Na_2MoO_4 + Na.$$

Na_3MoO_4 is a poor conductor $\rho = 10^8$ ohm-cm at 20°C.

$NaMoO_3$ and Na_2MoO_3

These compounds were observed in a high-temperature mass spectrographic investigation of gaseous molybdates[14]. The free energy functions, heat content functions and heats of formation were calculated from mass-spectrographic data and estimated molecular parameters. Similar values for gaseous Na_2MoO_4 also were reported.

Available Phase Equilibria and Thermochemical Data

Phase diagrams in the system Na_2O - MoO_3 are available[15] as well as one isotherm in the system MoO_3-MoO_2- Na_2MoO_4.[16]

Some preliminary work has been done in the system Na_2O-Al_2O_3-MoO_3 in this laboratory. Reau, Fuassier and Hagenmuller have noted[16] that the failures in early attempts to prepare molybdenum bronzes must be attributed to the very small range between temperatures of preparation and decomposition, and that the molybdenum compounds are very much less stable than their tungsten homologues. Confirmation of this statement is to be found in a list of enthalpies of formation and reaction for some oxide bronzes including $NaMo_6O_{17}$ at 298°C.[17]

Values for ΔH_f^o, ΔG_f^o, C_p and S are available for Na_2MoO_4 (c) at 298°K. These data together with the entropies and heat content functions for the appropriate elements permit a calculation of $\Delta G_f^o(T)$ for Na_2MoO_4(C) up to 1000°C (past T_m) as given in Table D1. Values of $\Delta G_f^o(t)$ for $NaMoO_3$(g) and Na_2MoO_3(g) are given in Table D2 based on data from reference 14. For the estimation of possible reactions involving the solid electrolyte, values for $a(Na_2O)$ over the alpha-alumina - beta-alumina two phase mixture are available[18,19]. Directly measured values of $a(Na_2O)$ over beta-alumina-sodium aluminate are not yet available. The latter can be calculated, however, from the relation

$$\ln a(Na_2O \text{ beta-}NaAlO_2) = \ln a(Na_2O \text{ beta-alpha-}Al_2O_3) + 2\,fV/RT \quad (1)$$

where V is the voltage of the cell

air Pt|$\alpha + \beta$-Al_2O_3 + liq|beta-Al_2O_3|+beta Al_2O_3+$NaAlO_2$ Pt air.

No data for beta''-alumina are available, but the differences in thermochemical properties between this phase and beta-alumina are expected to be small. Values of sodium oxide activity over the beta-alumina/alpha-alumina equilibrium are given in Table D3 together with measured values of V in equation 1.

Discussion

A study of the interaction of sodium and beta/beta''-alumina electrolyte has been reported previously[20]. There is evidence for a small absorption of sodium by the electrolyte, but no signs of a gross reduction reaction or of significant changes in mechanical integrity or ionic conductivity. In spite of

TABLE D1

T (°K)	ΔG_f Na_2MoO_4	
298	-323.69 (kcal/mole)	
400	-314.4	
500	-305.3	
600	-296.1	
700	-286.9	T_m = 959°K
800	-277.7	
900	-268.4	
1000	-259.2	
1100	-249.9	
1200	-240.6	

TABLE D2

ΔG_f^o (kcal/mole)

	Na_2MoO_3 (g)		$NaMoO_3$ (g)		Na_2MoO_4 (g)	
T (°K)	C_{2v}		C_{2v}	C_s	D_{2h}	C_{2v}
1000	-146.4		-107.2	-110.7	-206.4	-212.5
1200	-139.0		-102.1	-106.5	-194.7	-202.1
1400	-124.6		-93.6	-98.8	-176.0	-184.8
1600	-110.3		-85.0	-91.0	-157.4	-167.5
1800	-95.9		-76.4	-83.2	-138.9	-150.2

C_{2v}, C_s, D_{2n} molecular structure designations - see Ref. 14.

TABLE D3

Sodium oxide activity over beta-alumina/alpha-alumina equilibrium

From Ref. 18,

$$\ln a(Na_2O,\alpha-\beta) = -37,800/T + 8.29 \pm 4.6 \quad .$$

From Ref. 19,

$$\ln a(Na_2O,\alpha-\beta) = -26,460/T - .07 \pm 0.7$$

$$\ln a(Na_2O, \beta\text{-}NaAlO_2) = \ln a(Na_2O,\alpha-\beta) + 2fV/RT$$

$$V(\text{millivolts}) = 0.2427\ T\ (^oK) - 95.8 \quad .$$

TABLE D4

Calculation of $a(Na_2O)$ beta-alumina/gamma-alumina

$$\ln a(Na_2O,\beta-\gamma) + X/RT(\Delta G_f^o(\alpha) - \Delta G_f^o(\gamma)$$

where X is the stoichiometric number in the formula for beta-alumina Na_2O-X Al_2O_3. From phase equilibria, X is taken as 8.

T ^oK	$8/RT\ (\Delta G_{f\alpha} - \Delta G_{f\gamma})$
800	-19.043
900	-16.207
1000	-13.882
1100	-11.983
1200	-10.397
1300	- 9.055

past efforts there remains a need for a more complete understanding of the origin of the step increase in impedance in cells with molybdenum electrodes at high temperatures. Current interrupt tests suggest that the dominant effect is a loss of sodium permeability. If true, is this a result of homogeneous changes in the film i.e. from sintering or grain growth or could there be local effects near the electrode-electrolyte interface? The inference of sodium impermeability rests on the tenability of particular models for the equivalent circuit of a cell. For this reason, the possibility that the impedance rise may result from problems with charge exchange should not yet be excluded. A circumstance that will certainly contribute to an impedance increase is when the sodium oxide constituent of the electrolyte at the electrode interface is 'extracted' by vaporization or reaction with electrode material. As discussed previously, a voltage between an electrode metal on beta''-alumina and a liquid sodium reference electrode can be calculated from the equilibrium constant for the following reaction type,

$$1/y\ M + Na_2O\text{-}XAl_2O_3 \longrightarrow 1/y\ MO_y + X\ Al_2O_3 + 2\ Na.$$

Voltages for several metal electrodes are calculated and shown in Fig. D3. These voltages can be calculated by assuming that either gamma-alumina or alpha-alumina is the reaction product. The appropriate equations and data for gamma-alumina as the product are given in Table D4. Gamma-alumina is considered because this structure may more accurately represent the state of dealkalyzed beta-alumina at intermediate temperatures. The data in Fig. D3 are calculated for alpha-alumina as a reaction product.

When the condenser is very cold and when electronic conductivity is small, the open circuit voltage (OCV) of a cell is then controlled by the equilibrium in Eq. 1. In this case a dealkalyzation of the electrolyte will occur at open circuit since there will always be a sodium flux, however small, from electrode to condenser. Applied voltages greater than the OCV will also cause dealkalyzation. At lower voltages and higher sodium activity in the electrode, as realized by loading a cell, dealkalyzation is suppressed. In practice, with the condenser at room temperature, the OCV at high temperature <u>appears</u> to be governed by electronic conductivity. We have no results to suggest that a dealkalyzation occurs at open circuit or even as a result of applying higher voltages for short times. However, more systematic experiments are needed. Indeed, there is one recent observation[21] of a net transport of Na_2O at 1173 ^{o}K betwen two shorted platinum electrodes on a beta-alumina membrane separating two regions with different oxygen partial pressures. The presence of $NaAlO_2$ and Al_2O_3 at the beta''-alumina surface under the electrodes in these experiments was confirmed by X-ray diffraction.

In the past we have assumed that the consequence of dealkalyzation would simply be an increase in ohmic resistance. The step impedance increase in cells is, however, definitely not a simple ohmic contribution. A more realistic model of the dealkalyzed interface could be in accord with this fact. If a layer of soda depleted beta-alumina were sandwiched between a metal layer and a normal beta-alumina layer as in Fig. D4, then one might hypothesize that

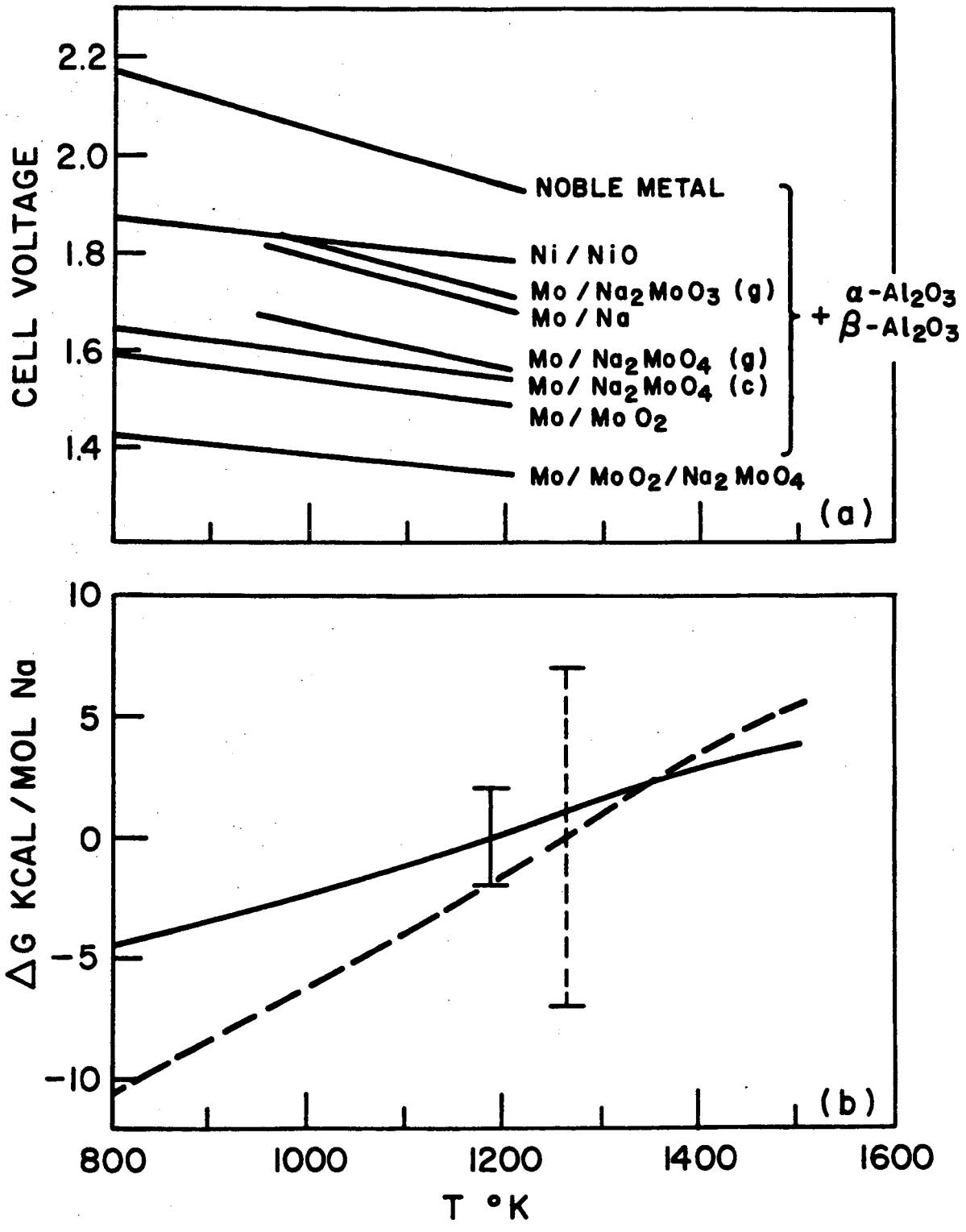

D1. a) Calculated voltage between electrodes on beta-alumina and liquid sodium vs. temperature using alpha-alumina as the reaction product. b) Calculated free energy differences.

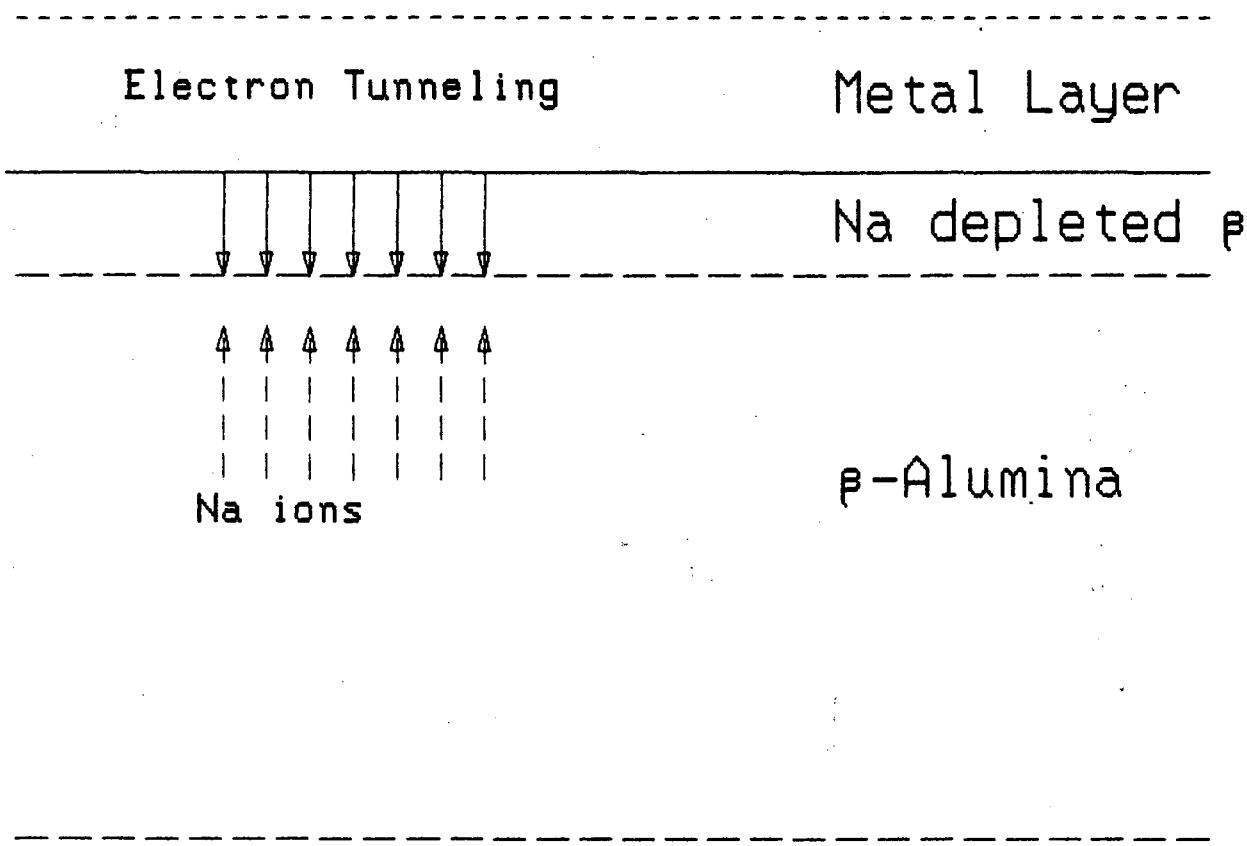

D4. Beta''-Alumina/Soda depleted beta''-alumina/metal

electrons tunnel through the ionic barrier to neutralize ions in the interior of the beta phase. Neutral sodium has difficulty in permeating through the oxide lattice and a substantial activity gradient is set up at relatively small currents. The voltage-steady state current relation expected from this model is most likely to be non-ohmic.

One experiment was designed to test this hypothesis. A degraded electrode was pulled off by a handle glued to it with epoxy. A new electrode was deposited by CVD on the same site and tested. The result was not clear-cut. The second electrode was inferior in performance to the initial performance of the first but better than the last observed state of that electrode.

In several instances, molybdenum electrodes were loaded slightly to lower the OCV and so to circumvent dealkalyzation. The usually small reservoir of sodium necessarily limited the current that could be practically drawn. No mitigation of the electrode degradation was ever realized by these attempts.

Recently liquid tin electrodes and tin-zirconium alloy films have proven to be stable for at least 100 hours. The opportunity exists for using these electrodes to deliberately create a dealkalyzed layer by back-biasing. Any impedance increase so produced, could then be studied without the effect of changes in the permeability of the film.

Another model of electrode behavior is perhaps worthy of test. According to this view, a liquid phase near the composition of Na_2MoO_4 forms at high temperature by reaction of the molybdenum electrode with oxygen and sodium. The presence of a molten salt might explain the good initial electrode behavior and its disappearance could account for the step impedance increase. There is evidence for the oxidation of ultrathin molybdenum films at measurable rates even at room temperature. At 500°C in oxygen at 10^{-3} to 10^{-6} torr, an initially clean metal surface is wholly oxide in 10^{-2} torr-sec[22]. During electrode testing in pumped vesels, oxygen can be trapped in an electrode from the gettering action of sodium on residual water vapor and water evolved from the electrolyte upon heating. Even without drawing current there can be a small sodium flux as a consequence of a small electronic conductivity of the electrolyte. In theory, this 'leakage' can be suppressed to any desired extent by back-biasing with the risk, of course, of decomposing the electrolyte. In short, it is likely that, without special precautions, molybdenum electrodes no matter how prepared will, after being applied to an electrolyte tube and heated in 'vacuum' up to 800°C in a test cell, become contaminated by sodium and oxygen. After consulting the available literature, one might expect to find in an electrode at 800°C in addition to Mo, molybdenum dioxide (MoO_2), possibly $Na_{0.66}Mo_2$, and a liquid phase with a composition near Na_2MoO_4. It is not unreasonable to propose that the actual multicomponent equilibrium is adequately represented by the equilibrium,

$$Na + MoO_2 \leftrightarrows 1/2\ Na_2MoO_4 + 1/2\ Mo$$

The equilibrium sodium pressures and maximum current densities at which these pressures occur are given in Table D5. The OCV of a cell where this equilibrium establishes sodium activity is plotted in Fig. D3. This reaction

TABLE D5

T (^{o}K)	ΔG^{o}(kcal)	Volts	P_{Na}(eq)(torr)	$i_{Na\ max}$(amps)
1000	-35.38	1.381	1.41×10^{-5}	0.52×10^{-3}
1100	-32.79	1.355	2.32×10^{-4}	8.2×10^{-3}
1200	-30.6	1.327	2.02×10^{-3}	68.7×10^{-3}

TABLE D6

Pressure-Flux relation for monatomic sodium according to the kinetic theory-Langmuir Relation. Na flux corresponding to 1 A/cm^2.

$$P = (2\pi MRT)^{1/2} i/F$$

T (^{o}K)	P(torr)
300	1.47×10^{-2}
400	1.70
500	1.90
600	2.08
700	2.25
800	2.41
900	2.55
1000	2.69
1100	2.82
1200	2.95

does not, of course, involve the beta''-alumina electrolyte. Using the Langmuir-kinetic theory relation between pressure and flux, we calculate the current density for formation of Na_2MoO_4 as 0.5 mA at 1000 ^oK rising to 68 mA at 1200 ^oK. This relation for sodium in the temperature range of interest is evaluated in Table D6. In such a reaction as Eq.2 is found a possible explanation for 'training'. As current is drawn and sodium activity rises, a molten salt forms and provides good ionic contact between metal electrode and solid electrolyte.

The possibility of further reaction of sodium or molybdenum with Na_2MoO_4 is tested by calculating ΔG for the reactions,

$$Na(g) + 1/6\ Na_2MoO_4 \longrightarrow 2/3\ Na_2O + 1/6\ Mo \qquad (3)$$

$$Na(g) + 1/2\ Na_2MoO_4 \longrightarrow Na_2O + 1/2\ MoO_2 \qquad (4)$$

$$Mo + 2\ Na_2MoO_4 \longrightarrow 2\ Na_2O + 3\ MoO_2 \qquad (5)$$

The results are tabulated in Table D7. The first reaction proceeds only when the calculated current density is 45 A/cm^2 at temperatures above 800^oK. We might also argue that the loss of Na_2MoO_4 liquid by vaporization of Na_2MoO_4 and Na is the source of the impedance increase at high temperature. From the vapor pressure[7] and density[23] of Na_2MoO_4 we calculate the loss in microns/hour as 0.2 at 800^oC and almost 3 at 900^oC (see Table D8). Both the absolute magnitude and temperature dependence of this rate are consistent with the observed electrode power degradation rates at 800 and 900^oC.

As described earlier, one test strongly pointed to a reaction involving beta''-alumina electrolyte in the vicinity of an electrode. An Mo electrode was loaded and operated in vacuum after being biased at 3 volts positive while being heated to 800^oC in one atmosphere of hydrogen. After the electrode was pulled off after testing, aluminum was found on the surface near the electrolyte, and XRD analysis of this surface revealed a major phase indexed as $MoAl_3$.

From the recent phase equilibrium study in the system Na_2O- Al_2O_3-MoO_3 (see Chapter F), the compositions of liquid in equilibrium with beta-alumina at about 900^oC are close to Na_2MoO_4 but contain several mole percent of Al_2O_3. In attempting to account for the presence of $MoAl_3$ in the singular electrode, a scheme involving the formation of $MoAl_3$ by the reduction of a molten salt is more plausible than any involving a solid oxide.

These views of molybdenum electrode behavior might be tested by carefully analyzing V-I curves up to 680^oC to find evidence of a melting transition. Direct observation of the desorption of Na_2MoO_4 from an electrode might be possible with a mass spectrometer.

TABLE D7

Possible reactions in Mo-Na-O Electrodes

$$Na(g) + 1/6\ Na_2MoO_4 \longrightarrow 2/3\ Na_2O + 1/6\ Mo \qquad (3)$$

$$Na(g) + 1/2\ Na_2MoO_4 \longrightarrow Na_2O + 1/2\ MoO_2 \qquad (4)$$

$$Mo + 2\ Na_2MoO_4 \longrightarrow 2\ Na_2O + 3\ MoO_2 \qquad (5)$$

T (^oK)	ΔG_3 kcal/mol	ΔG_4 kcal/mol	ΔG_5 kcal/mol
800	-10.403	4.633	90.216
900	-7.701	7.517	91.31
1000	-5.039	10.136	91.04
1100	-2.462	12.695	90.94
1200	+0.212	15.613	92.41

TABLE D8

Pressure and flux into vacuum of Na_2MoO_4

$$\ln P\ (torr) = -33390/T + 22.18 \quad \text{(Ref. 7)}$$

T (^oC)	P (torr)	J ($g/cm^2 sec$)	μ/hr
700	5.4×10^{-6}	6.99×10^{-10}	9×10^{-3}
800	1.3×10^{-4}	1.62×10^{-8}	0.21
900	1.9×10^{-3}	2.21×10^{-7}	2.98
1000	1.7×10^{-2}	1.99×10^{-6}	27.4

Density $d(g/cm^3) = 3.407 - (.629 \times 10^{-3})\ T\ (^oK)$ (Ref. 23)

Roger Williams of the Jet Propulsion Laboratory in Pasadena has observed Na_2MoO_4 and weak signals from $Na_2Mo_3O_6$ by x-ray diffraction in an electrode that was originally MoO_2 heated to 800°C in vacuum and loaded to 0.2 volts in a SHE configuration. No Mo metal was found. The MoO_2 was applied to a beta''-alumina tube as a past anode with 'Nicrobraz' cement. As part of the same study, an Mo electrode prepared by sputtering was held at open circuit at 800°C. This electrode also was examined by XRD and found to contain a small amount of Na_2MoO_4. Samples were obtained by scraping off the film electrodes in a glove box. The XRD was performed with a Guinier camera equipped with a copper monochromator.

TITANIUM NITRIDE ELECTRODES

Films of TiN have also been tested as SHE electrodes. This material provides a number of interesting possibilities which put it in a different class from the molybdenum standard electrodes. Titanium is a chemically 'active' metal (a constituent of many of the 'active metal' brazes used to join metal components to BASE) and adheres tenaciously to beta''- alumina. The ability of Ti films to scavenge oxygen leads to partially or fully oxidized films which have sheet resistances too high for practical SHE operation. TiN films, however, exhibit a resistivity of approximately 30 micro-ohm cm, lower than that of pure Ti films by as much as a factor of 2 to 2.5. In addition they are extremely hard, abrasion resistant and relatively inert chemically. Further, if adhesion to the BASE should emerge as an important problem, it should be possible to deposit pure Ti as a bonding layer between the BASE and TiN. A second aspect is that TiN films appear to offer no reasonable options for a molten salt or other liquid layer at the interface with the BASE. As discussed in the previous section on molybdenum electrodes, such layers appear to be the rule in molybdenum, tungsten, and probably niobium electrodes. The excellent initial performance of these electrode materials appears to be due to the presence of such interlayers and performance degradation to their loss by evaporation or decomposition. Thus, studies of TiN electrodes and others of this general type may be able to elucidate the behavior of the clean solid-solid interface in new ways.

The deposition of TiN films by reactive sputtering of Ti in a nitrogen atmosphere is a subject of considerable current interest in part due to their possible applications as wear resistant and decorative coatings. Experience appears to indicate that the color of the deposited films is rather well correlated with their purity.

Testing of the SHE performance of TiN electrodes was carried out by the usual screening approach using small (approx. 1 cm^2) patch electrodes in non-recirculating systems. Current-voltage curves for several such electrodes are shown in Figure D5. The performance of these electrodes does degrade with time at high temperatures but the rate and degree to which this occurs appears to depend importantly on the deposition conditions. The rate at which the maximum power decreases for the TiN system is discussed below, together with the performance characteristics for a selection of individual electrodes. We have examined samples of these films before and after operation at high temperatures using standard SEM equipment (see Figure D9).

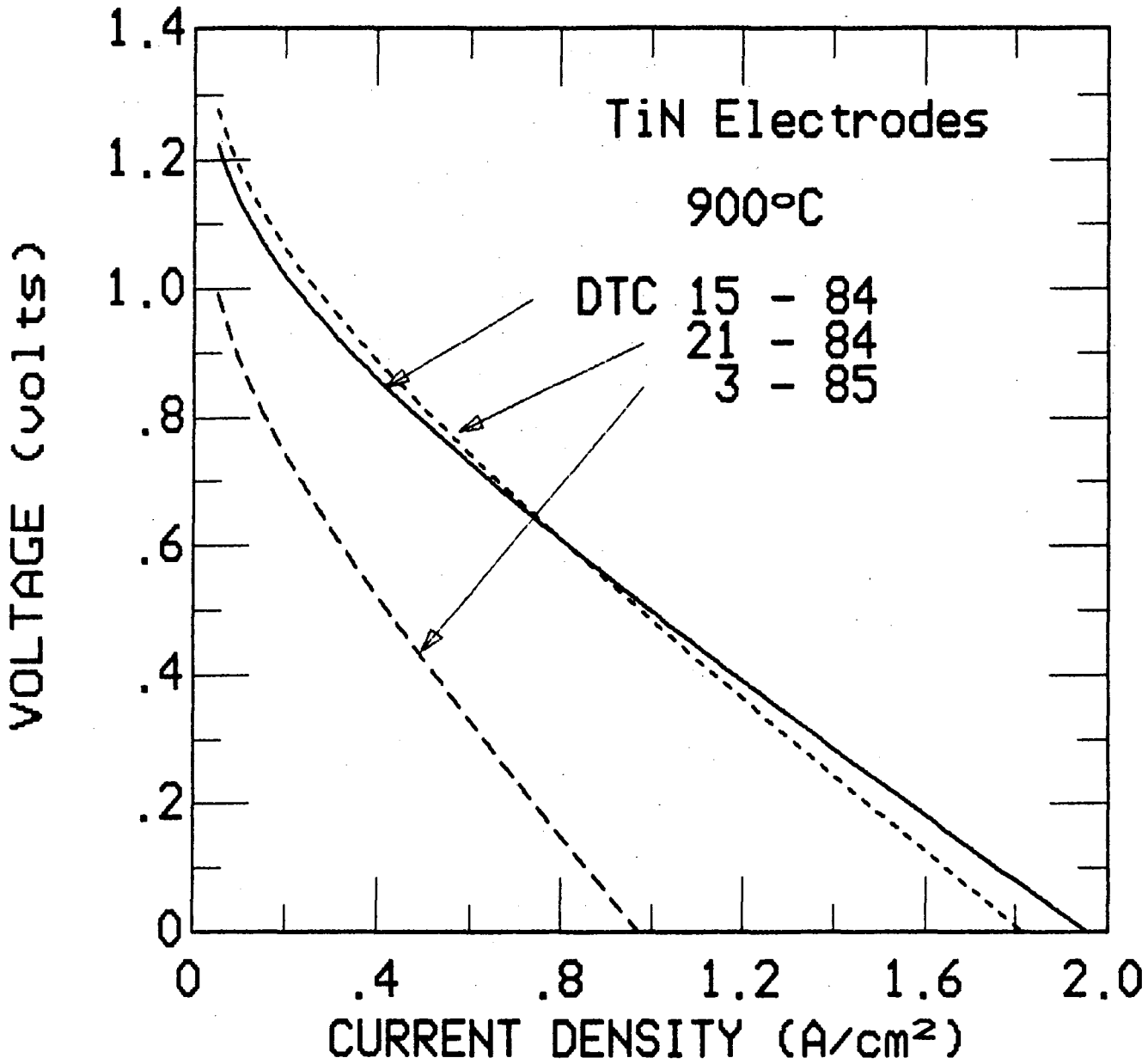

D5. Current-voltage data for several representative titanium nitride sputtered electrodes.

TiN Electrode Preparation:

A sputtering system suitable for the deposittion of TiN electrodes on BASE tubes is being operated in the metallurgy department at Ford, and the deposition of the TiN films studied during this contract effort was carried out by Mr. Duane Schmatz of that department. Tests have been conducted on a series of 13 TiN electrodes in order to investigate the effects of the sputtering parameters such as N_2 pressure and film thickness on SHE performance. Table D9 shows the electrode parameters and the major results for all electrodes in the series. While the details of the BASE tube preparation may affect the interfacial layer between the BASE and the TiN, other important parameters appear to be nitrogen pressure and electrode thickness.

To provide nitrogen for reactive sputtering, N_2 was mixed with argon in a ratio $4cm^3$ $N_2/16$ cm^3 Ar (20% N_2). Other experiments have shown that the normal film parameters (stress, stochiometry, adhesion) are not sensistive to this ratio and it was held constant for all of the tests. It is important to keep the N_2 flow rate below the level at which the nitrogen reacts with the Ti target surface faster than the Ti is removed by the sputtering. Coverage of the target by a layer of TiN can be detected as a rapid drop in the sputtering voltage and this is followed by a reduction in the sputtering rate and the production of nitrogen rich films. The N_2 flow rate determines the ratio of titanium to nitrogen. The sputtering system is normally operated in a current controlled mode. The variations in sputtering voltage at a given pressure indicated in Table D9 appear to occur primarily as a result of target erosion which changes the sputtering geometry and thus the maximum allowable N_2 flow rates. Within limits set by the pumping system, the flow rate and pressure of the nitrogen/argon mixture can be adjusted to compensate for such changes in voltage so that the reaction rate of nitrogen and titanium remains constant. Low gas pressure (below about 2.5 mtorr) tends to yield a stochiometric film with low porosity. Higher gas pressures can also produce stochiometric films but may adversely affect their quality since the flow rate of the N_2/Ar mixture must be substantially reduced due to pumping limitations. Contaminants arising from outgassing of the walls and other components during the sputtering operation are not purged from the system as completely as at the higher flow rates associated with low pressure sputtering. SEM photographs show a higher porosity in the films sputtered at higher pressures.

Samples other than BASE tubes indicate that the details of the sputtering procedure may be important. An initial 'pre-sputtering' discharge, performed at low pressures, is generally carried out in order to assist in cleaning the system. During pre-sputtering in these tests, the end of the sample may have been exposed to the plasma and an extremely thin film of impure TiN may have formed prior to the actual sputtering operation. This may account for some of the differences in electrode performance. This situation has been corrected by shielding the samples until the main sputtering operation begins.

Another problem with the BASE tubes is that because of the heating during the sputtering operation, some tubes apparently outgas considerably when sputtering begins (a rise in the pressure is seen). This suggests that in future work the tubes should be baked out at a reasonable temperature (200-300°C) under a good vacuum before sputtering is initiated.

TABLE D9: Sputtering parameters and performance characteristics of TiN test electrodes.

DTC #	Comments	Sputtering Pressure (m. torr)	Sputtering Current (A)	Sputtering Voltage (V)	N_2 Flow cc/mm	Time	Electrode[2] Thickness μm	Sheet Resistance Ohms	Test Temp. °C	Initial Power Watts	Final Output Power Watts	Test Duration Hours
2-84		2.5	2.5	400	5.0	30 min.	2.0	3.1	800	.051	.051	200
4-84	(Fractured)	3.5	1.8	330	3.0	1 hour	2.5	2.7	507	.03		
15-84		2.5	1.55	425	4.1	1 hour	3.0	1.19/.39*	900	.51	.345	143
16-84	(Fractured)	1.6	1.45	450	4.08	1 hour	1.5	.60/.57*				
17-84		2.5	1.5	495	3.75	1 hour	2.0	1.02	900	.50	.180	168
								3.78	850	.44	.32	168
18-84	(Fractured	1.5	1.45	440	4.1	1 hour	3.0	.48/.52*	800	.243		
19-84	(Fractured)	1.5	1.45	435	4.0	35 min.	1.5	1.41/2.0*	900	.46	.312	119
21-84		3.5	1.7	355	3.7	1 hour		1.6/1.5*	900	.45	.226	458
2-85		3.5	1.5			.5 hour	1.0	4.7	850	.192		
	1 μm Moly overcoat						1+(1.0)	1.9	789	.076		
3-85A[1]	(a) Ti/TiN	2.5	1.6	365	3.6	40 min.	2	1.4	900	.16		
	(b) Moly overcoat						2+(.13)	.26	871	.18		
	(c) High density wire wrap						2+(.13)	--	914	.12		
3-85B[1]	(a) Ti/TiN	2.5	1.6	365	3.6	40 min.	2.0	1.89	--	--		
	(b) Moly overcoat						2+(.13)	2.1	900	.5		
	(c) Medium density wire wrap						2+(.13)	--	850	.308		
4-85	(a) TiN over Moly	2.4	1.6	360	3.4	45 min.	2+(.2)	1.26	850	.249		
	(b) TiN						2.0	1.49	874	.28		
	(c) Medium density wire wrap over TiN+moly						2+(.2)	--	838	.15		
6-85	TiN	2.0	1.6	440	4.35	60 min.	3.0	.86	800	.521	.469	246

* Two electrodes/tube

[1] Same tube, same electrodes

[2] Note: Thickness is determined by sputtering on a flat glass slide under the same conditions and measuring with a microscope or profilometer.

The following paragraphs describe the features of some of the most interesting members of the series of TiN electrode investigated in the present program.

DTC-15-84 : Figure D6 shows the output performance of this electrode as a function of time. This electrode is significant in that the output levels out at slightly below 0.4 W/cm^2. The final drop off may reflect a dropping sodium level in the BASE tube (approaching the maximum time limit on the sodium supply).

DTC-21-84 : The electrode tested in DTC 21-84 was sputtered at high pressure and showed signs of physical separation from the BASE tube after 465 hours of operation, as can be seen in the photograph in Figure D7. This test was run for approximately 458 hours at 880°C with the power decreasing from an initial 0.45 W/cm^2 to 0.225 W/cm^2. The cell was refilled twice and this exposure to the atmosphere and handling may have contributed to the decrease in output power since the wire electrodes may have been bumped or moved slightly. The thin film electrodes sputtered at low pressure in this series seem to degrade less than the one sputtered at high pressure. The best TiN electrode endurance measured to date was on DTC-6-85, sputtered at 2 mtorr pressure from a new titanium target.

Figure D8 shows the output power vs. time. Figs. D9a,b and c are scanning electron micrographs at similar magnifications showing before and after microstructures of thin TiN electrode films (not on the same BASE tube but sputtered simultaneously). Note the difference in Figs. D9a and b. The film in D9a, the as-sputtered surface, has a 'fuzzy' appearance and what may be two distinct grain sizes, one definitely sub-micron and one in the range of 1- 15 microns. The film in Fig. D9b has a completely different structure almost indicating a third range of grain sizes on the surface between the other sizes. Figure D9c is a new low-pressure electrode, note the absence of the two grain sizes. (The large chunk of matter on the right side may be residual from cutting the sample.) This electrode appears to be more uniform than the other electrodes.

DTC-3-85 : The electrodes in DTC-3-85 were made possible by the addition of a computerized controller to the sputtering apparatus. They consisted of an initial layer of titanium metal whose composition was then graduated to fully stochiometric TiN by slowly increasing the N_2 flow in the system. Three patch electrodes were deposited on the BASE tube and a 0.13 micron thick molybdenum overcoat was sputtered on top of one of the electrodes. The current collection arrangements were also different. One Ti-TiN electrode having the conventional arrangement of 2 copper wrapped molybdenum wires (see Figure D10) for current gathering was used as a control and yielded 0.16 W at 900°C. The second had the same current gathering arrangement but the Ti/TiN had the additional Mo overcoat and yielded 0.18 W at 871°C. The third electrode had a 'tight' molybdenum wire wrap (the current collection wires visually obscure approximately 1/2 of the electrode area) over the Ti/TiN and yielded 0.12 W at 914°C. The cell was shut down due to a heater failure, opened to the atmosphere at room temperature and refilled. The tube and the electrodes were salvaged, and two of the electrodes were tested in a second run. This time the second electrode, with the Mo overcoat and conventional current collection set-up, was tested in the same current collection configuration and yielded 0.15 W at 900°C (slightly reduced from 0.18 W at 871°C before). The third electrode

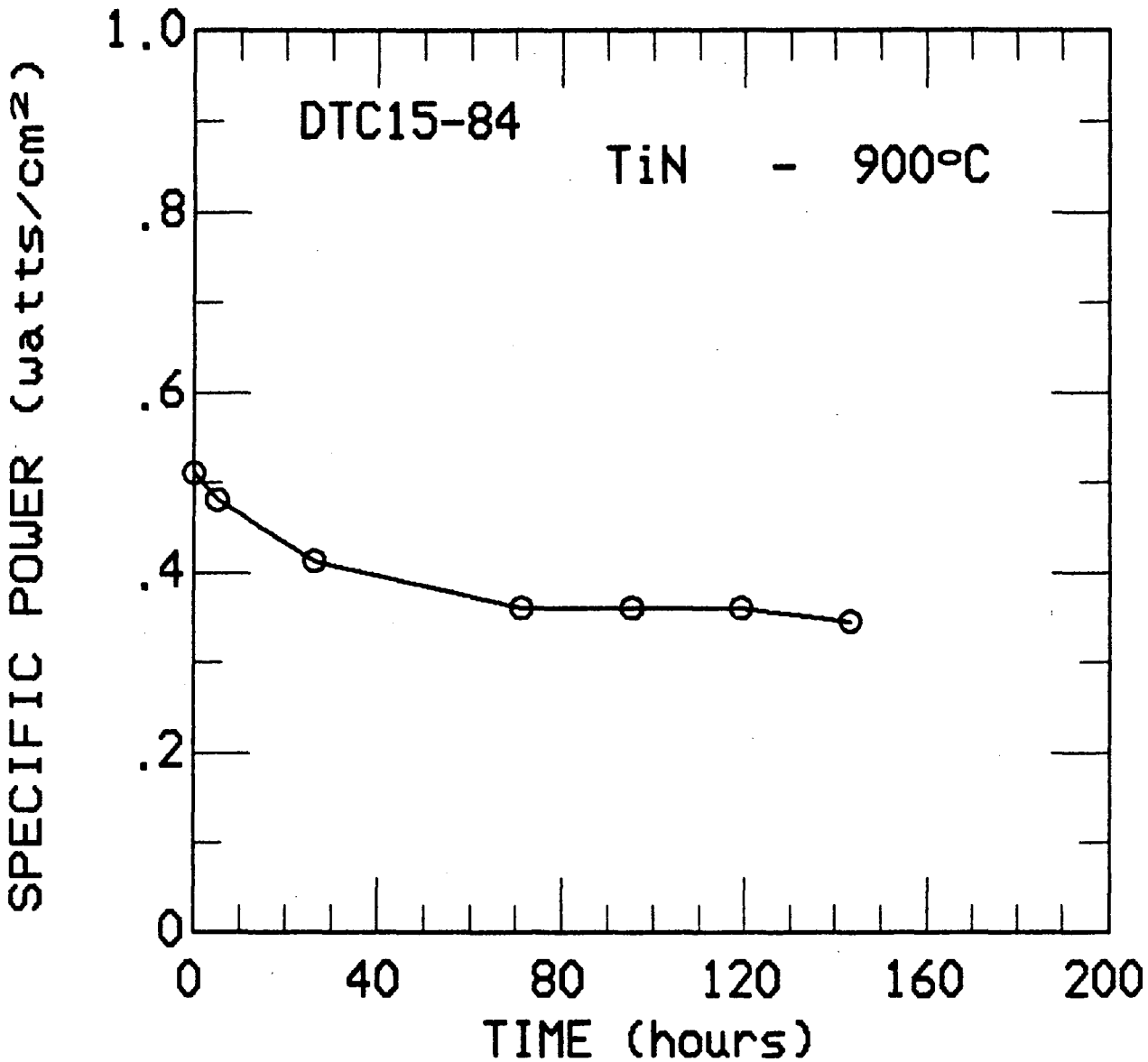

D6. Maximum output power of TiN electrode vs. time.

D7. Photograph of TiN electrode, deposited at high sputtering pressure, showing separation from the BASE substrate.

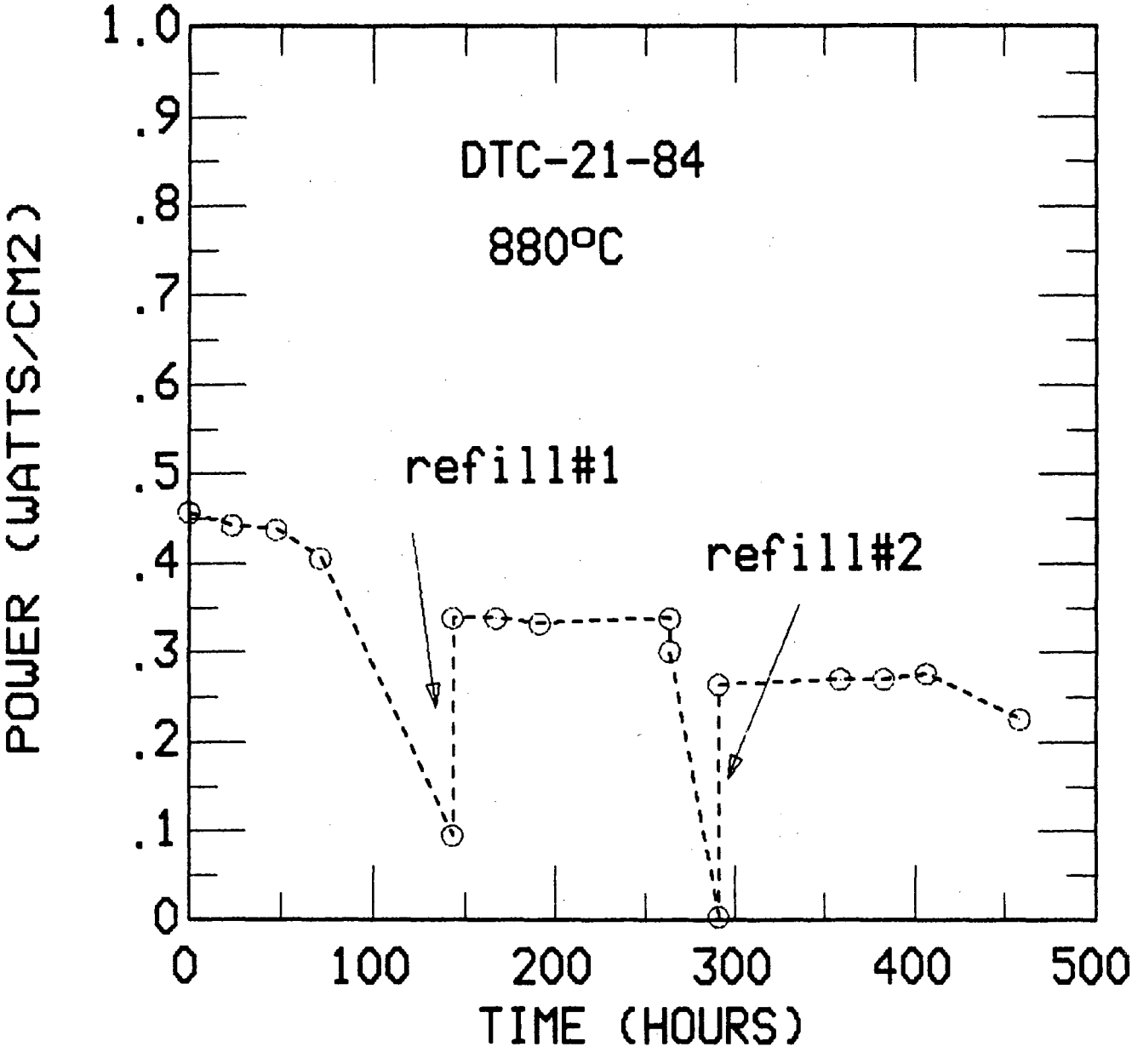

D8. Maximum output power of high pressure sputtered TiN electrode. Times at which sodium was added to system are noted.

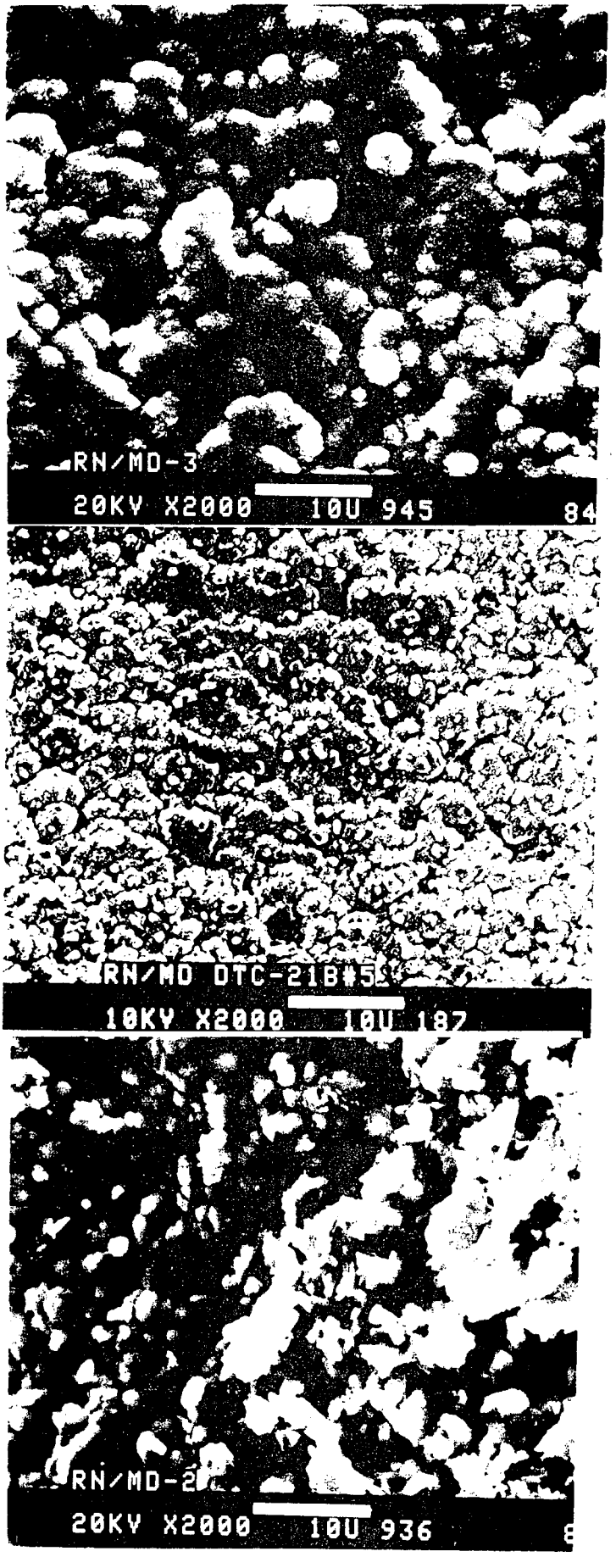

D9.

Scanning electron micrographs of TiN film sputtered at the same time as the electrodes of Fig. D8. a) as sputtered, b) after 465 hours at 880°C and c) a new electrode sputtered at low pressure.

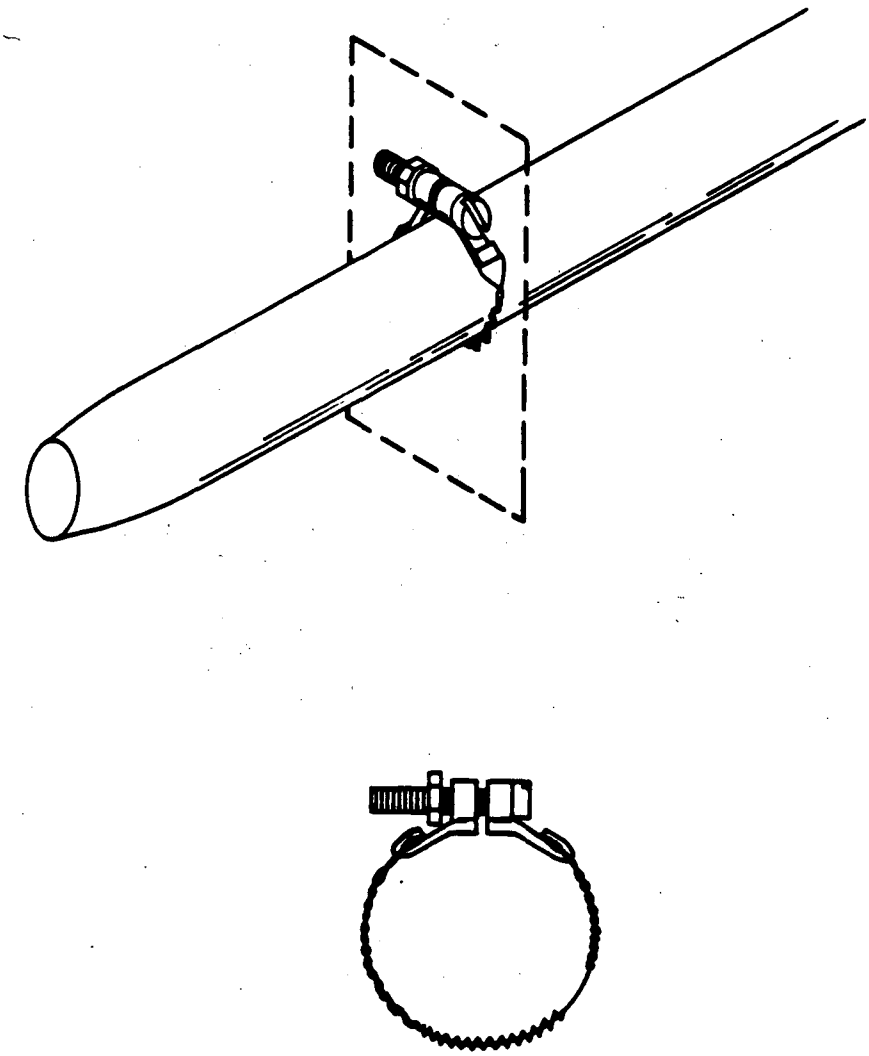

D10. Current pick up system for contacting patch electrodes showing secondary wire wrapping on tension strand.

was changed from the 'tight' wire wrap to a wrap with at least a 2-wire width spacing between each wire. This yielded 0.308 W at 850°C, a significant increase above the 0.12 W at 900°C observed in the previous test. This suggests that choices for the bus wire configuration can substantially affect the power output of SHE electrodes under certain conditions. Other experiments, still in a preliminary stage, have indicated that occlusion of the SHE electrode surface area by tightly wrapped molybdenum collection wires (wrapped closely enough to completely obscure the surface area of the thin film electrode visually) has a minimal effect on the electrode output. The role of the current collection system in electrode performance requires further experimental clarification.

DTC-4-85 : The electrode tested as DTC-4-85 consisted of a TiN layer deposited over a 0.1-micron layer of Mo. The results from this single attempt were disappointing since it yielded only 0.24 W/cm^2 at 850°C, but this test must be regarded as somewhat inconclusive since it appears that there was a problem with the sputtering apparatus. This electrode composition should be repeated.

DTC-6-85 : For this test a new Ti sputtering target was installed in the system (voltage went up to 440 V) prior to deposition. Thin test films on glass slides showed the normal TiN gold coloring at the interface between the TiN film and the glass indicating the presence of a high density, high quality TiN film at the interface. This was the best TiN electrode tested in the entire series. Current voltage curves for this electrode are shown in Figure D11. It maintained an output of greater than 0.45 W./cm^2 for 246 hours at 800°C. Figure D12 shows the maximum power vs. time relation for this cell which contained more sodium in order to permit a long run before refilling became necessary. Power dropped off sharply in the initial run of 50 hours, and the unit was shut down for several days and restarted (the unit was under vacuum during shut down). After 24 hours of operation the electrode improved substantially between two back to back I- V curves. While the reason for this behaviour is not clear, the electrode subsequently maintained the higher output level until the end of the test. Microscopic inspection of the electrode showed no signs of delamination or discoloration of any kind. The improvement in the quality of TiN at the interface may account for the improved performance relative to earlier electrodes.

In conclusion, the evidence indicates that TiN would make an acceptable electrode at modest power levels (0.4 to 0.5 W/cm^2 at 800°C). More work is needed in the area of surface preparation of BASE and the optimization of film thickness for more consistent performance. Additional results on the effects of electrode occlusion by current bus collection wires may lead to an increased emphasis on thinner, more resistive films whose resistance may be overcome by more densely wrapping the collection system. In addition, the present sputtering system cannot uniformly coat an entire tube and would have to be modified. An investigation of the chemical reactions (if any) between TiN and Na will be required for a complete understanding of the system.

Liquid Metal Electrodes - Tin, Tin-Zirconium

Investigation of the stability of SHE electrode performance for a variety of SHE electrode materials has suffered from a certain ambiguity as to the

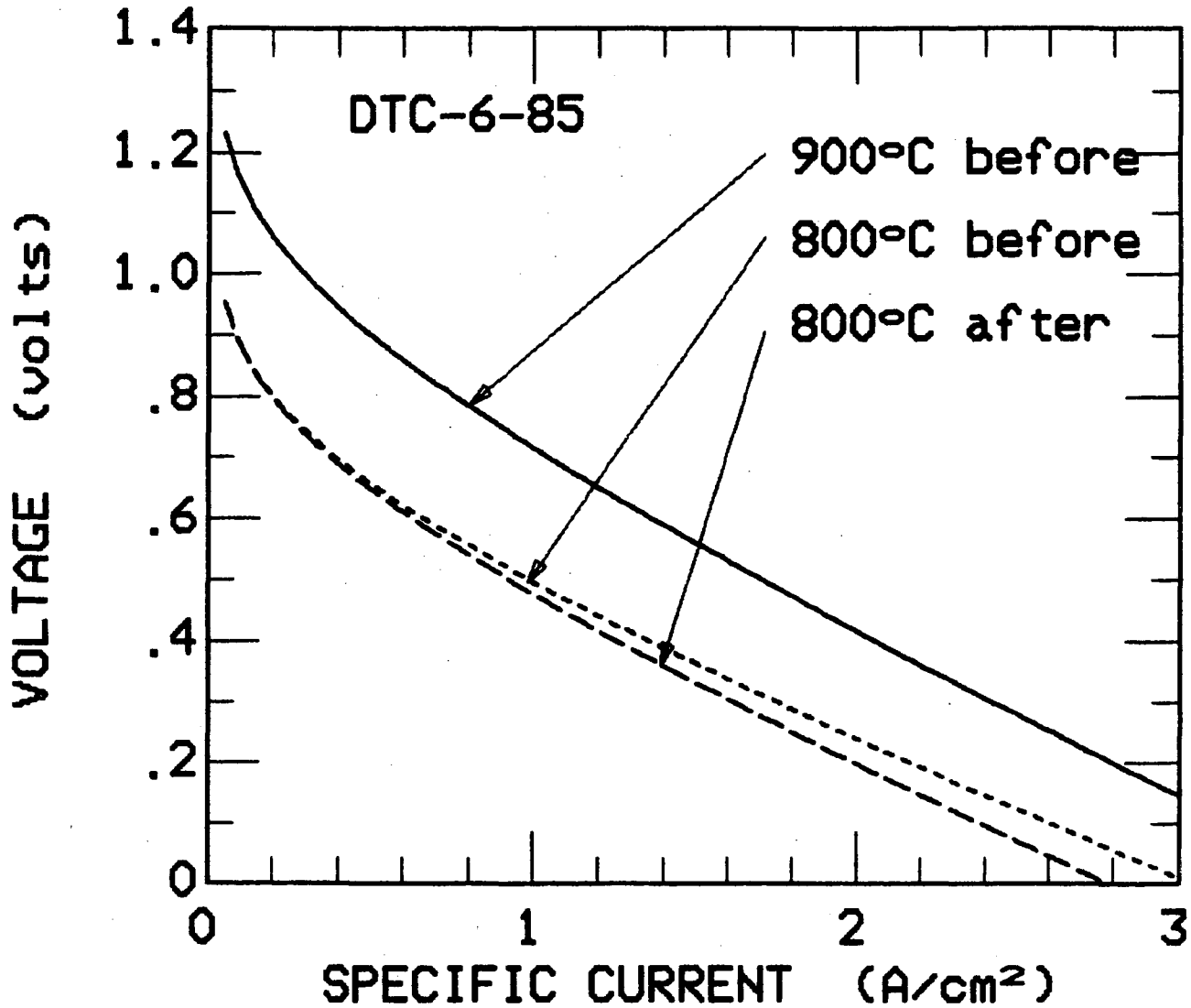

D11. Current-voltage data for the best of the TiN electrodes tested to date.

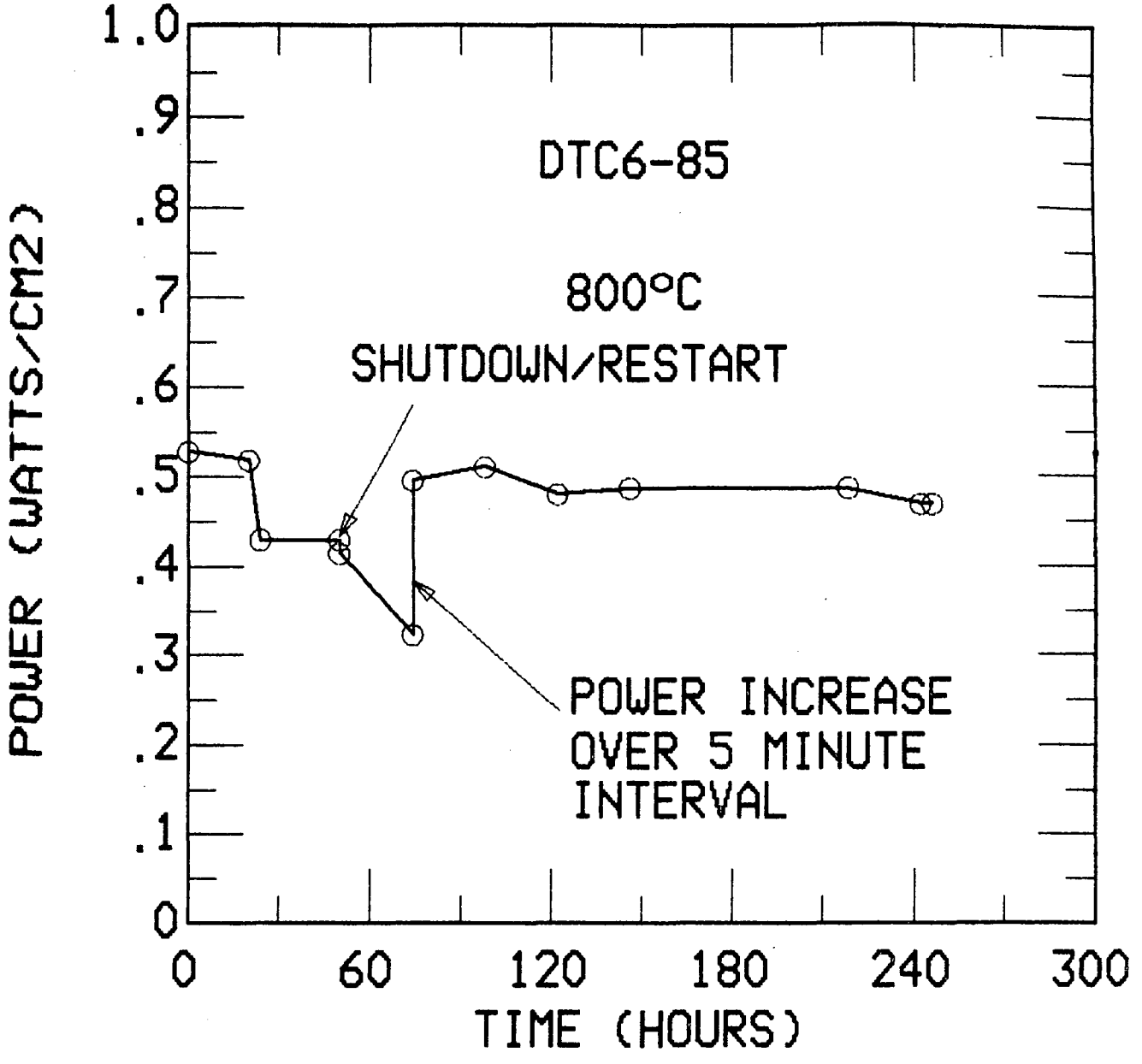

D12. Maximum output power vs. time for high purity TiN electrode.

exact site of the changes leading to the apparent decrease in electrode permeability. In order to examine the electrode-electrolyte interfacial properties experiments were carried out using liquid metal electrodes for which no change in the bulk electrode properties would be anticipated. Under these circumstances it would be expected that any observed degradation of the system performance would be readily attributed to the BASE. Furthermore, since previous experiments appear to have eliminated changes in the bulk BASE properties as a direct cause of the observed performance loss, degradation observed in this experiment would direct attention to possible changes in the surface layers of the BASE.

In this connection, liquid tin provides an electronically conductive, relatively low-vapor-pressure electrode material with a fairly high sodium solubility at normal SHE operating temperatures. In order to run such a system it is necessary to provide a means for holding the tin against the BASE as well as making appropriate electrical connection to it. Two principal methods were used and they are shown schematically in Figure D13.

In the first diagram, a cone of molybdenum metal is shown strapped to the BASE tube with the tin placed as shown. Approximately 2.3 g of Sn were placed in the conical 'boat' and a molybdenum lead wire spot welded to the cone using a titanium interlayer. The simple geometry of the boat permits a simple calculation of the BASE area exposed to the Sn as a function of the total mass of tin used. Because the tin does not wet the BASE it does not leave the conical reservoir by flowing down the tube wall. With 2.2 g of pure Sn (note that the tin is saturated with molybdenum due to the cone and lead wire) this electrode configuration produced a consistent i-v relation for 307 hours at 800°C. The maximum power density was 0.26 W/cm^2. Over the test period, which involved refilling the tube with sodium, no changes in the output curve were observed. At 800°C the conventional sputtered molybdenum film electrode exhibits substantial loss of maximum output. Nevertheless the total output from this test was small and general conclusions are not obvious. It should be noted that the thickness of the Sn electrode was large, and the path for the neutral sodium far longer than in the conventional thin film electrodes.

The influence of the Na charge carrier concentration in the Sn was also examined. Because of the high solubility of Na in Sn at SHE operating temperatures, an attempt was made to restrict this solubility, and hence the charge carrier concentration, by alloying the tin with an equal weight of copper for which the sodium solubility is far smaller. The output of this system was found to be much lower reaching a maximum of 0.108W/cm^2 at 800°C. Following the tests of this electrode, the beta''-alumina was observed to be stained in the electrode-electrolyte interface area. Electron microprobe examination of this area revealed traces of Cu, Sn and Mo but no indication of sub-surface penetration of these elements was found. This result tends to support the conclusion that a reduction in the number density of sodium atoms in the electrode will reduce its neutral sodium permeability. I-V curves of these conical liquid electrodes are shown in Figure D14.

While the conical reservoir provides a combination of small evaporative surface area and large capacity for the liquid electrode, it also leads to a relatively long path for sodium transport through the electrode, and for this reason, a relatively low power output. In order to allow more rapid transport

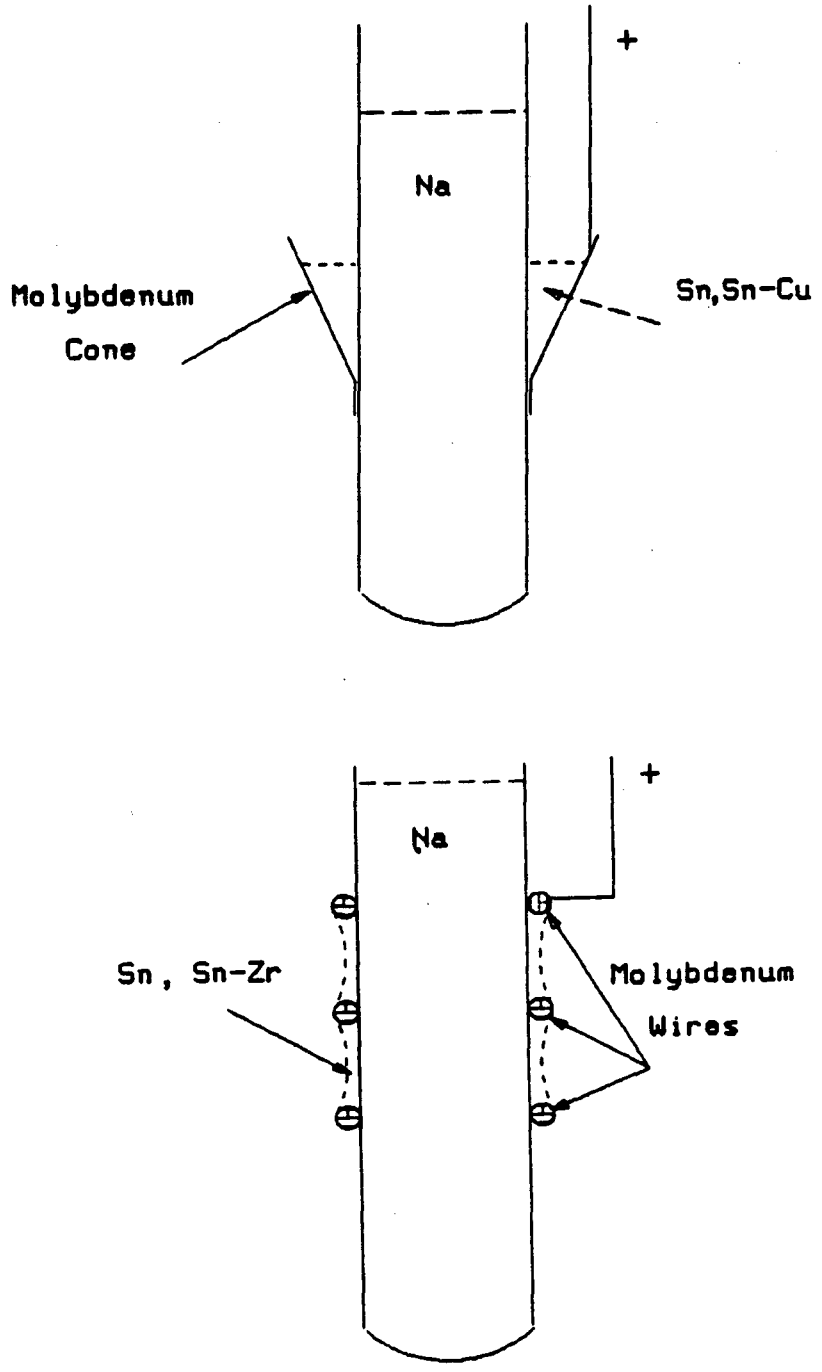

D13. Schematic diagram showing two methods for holding a liquid metal electrode against a beta''-alumina tube.

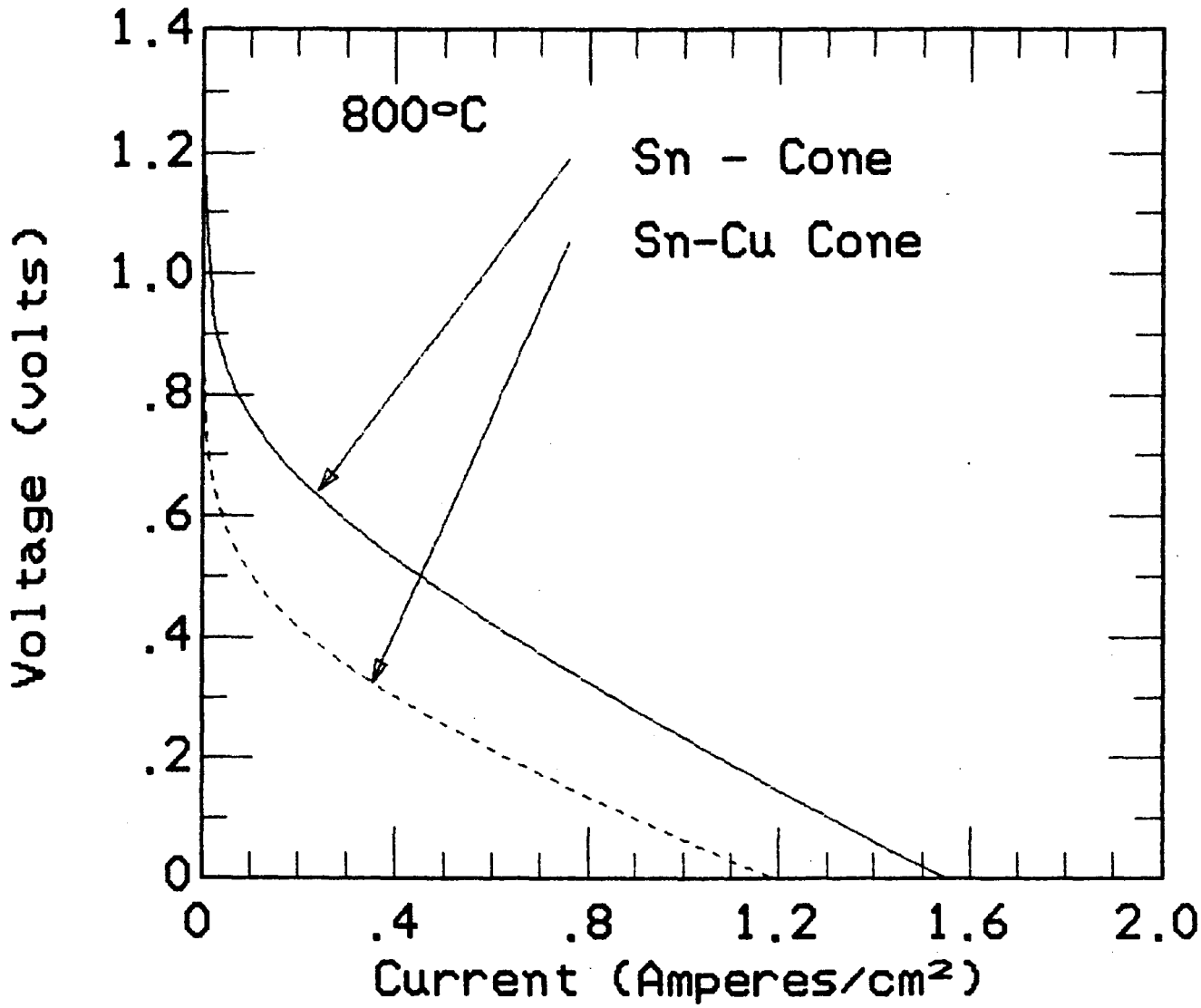

D14. Current-voltage data for conically supported liquid tin and liquid tin/copper electrodes.

through a liquid electrode, a wicking structure composed of molybdenum wire (0.006-inch diameter) wrapped around the BASE tube was used to hold the liquid Sn and Sn-Zr alloy against the BASE surface, as shown in the second diagram in Figure D13. The tin was applied to the wire in a separate operation by the reduction of a stannous oxide/water paste in flowing hydrogen at 800°C for one hour. After wrapping the BASE tube with this wire, a stannous oxide/alcohol slurry was applied with a small brush and hydrogen reduction performed at 700°C with the DTC assembled in the condenser can. The current-voltage relation for this electrode is shown in Figure D15.

An experiment with a 33 wt% Cu in Sn electrode was carried out using the wire/wick geometry but no benefits were observed from this combination. The wicking wire wrap achieved a 50% coverage of the surface area of the beta''-alumina. Incomplete wetting of the 'wicking' wires by the electrode material appeared to have been a problem. In order to improve the wetting of the collection wires by the Sn-Cu alloy, zirconium was added to the alloy by applying a ZrH_4/ alcohol slurry to the wire alloy system. Operation of the cell with sodium passage was expected to reduce the hydride, thereby freeing the Zr for the promotion of wetting both for the molybdenum wires and for the BASE. The current voltage relation for the modified liquid film electrode is shown in Figure D16.

Experiments with a copper-free tin/zirconium alloy film were also performed. ZrH_4 powder at 9% by weight was added to the Sn. Figure D17 show the measured current-voltage relations for this electrode as a function of temperature. The maximum power density at 900°C reaches 0.60 W/cm^2. This value is remarkable when it is noted that the thickness of the Sn layer is substantially greater than the 1-2 microns generally applicable to the conventional molybdenum film electrodes. Figure D18 shows the equally remarkable constancy of the maximum power output of this electrode over the period up to 140 hours. Also shown is the time/output performance of a normal molybdenum electrode. When the test duration was extended by refilling the BASE tube with sodium, the output decreases remained small and can probably be accounted for by the increased electronic resistivity of the electrode as a result of the gradual loss of tin due to evaporation.

Additional experiments were undertaken to examine the electrode performance of bare wires wrapped directly on BASE tubes. These results allow limits to be placed on the possible contributions of the wires used to measure more conventional electrodes. The total current contributed by these wire electrodes appears to be neglible with respect to the normal currents achieved with sputtered film electrodes. Wires of both molybdenum and rhenium were tested and the I-V results are presented in Figure D19. The performance vs. time was also monitored and both showed a significant drop off with time which reached a nearly stable value after about 100 hours. While the molybdenum wires perform somewhat better initially than the rhenium, the difference is not great and it reverses after a few hours. We do not feel that more detailed conclusions in this special case are warranted at this time.

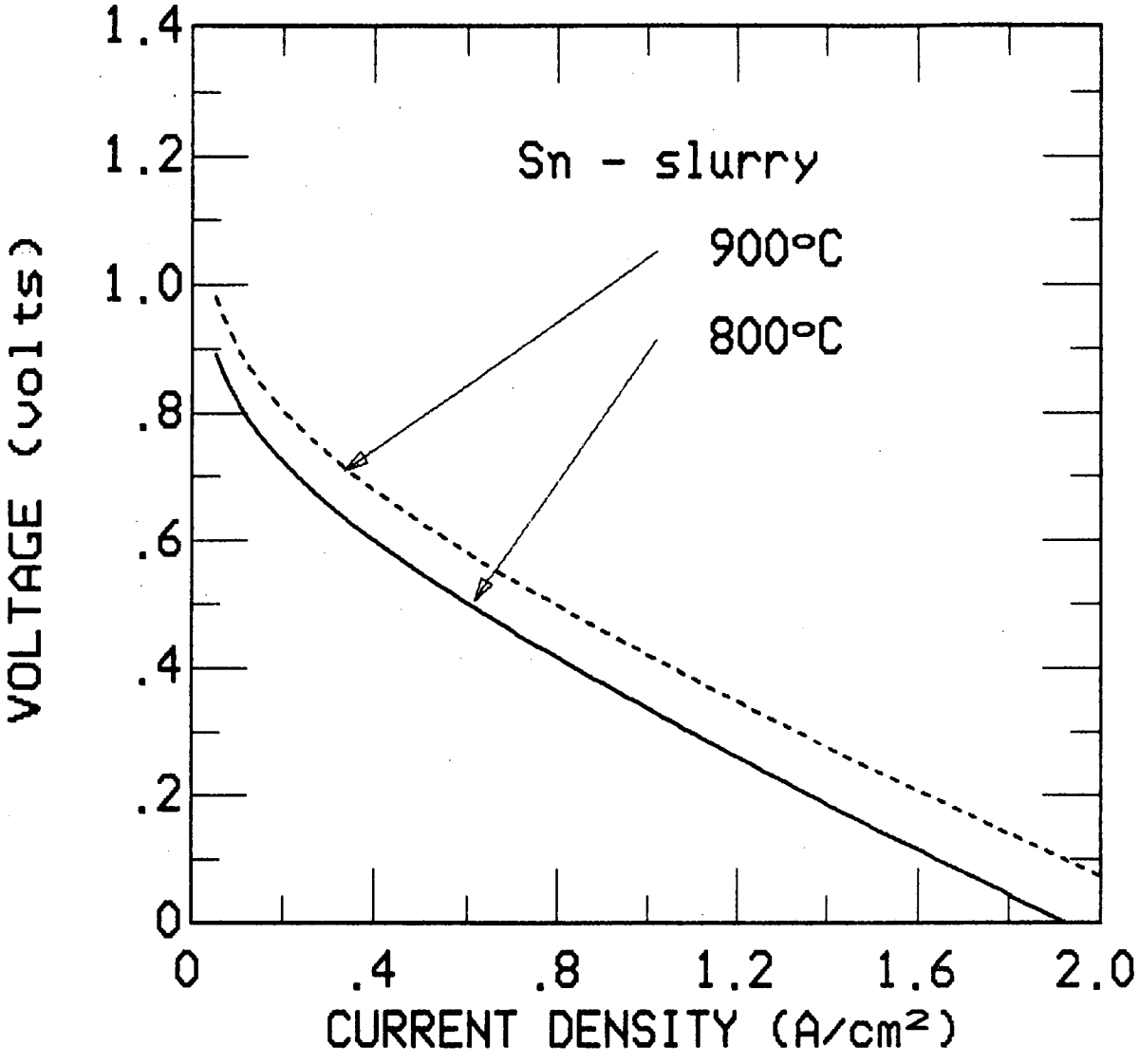

D15. Current-voltage data for a wire supported, slurry deposited liquid tin electrode.

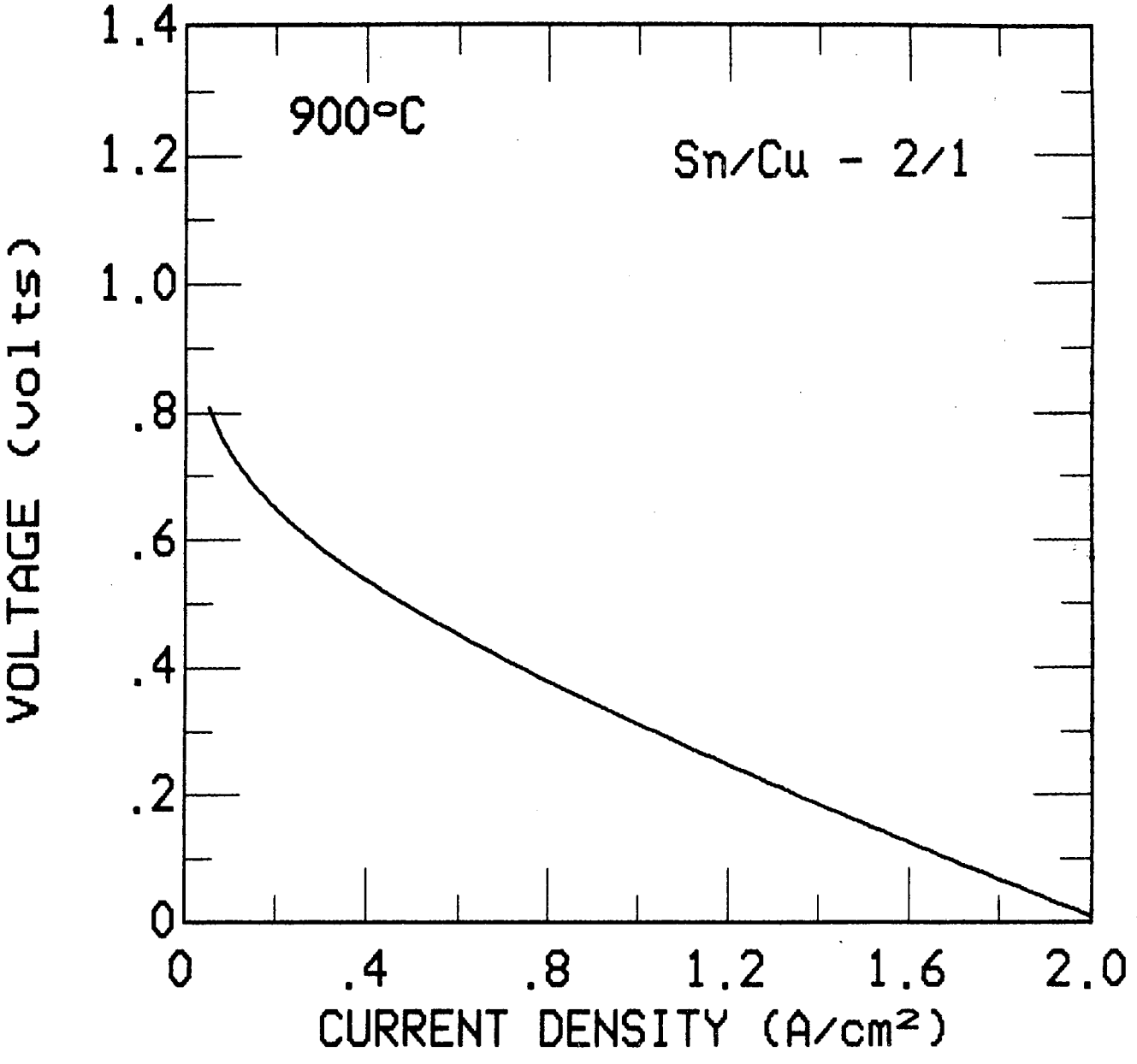

D16. Current-voltage data for a wire supported tin/copper electrode. having a composition of 67% tin and 33% copper.

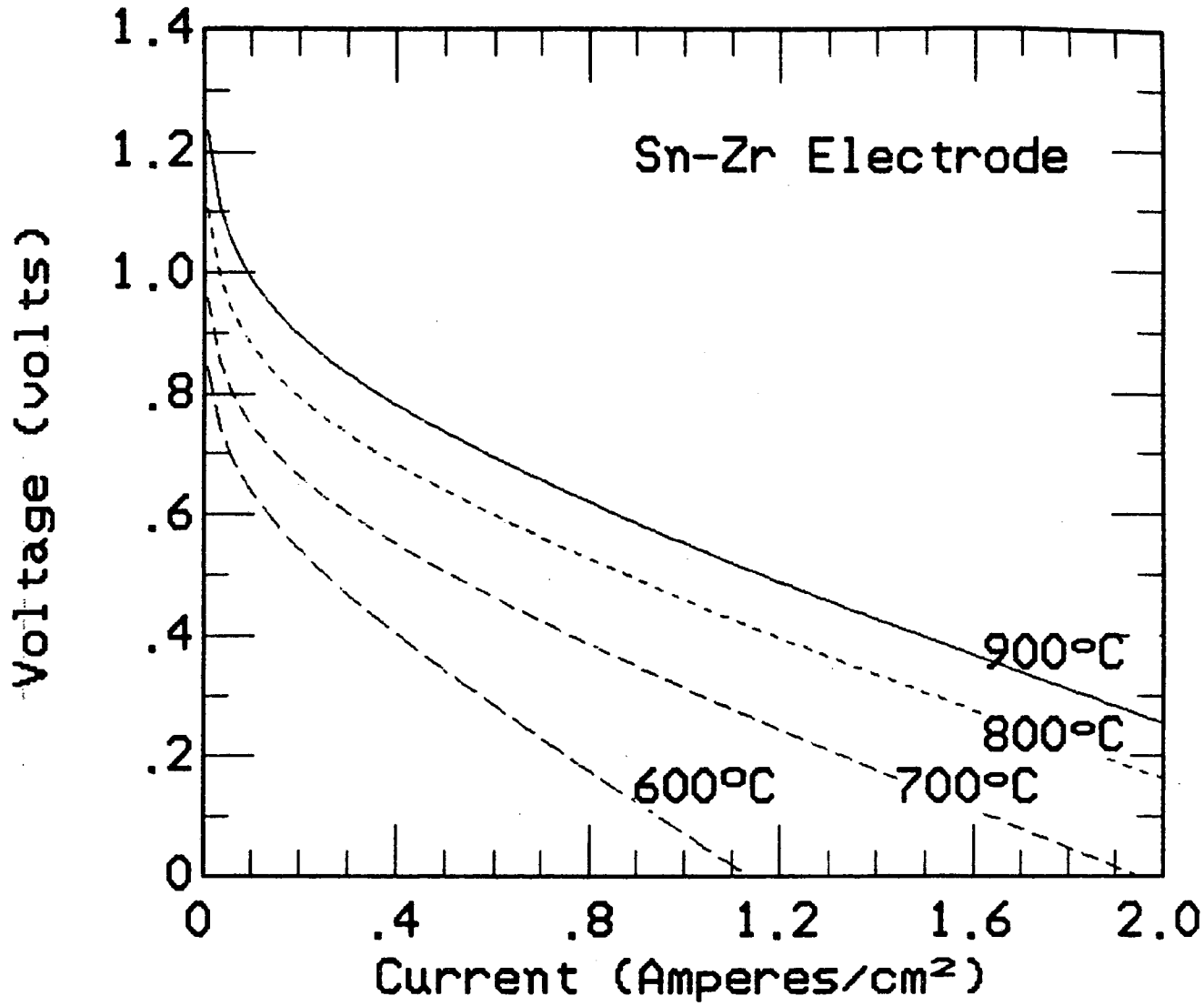

D17. Current-voltage data at several operating temperatures for a wire supported tin/zirconium alloy liquid metal electrode.

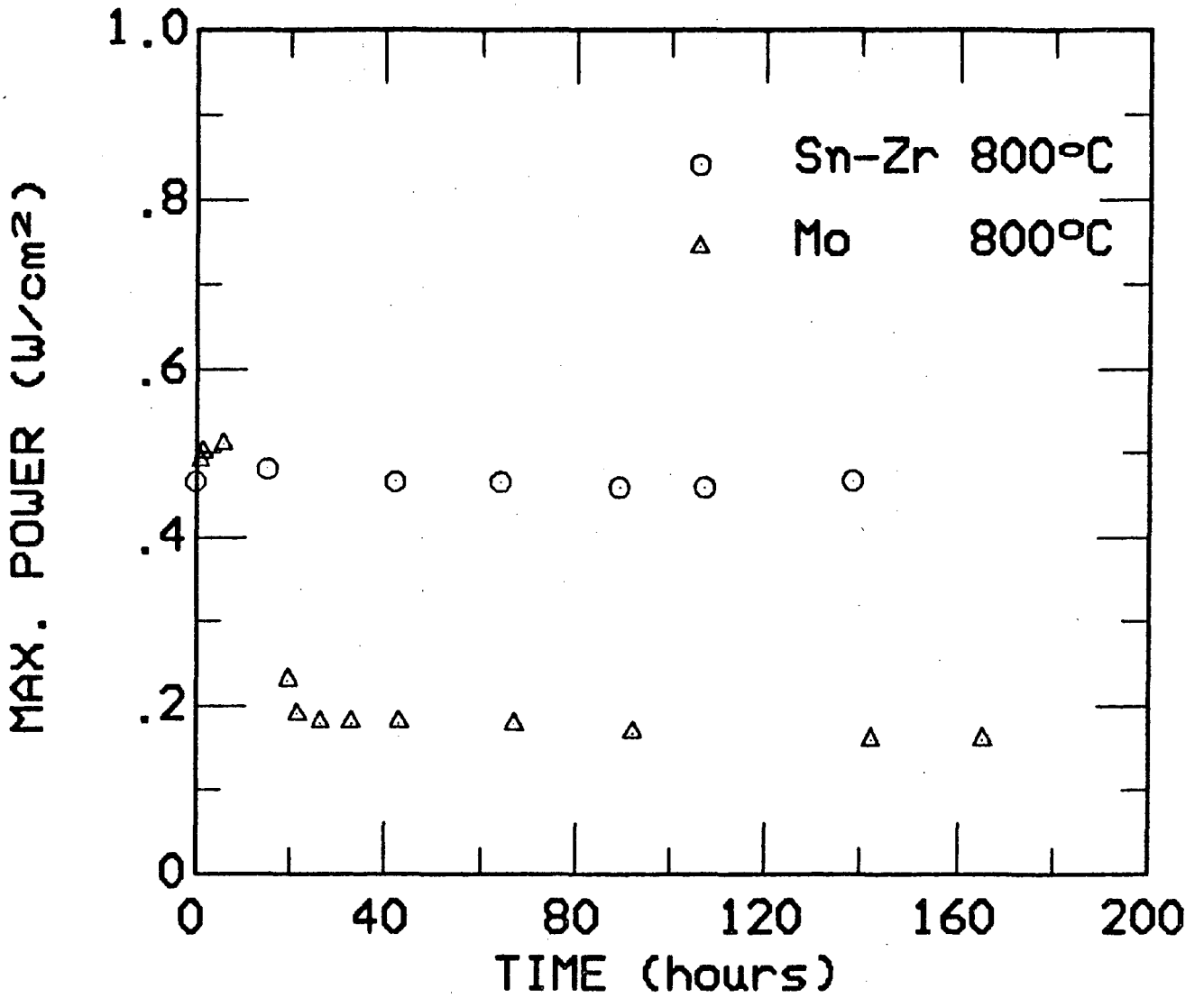

D18. Maximum power vs. time for tin/zirconium liquid metal electrode showing improved endurance by comparison with a standard molybdenum film electrode.

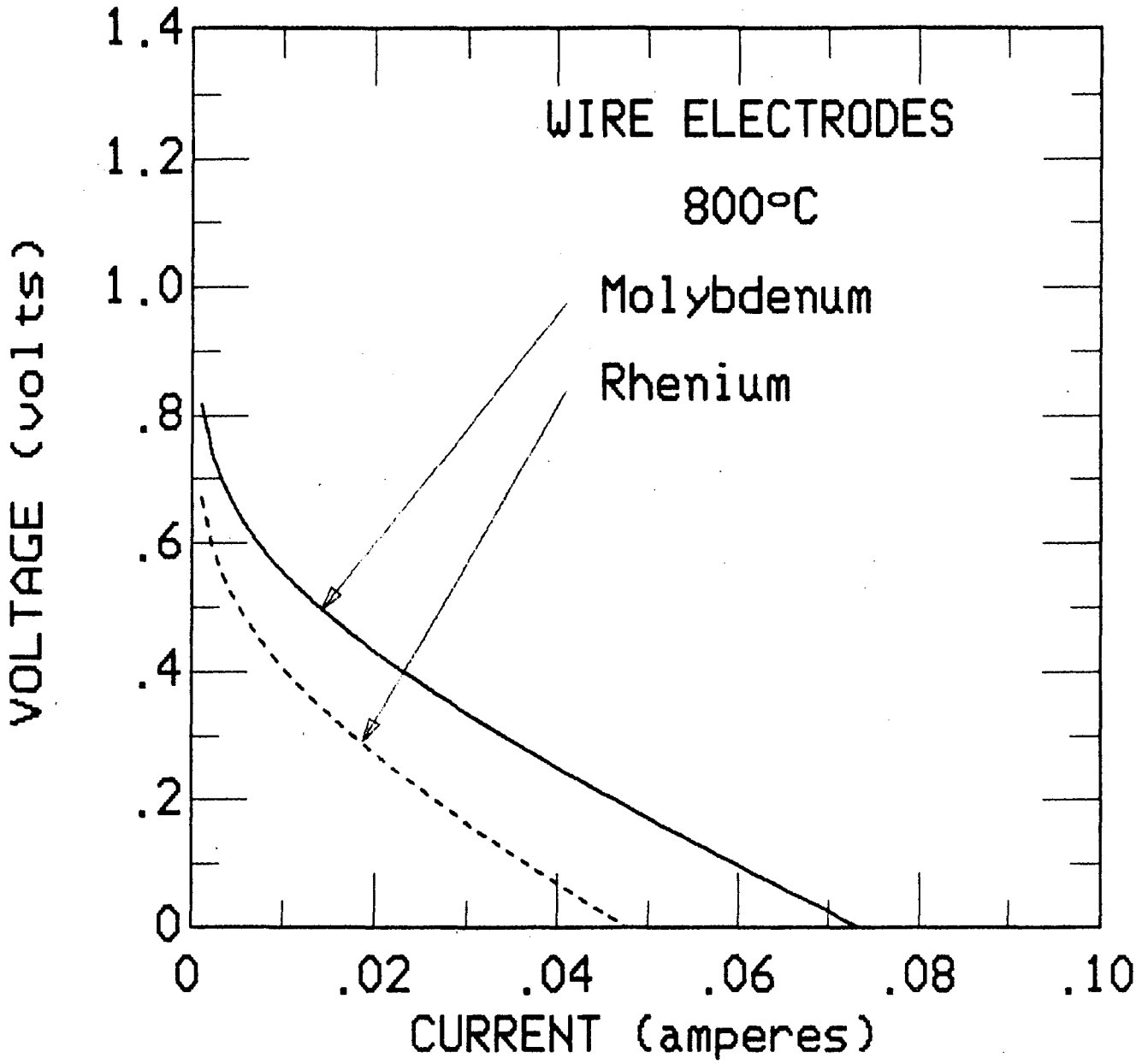

D19. Current-voltage data for bare wire electrodes on BASE tubes showing results for molybdenum and rhenium wires.

Cermets

There are a number of methods for producing SHE electrodes having the basic characteristics of a ceramic/metal composite. Some have a fine-scale structure with the metal particles in sufficiently close proximity that bulk electronic conduction is possible. Others rely on the absorption of metal particles on 'internal' surfaces which are adequately interconnected to produce the necessary conductivity. We discuss two principal methods, absorption in porous beta''-alumina films deposited on standard BASE tubes, and flame-spraying of the composite material directly onto such BASE tubes in a single step.

Flame Sprayed Cermet Electrodes

It is known that surface coatings of a variety of high-temperature materials can be deposited on suitable substrates by feeding powders of the coating materials into a high-power electrically generated plasma or combustion flame and spraying the substrate with the torch-heated material. In this study an oxy-acetylene flame-spray gun has been employed in order to deposit on a BASE tube, a cermet electrode that has open porosity and both electronic and ionic conductivity. The flame-spray equipment (manufactured by Metco Industries) consists of a hand-held gun with controls for the oxy-acetylene flame and a powder feeder unit using N_2 as a carrier gas for injecting the powder into the flame. The unit is capable of producing gas temperatures in excess of 2600°C (plasma-spraying operates with temperatures in excess of 16,000°C). Figures D20 and D21 illustrate schematically both the equipment and the process geometry of the complete flame-spray setup.

The high thermal efficiency of the flame-spray system makes it practical to deposit a powder with a structure as complex as β-Al_2O_3. The very short heat/cool cycle prevents the loss of major amounts of sodium from the structure, though a small amount of sodium must be lost since the flame exhibits the characteristic bright yellow color.

There are a number of important process parameters which may be adjusted in order to influence properties of the sprayed coating.

A. The powder flow rate strongly influences the temperature reached by the powder before it impacts the surface of the substrate. Higher flow rates lead to lower powder temperatures since only a given amount of heat is available in the flame. Conversely, lower powder flow rates yield higher powder temperatures. No method has been developed for reliably measuring the powder temperature in the flame.

B. The flow rate of the N_2 carrier gas is conditioned to some extent by the powder flow rate. High powder flow rates require a high gas flow rate to prevent clogging of the lines. The high gas flow rate means that the powder will spend less time in the flame, absorbing less heat, reaching a lower peak temperature and will impact the substrate surface at a higher velocity.

C. The oxygen/acetylene ratio can be adjusted, within manufacturer's specifications, to affect the flame temperature, but is always kept on the rich side of stochiometry. As a result, the powder is effectively shielded from the oxidizing atmosphere until after it is quenched on the surface.

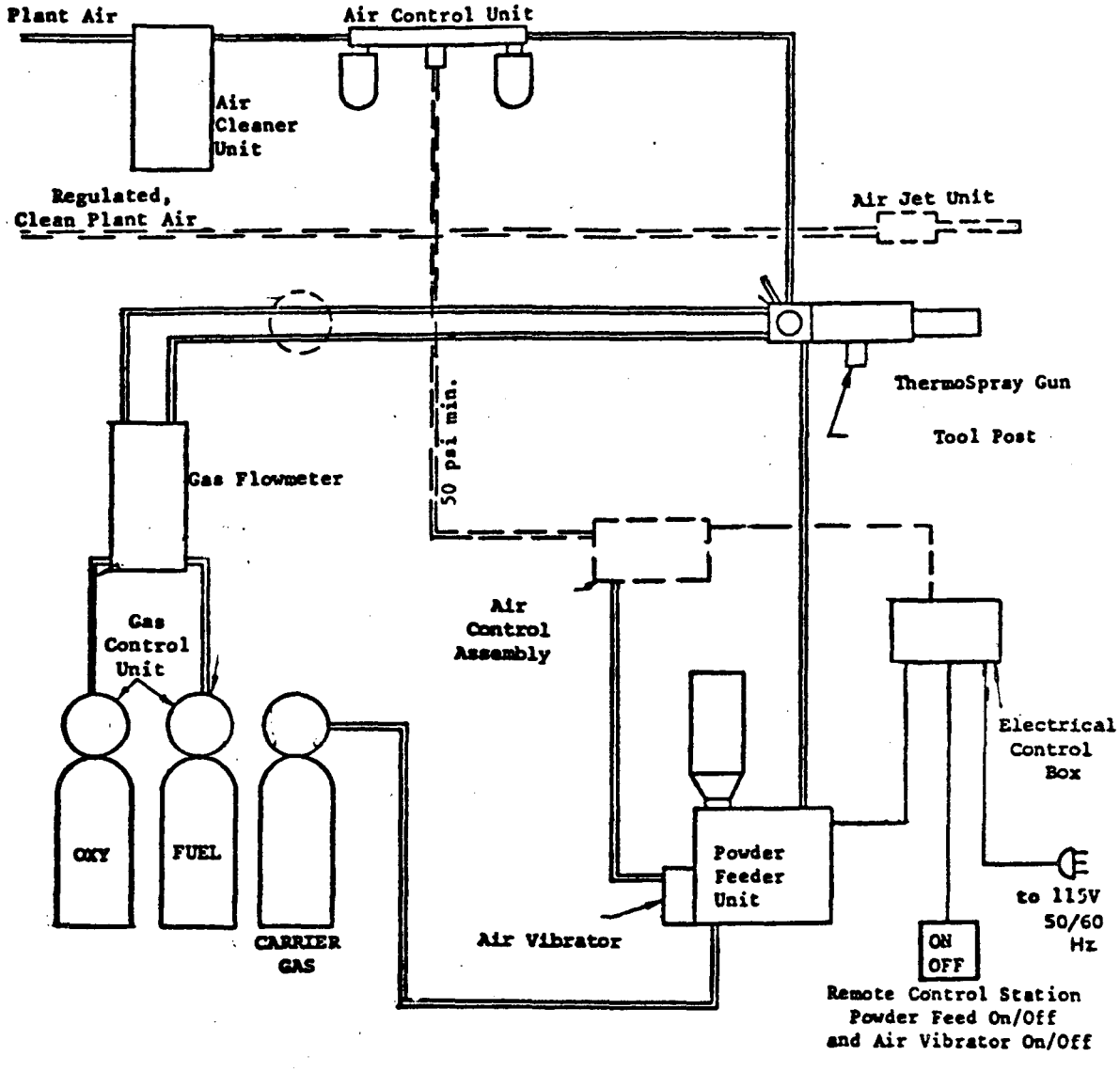

D20. Schematic diagram of Metco flame-spray apparatus used for the deposition of beta''-alumina and cermet electrode layers.

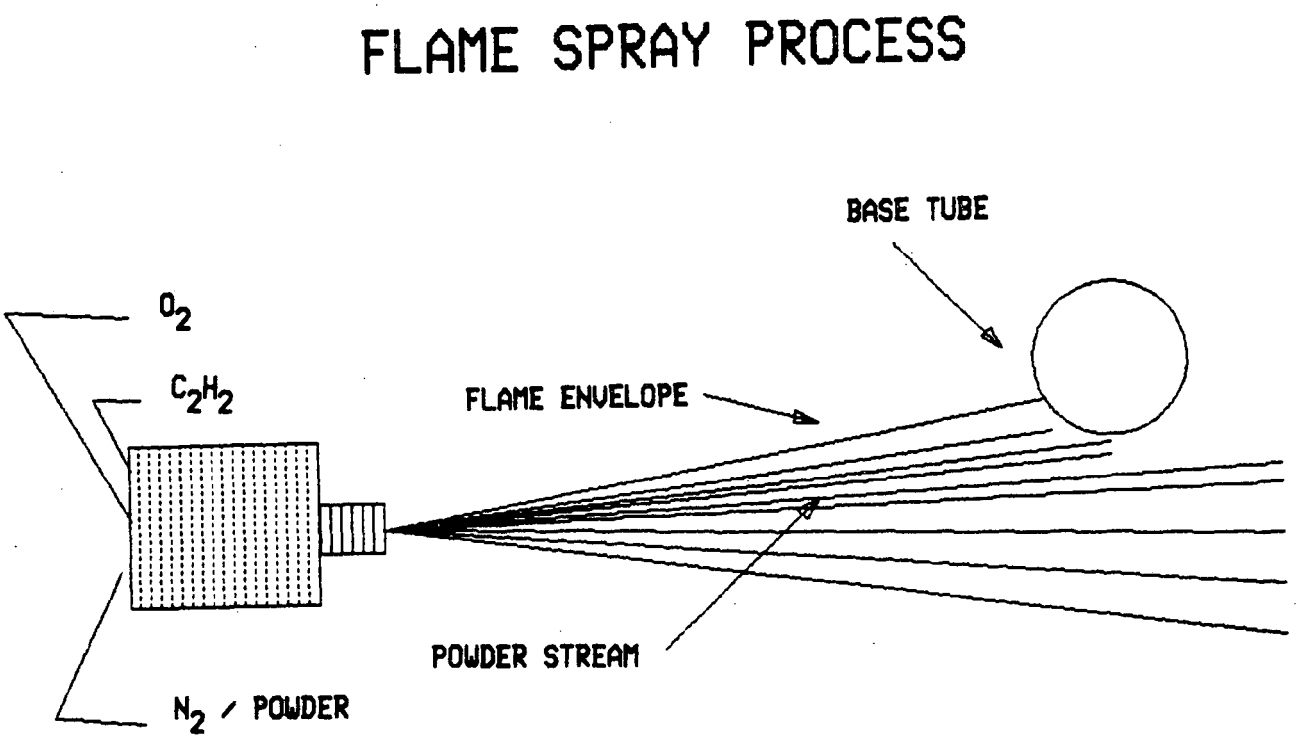

D21. Schematic illustration of the flame-spray process geometry showing gas and powder feed lines.

D. The speed of rotation or linear surface velocity of substrate past the spray nozzle will affect the relative impact velocity of the powder as it strikes the substrate surface.

E. Speed of gun over target. This affects both the uniformity and thickness of the coating. The present experiments were carried out with a hand held gun which was quite suitable for the patch electrodes but it can be anticipated that a lathe-type setup will be required to coat an entire BASE tube uniformly.

F. Auxiliary N_2 and air may also be used. Additional N_2 can be injected at the nozzle to produce denser coatings. Air jets placed internally in the flame can be used to inject high-velocity air into the spray stream to increase powder velocity.

G. Powder size and composition must be in the appropriate range if good coatings are to be possible with any combination of the above parameters. These factors are discussed in detail below.

Powder Preparation Techniques

The powder required by the Metco flame spray system is fairly coarse at 50 to 100 microns diameter. This size requirement is necessary if the powder is to flow smoothly through the powder feeder, hose and gun. Unfortunately this particle size gives coatings with a coarse microstructure not suitable for a SHE electrode. In order to produce a suitably fine-grained microstructure in the finished coating, a particle size of 1 to 10 microns or less is required. It is therefore necessary to cause the powder to agglomerate into 70 to 100 micron size particles before spraying. This is done by mixing an acrylic binder dissolved in acetone with the β-Al_2O_3 and/or molybdenum metal powder. The slurry is then mixed continuously while the acetone is allowed to evaporate. In this way the viscosity of the mixture slowly increases and this prevents the denser molybdenum from settling. The mixture is then dried overnight in a vacuum oven and milled until 100% of it passes a 200 mesh sieve. In this process the powder must be kept dry until it is used.

Composition

The powders tested during this portion of the study were primarily β-Al_2O_3 and molybdenum cermets. The β-Al_2O_3 was not fully calcined and had both beta and beta'' phases. This was done to keep the particle size as fine as possible. Figure D22a shows the X-ray diffracton pattern taken from the calcined beta/beta''-alumina powder, and Fig. D22b shows the diffraction pattern taken from material removed from the flame-sprayed coating deposited on a BASE tube. The beta and beta'' lines are marked and appear to be accurately matched. In the direct deposition of cermets, three sizes of molybdenum metal powder were used: - 200 mesh (74 microns), - 325 mesh (44 microns) and 1-5 micron. The molybdenum metal was added in the form of $(NH_3)_4(Mo_2O_7)_2$ and reduced in H_2. This was done in some cases to coat the β-Al_2O_3 particles with a thin coat of molybdenum and in others to impregnate flame sprayed β-Al_2O_3 electrodes. Compositions of the coatings ranged from 15

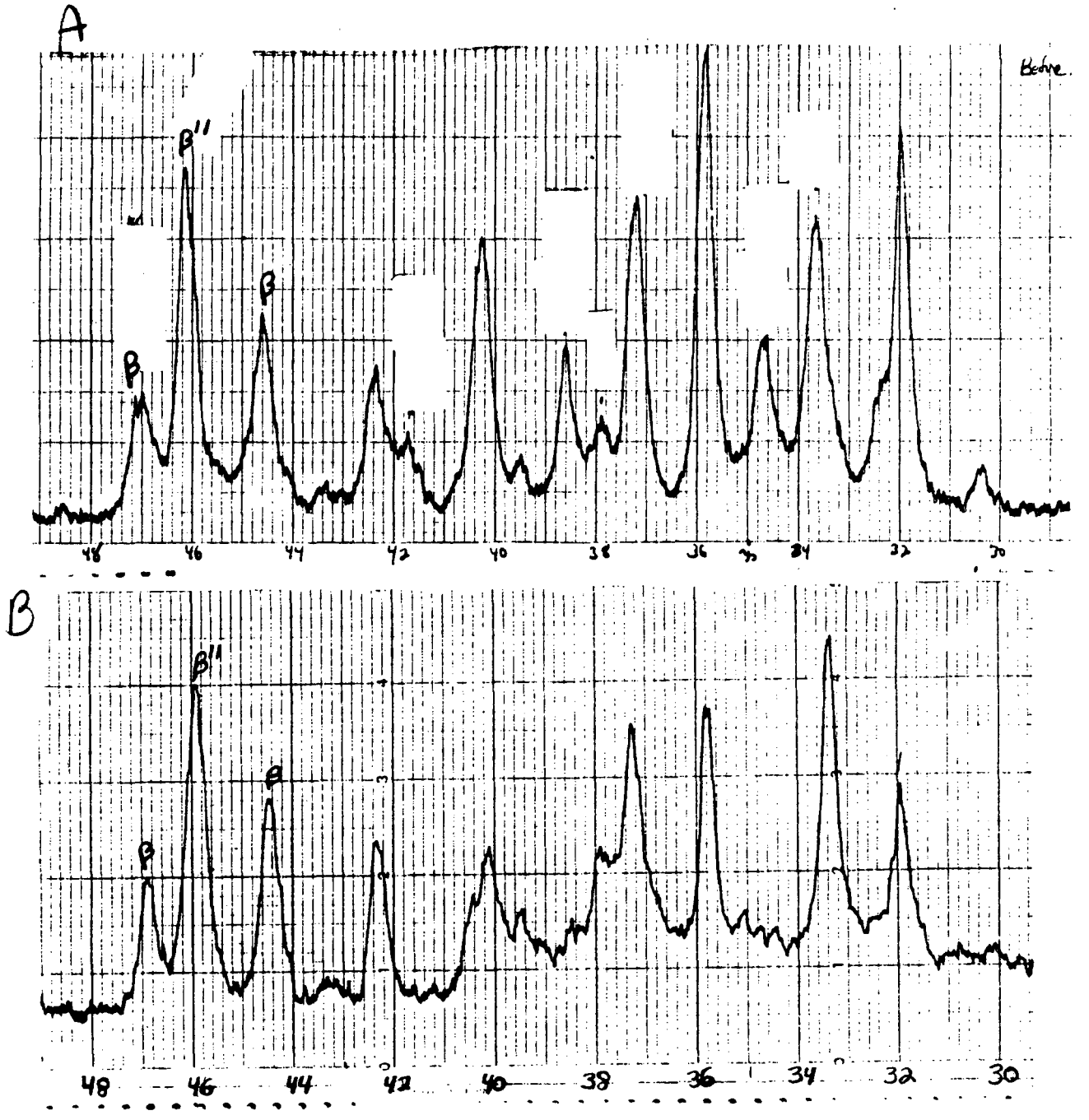

D22. X-ray diffraction patterns taken from a) the calcined beta/beta''- alumina powder and b) from scrapings of the flame sprayed deposit on a BASE tube.

to 50 volume percent molybdenum. Copper and titanium metal powders were also tested as spray powder additions, in amounts of 15 and 20 volume percent, respectively.

The BASE tubes were prepared by 'grit blasting' their outer surfaces with 1 micron alpha alumina powder. An attempt was made to preheat the BASE tube prior to the actual electrode deposition. This was done to minimize the potential for thermal shock, but due to the high volume of air drawn in by the vent hood, the propane fired preheater was overwhelmed. More effective preheating appears to be possible if one makes several quick passes over the surface of the tube with the oxy-acetylene flame before the powder feed is turned on. Of the 15 attempts to produce patch electrodes on full length (30 cm) BASE tubes, only the first five were preheated with a flame. Two of these cracked, the cracks occurring at the ends of the tubes (one at the open and one at the closed end). If the hot zone of the flame is kept at least 3/4 to 1 inch from the ends, there seems to be no problem.

In preliminary testing, a number of flat Al_2O_3 substrates were flame-sprayed in order to work out the spraying parameters such as the powder and carrier gas N_2 flow rates. The best distance between the gun and the BASE tube was found to be 6-8 inches (Metco recommends 4-10 inches). In order to produce a porous coating, a low powder velocity was necessary to prevent the molten particles from splattering on the surface. The surface of the coating is extremely rough and varies in thickness from $< 50\ \mu$ to about $250\ \mu$. If the coating is much thicker, it will flake off the BASE tube. The adhesion of most of the electrodes can be described as good and they required considerable effort to scrape off. At this time, however, we have no reliable quantitative test for adhesion. The electrode coating was applied in layers and the point to point resistance of the films checked after each application. This was used as the main control for thickness, with the electrode considered complete when the desired 1-3 ohms resistance was reached. With this approach, the final electrode thickness varied with its composition, with more conductive powders leading to thinner electrodes.

The β-alumina tube substrate is held by its open end in a chuck and rotated at approximately 475 rpm. The cermet powder is then sprayed on the receding edge in order to reduce the powder impact velocity as much as possible. This is a standard method for increasing the porosity of flame-sprayed coatings.

Scanning electron microscope photographs reveal considerable porosity in the flame-sprayed coatings. They also indicate that the beta-beta'' powder appears to be melting in the flame and quench cooling on the surface. Figures D23 and D24 show a fibrous structure. Figure D25 shows Mo particles that appear to have had a liquid phase. While molybdenum metal melts at 2610°C, there is a known eutectic of beta and sodium aluminate that melts as low as 1560- 1580°C, well within the range expected in the oxy-acetylene flame. Evidence for a molten state of beta-alumina is also supported by the strong adhesion to the surface of the beta-alumina tube. No post-treating was done to minimize residual stresses. The elemental analysis conducted with the SEM indicates that the molybdenum and beta''-alumina are quite well dispersed. The SEM beam diameter was 2 microns and almost all topographical features of the sample surfaces showed both molybdenum and aluminum peaks.

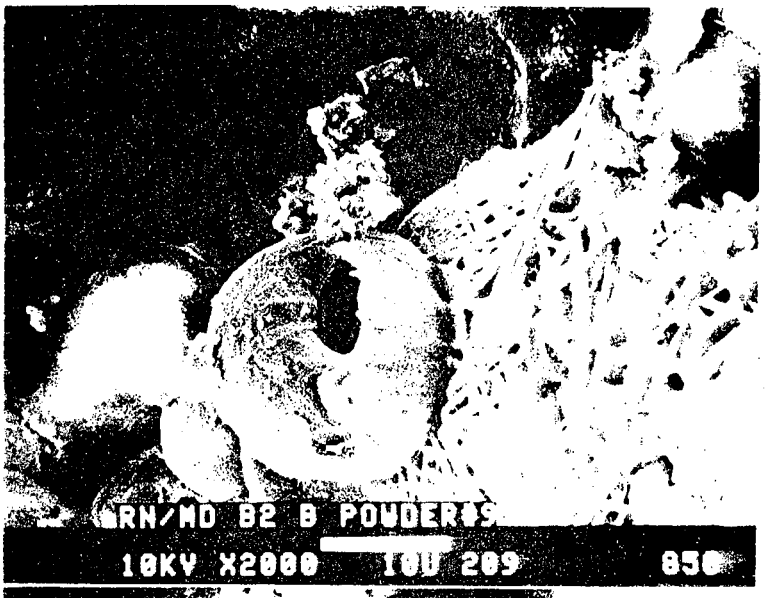

D23.

Scanning electron micrograph of flame-sprayed beta''-alumina film.

D24.

Scanning electron micrograph of flame-sprayed BASE film.

D25.

Scanning electron micrograph of flame-sprayed beta/moly cermet film.

The starting powder in this case was not fully calcined to beta'', and thus contained a large amount of beta and a little unreacted Al_2O_3. The X-ray diffraction results presented in Figs. D22a and D22b show that the beta and beta'' structures are preserved during the flame-spray process.

Table D10 summarizes the data on all of the flame-sprayed electrodes tested to date. The most significant electrode on the list may be DTC-23-84 which yielded 0.57 W/cm^2 at 900°C. After 40 hours, the performance of this electrode fell rather sharply to 0.269 $W.cm^2$ in a manner characteristic of thin film molybdenum electrodes. Figure D26 shows the output of the patch electrode at its start-up condition and after the 40-hour period. Figure D27 shows the maximum output power as a function of time. It becomes necessary to increase the volume percentage of the Mo metal in order to keep the sheet resistance of the electrode down to an acceptable level. The goal is to obtain the highest amount of surface contact area between the BASE and the Mo metal. Two of the early electrodes (DTC-5-84 and DTC-6-84) were literally blown off the surface. The reason for this may be a combination of low porosity with low resistance. This can lead to an extremely high Na pressure between the BASE tube and the electrode. Other electrode compositions (using Cu and Ti) did not perform as well as expected, with neither electrode producing more than 0.17 W/cm^2 at 800°C. The first electrode, DTC-3-84, was a flame-sprayed beta/beta'' coating which was later impregnated with molybdenum using an ammonium dimolybdate solution. The entire tube system was subsequently reduced by heating in hydrogen. While the power output was low, the beta coating may not have been as porous as the later coatings made with the improved techniques. Similar types of electrodes will be attempted in the future.

There are two flame-sprayed cermet electrode concepts that should be pursued. In the first two continuous phases of Mo metal and beta'' are present throughout the electrode. In the second a fine grained high porosity beta'' structure is produced with a thin molybdenum film over the entire surface. The operation at high interfacial surface area, coupled with low current density, may yield a medium power long-life electrode.

Conclusion

The flame-spray process should continue to be developed because it appears to offer the capability for the deposition of both an oxide ceramic and an unoxidized metal at the same time. This would be an excellent process for manufacturing since the coating time for a single BASE tube may be less than 4 minutes. If durability of the current, modest power-level electrodes (initially approx. 0.5 W/cm^2) can be improved, this method will provide a means for achieving low-cost electrodes for the SHE. The possibilities for the fabrication of beta''-alumina articles of thin cross-section and/or unusual shape also appear to be worthy of further investigation.

TABLE D10 : Performance characteristics of flame-sprayed beta'' and beta''-alumina/metal cermet electrodes.

FLAME SPRAYED CERMET ELECTRODE SUMMARY

DTC #	By Volume Cermet Composition	Electrodes	4 Pt. Ress.	Initial Power w/cm^2	Power at Time(T)	Time (T) (hrs)	Temp. C^o
3-84	β + $(NH_3)_4$ Mo_2 O_7[1]	Moly	2.43	.12	.02	300	800
5-84	50% β + 50% Moly[2]	Moly	.133	---	---	---	---
6-84	85% β + 15% Moly[2]	Moly	2.45	---	---	---	---
7-84	75% β + 25% Moly[2]	Moly	1.68 2.50	.188 .45	--- .035	--- 90	800 900
8-84	75% β + 25% Moly[3]	Moly	9.67	.123	.120	288	800
9-84	75% β + 25% Moly as $(NH_3)_4$ Mo_2 O_7	Moly	.29	.152	.024	162	800
10-84	75% β + 25% Moly	Moly	.29	.208	.208	24	800
11-84	65% β + 35% Moly	Moly	.56	.54	.08	90	900
12-84	70% β + 15% Mo + 15% Cu	Copper/Moly	1.43	.175	---	---	800
13-84	55% β + 45% Moly	Copper/Moly	1.24	.315	---	---	900
23-84	55% β + 45% Moly	Copper/Moly	.35 .65	.57 .48	.269 ---	40 ---	900 917
1-85	30% Mo + 50% β + 10% Ti	Copper/Moly	.42 1.49	.08 .066	.032 .020	20	850 848
5-85	50% Mo - 50% β (vol) (1-5μ Moly Powder)	Copper/Moly Copper(13 wire) Nichel(12 wire)	1.72 --- ---	.21 .25 .152	.16 .108 ---	134 134	850 852 842

1 Solution impregnated.

2 -200 mesh (74m) Moly powder

3 -325 mesh (44m) Moly powder

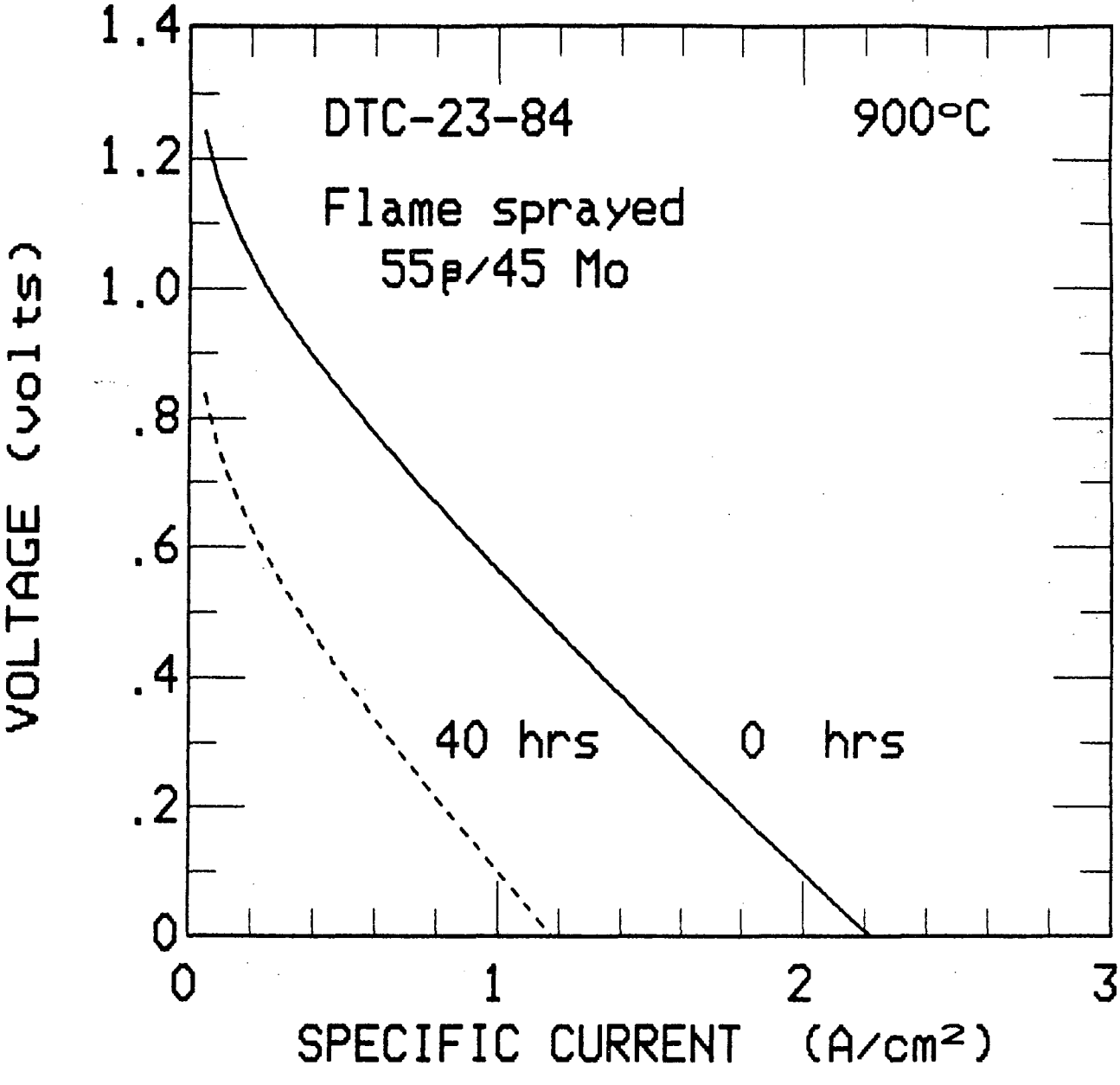

D26. Current-voltage data for a flame-sprayed cermet electrode having a composition of 55 volume percent BASE and 45 volume percent molybdenum.

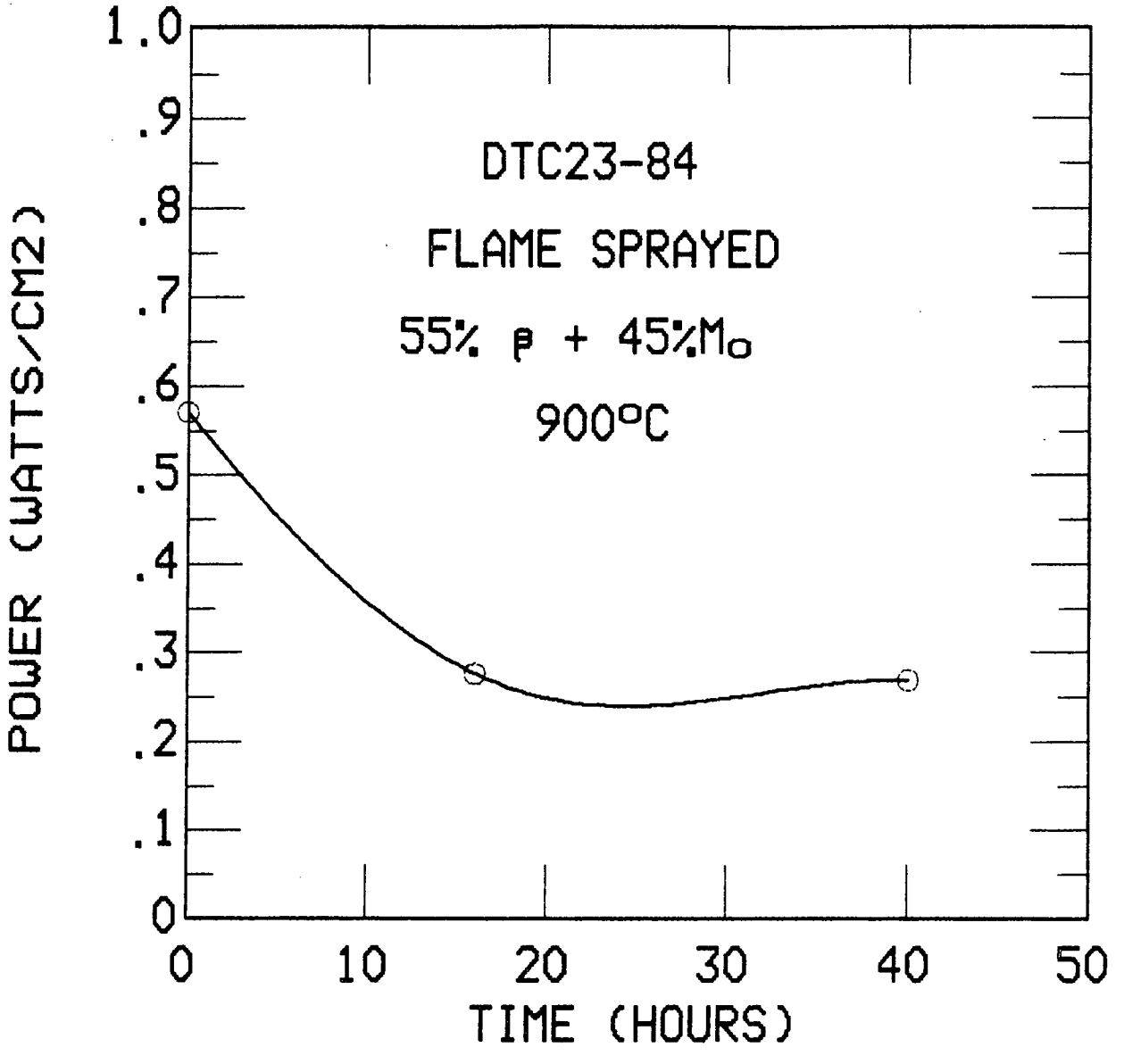

D27. Maximum power vs. time for flame sprayed cermet electrode.

References

1. N. Weber, 'A Thermoelectric Device Based on Beta-Alumina Solid Electrolyte', Energy Conversion, 14, 1 (1974).

2. T.K. Hunt, N. Weber and T. Cole, Proceedings of the 10th Intersociety Energy Conversion Engineering Conference, Part II, p.231 (1975).

3. T.K. Hunt, N. Weber and T. Cole, 13th Intersociety Energy Conversion Engineering Conference, p. 2011, (1978).

4. T.K. Hunt and N. Weber, 30th Power Sources Symposium, p.241 (1982).

5. T.K. Hunt and N. Weber, Proceedings of the SERI Workshop on Thermally Regenerative Electrochemical Systems, Alexandria, VA 1981., p. 143.

6. George A. Tsigdinos, Fred W. Moore, 'Simple Molybdates of the Elements', Climax Molybdenum Co. Division of AMAX Inc., Ann Arbor, MI.

7. I.O. Ermilora, E.K. Kazenas and G.N. Zviadadze, Zh. Fiz. Khim., 50, 2172 (1976).

8. J.W. Kissel, W.A. Glaesev and C.M. Allen, Wear, 5, 446 (1962).

9. T.A. Bither, J.L. Gillson and H.S. Young, Inorg. Chem., 15, 1559 (1966).

10. A. Wold, W. Kunnmann, R.J. Arnott and A. Ferreti, Inorg. Chem., 3 545 (1964).

11. N.C. Stephenson, Acta. Cryst., 20, 59 (1966).

12. H. Kessler, A. Hatterer and C. Ringenbach, Proc. International Conference of Liquid Alkali Metals, Mary Monroe Ed., Brit. Nucl. Eng. Soc., London, England (1973).

13. D. H. Hubert, Comptes Rendus Acad. Sci., 262, 1189 (1966).

14. U.V. Choudary, K.A. Gingerich and J.E. Kingcade, J. Less Common Metals, 42, 111 (1975).

15. Phase Diagrams for Ceramists, E.M. Levin et al Eds., American Ceramic Society, Columbus, Ohio (1964), Figs 4291 and 2288.

16. Jean-Maurice Réau, Claude Fuassier and Paul Hagenmuller, J. of Solid State Chem., 1, 326 (1970).

17. D.G. Dickens and P.J. Wiseman, 'Oxide Bronzes and Related Phases', Vol.10 Solid State Chemistry, L.E.J. Roberts Ed., Inorganic Chemistry Series Two, International Review of Science, University Park Press (1975).

18. F.A. Elrefaie and W.W. Smeltzer, J. Electrochem. Soc., 128, 1443 (1981).

19. Alain Debreuil, Martin Malenfant and A.D. Pelton, J. Electrochem. Soc., 128, 2006 (1981).

20. T.K. Hunt and N. Weber, 'Research and Development on a Sodium Heat Engine' Final Report DOE Contract No. DE-AC02-79ER10347, (1982).

21. K.T. Jacob, Journal Appl. Electrochem., 13, 469-72 (1983).

22. T. Miura and Yutaka Tuzi, Proc. 2nd Int. Conf Solid Surfaces (1974), p. 85, Edited by Hiroo Kumagai and Tomiyuki Toya, Japanese Jour. Appl. Phys.

23. George J. Janz, Molten Salt Handbook, Academic Press, New York, NY p.42 (1967)

E. STABILITY OF BETA''-ALUMINA AT HIGH TEMPERATURES

The long term chemical and mechanical stability of the solid electrolytes, beta and beta''-alumina, in contact with potentially reactive elements and compounds is an important issue in the design and operation of energy storage and conversion devices based on these materials. A number of possible interactions related to the materials used in the Sodium Heat Engine have been studied and the results are discussed in this chapter.

In the operation of the Sodium Heat Engine [1,2], these beta-alumina solid electrolytes (BASE), in the form of dense ceramics (conveniently in the form of closed end tubes), are operated in contact with liquid sodium on one side and a solid or molten salt electrode on the other side, at temperatures up to 900°C. The criteria for choosing the electrode material are several. Low vapor pressure, high electronic conductivity, and permeability to sodium at low activity are essential characteristics. Other properties to be considered are chemical reactivity to sodium and the electrolyte, resistance to densification and cost.

In work more specifically directed toward SHE development, we have investigated the interaction of sodium with beta''-alumina and mixed beta/beta''- alumina ceramics at temperatures up to 900°C. Electrodes based on molybdenum and other refractory base metals have been tested, and our observations relating to the interaction of the ceramic electrolytes with certain of these electrode materials are also included in this section.

Chemical Considerations

Two representative chemical reactions of basic concern in these studies may be written

$$Na + (2/3(X-1))Na_2O \cdot XAl_2O_3 \rightarrow ((3X+1)/3(X-1))NaAlO_2 + 1/3\ Al \quad (1)$$

$$(1/y)M + Na_2O \cdot XAl_2O_3 \rightarrow (1/y)MO_y + XAl_2O_3 + 2Na\ . \quad (2)$$

Reaction (1) is the sodium reduction of beta-alumina to sodium aluminate and aluminum. Reaction (2) describes the dealkalization of beta-alumina by an electrode metal that forms an oxide or more simply by vaporization of the soda component from the ceramic at high temperatures. An indication as to whether or not these reactions will proceed, especially at temperatures above 1000°K where reaction rates may not be insignificant, may be obtained from an estimate of their equilibrium constants. If one knows the Na_2O activities over the two-phase equilibria β-$NaAlO_2$ and β-Al_2O_3, then by assuming that in subsequent equilibria all of these oxides can be described as compounds only of Na_2O and Al_2O_3, one can calculate the constants sought. No direct measurements of Na_2O activity over the β-$NaAlO_2$ equilibrium are available. There have been several measurements of soda activity for the β-α-Al_2O_3 system reported in the literature, most recently those by Elrefaie and Smeltzer[3] and Dubreuil, Malenfant and Pelton[4]. By combining their values with those obtained from a study[5] of the cell

$$\text{air(Pt)} \mid \alpha \text{ and } \beta \mid \beta \mid \beta \text{ and } NaAlO_2 \mid \text{(Pt)air},$$

the Na_2O activity a, for the β-$NaAlO_2$ equilibrium can be calculated from the expression

$$\ln(a)_{(Na_2O,\beta\text{-}NaAlO_2)} = RT\ln(a)_{(Na_2O,\beta\text{-}\alpha\text{-}Al_2O_3)} + 2FV/RT ,$$

where V is the voltage of the cell referred to above. Reaction (1) is appropriately characterized by the free energy change ΔG, and reaction (2) by the voltage between the electrode metal and liquid sodium. Under certain circumstances the alumina produced in reaction (2) may have thermochemical properties more nearly like those of γ-Al_2O_3 than α-Al_2O_3. Most of the BASE ceramics are made slightly soda-rich (to promote liquid phase sintering) and should not have nuclei of α-Al_2O_3 present. Because the data of Refs. 3 and 4 were taken with respect to α-Al_2O_3, the calculation of the cell voltage requires a value for the stoichiometric number X only for the γ-Al_2O_3 case. Thus we find

$$\Delta G_1 = (2/3)\Delta G_f^\circ(Na_2O) - (1/3)\Delta G_f^\circ(NaAlO_2) + 4/3FV + (2/3)RT \ln(a)_{(Na_2O,\beta\text{-}\alpha)} - \Delta G_f^\circ(Na_{liq}) \qquad (3)$$

$$V_1 = (F/2)[-\Delta G_f^\circ(Na_2O) + (1/y)\Delta G(MO_y) - RT \ln(a)_{(Na_2O,\beta\text{-}\alpha)} - X[\Delta G_f^\circ(\alpha) - \Delta G_f^\circ(\gamma)] + 2\Delta G(Na_{liq})] . \qquad (4)$$

Calculated values of V and ΔG for X = 8 are plotted vs. temperature in Figure E1. It appears from this estimate that beta-alumina is weakly unstable in liquid sodium below about $1200^\circ K \pm 200^\circ K$.

Ceramic Characteristics

Selected properties of the two ceramics studied are listed in Table E1. Sample tubes were chosen from the same lot as those used for a previous study of electrical conductivity.[7]

TABLE E1

Sample Type	A	B
Composition (wt %)		
Na_2O	8.89	8.0
Li_2O	0.75	0.0
MgO	0.0	2.0
Al_2O_3	90.4	90.0
Phase	β''	0.6β - 0.4β''
Density	3.22	3.267
Grain Size	~10μ	1-2μ
Source	Ceramatec Inc.[8]	Chloride Silent Power[9]

Ceramic Interaction with Electrodes

There are a number of chemical interactions which may disturb the performance of the interfaces between the electrolyte and its electrodes. Reaction of electrode materials such as molybdenum, tungsten etc. with the oxygen in the beta-alumina may denature the electrolyte, resulting in a thin, partially insulating layer having a weakened physical contact with the solid electrodes.

Experience With SHE Cells

Above 500°C, and when the sodium pressure at the condenser is not voltage controlling, the open circuit voltage of a SHE cell with a molybdenum electrode is always several tenths of a volt below the calculated curve in Figure E1 e.g. 1.5 volts at 900°C. If reaction (2) was voltage determining, the sodium flux to the condenser would require the electrode (1-3 μ thick) to be converted to an oxide within a few hours. This is not observed. We believe that the lower voltage is a manifestation of a small electronic conductivity in the ceramic[1]. Additional evidence to support this interpretation is found in the observation that the volume of sodium in sealed SHE cells left at open circuit at 900°C decreases by several cm^3 per week. One may ask if reaction (2) can be forced. The application to the electrode of a positive voltage, above the decomposition potential of beta-alumina, might be expected to result in a permanent increase in the cell impedance. Our experiments show no such increase after the application of voltages up to 6 volts for several hours at temperatures up to 900°C.

Reaction with Carbon

In a further study of possible dealkalyzation reactions, sintered ceramic discs of type A were coated with several varieties of carbon - graphite and polymers that carbonize on heating in vacuum. These were heated for 24 hrs at 850°C in vacuum and then for a short time in air to burn off the carbon film.

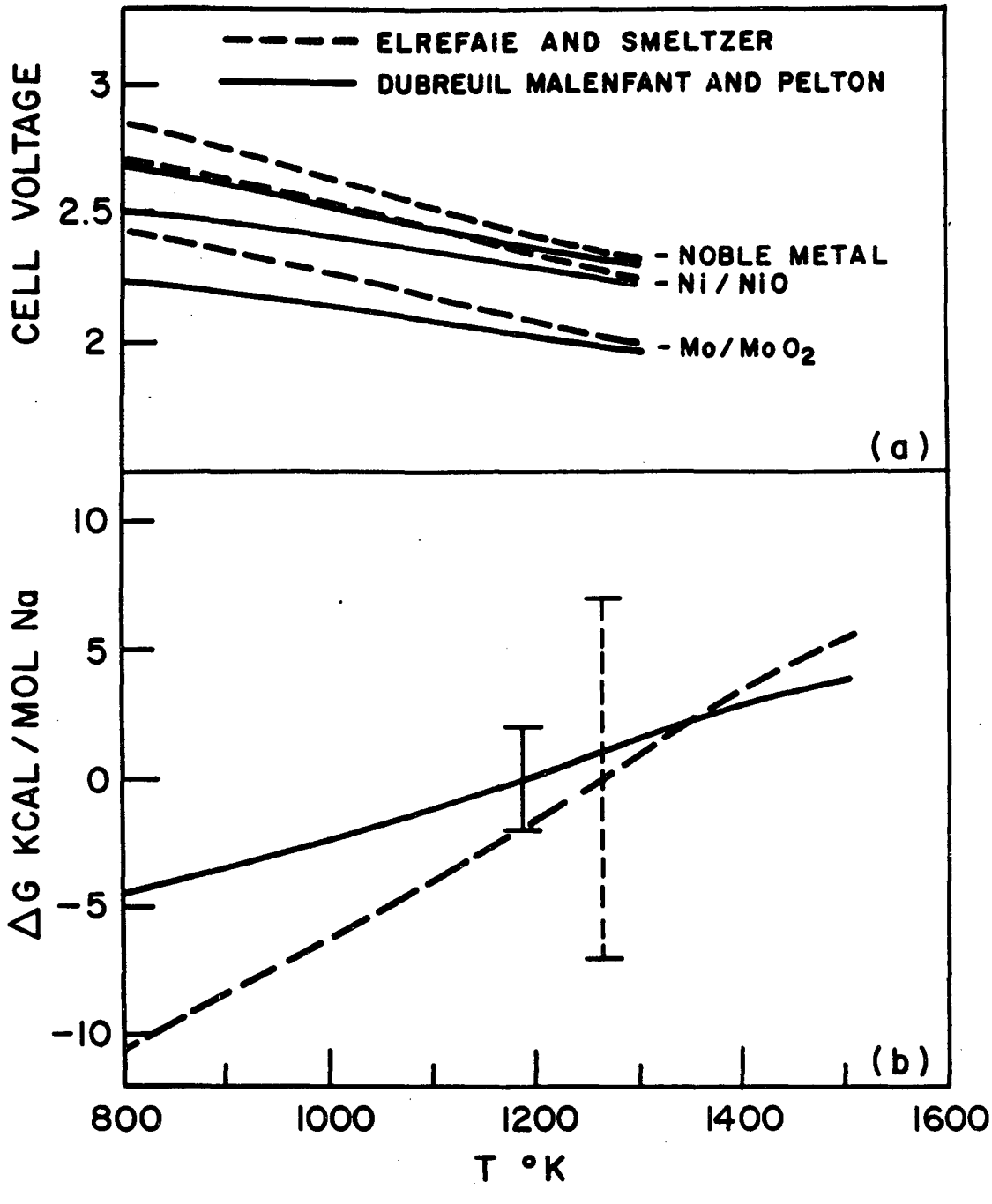

E1. a) Calculated voltage between electrodes on beta-alumina and liquid sodium vs. temperature. b) Calculated ΔG of reaction (1) vs. temperature.

The room-temperature resistances were measured before and after treatment by a simple technique employing filter pads soaked in NaOH solution to make contact between Ag - Ag_2O electrodes and the ceramic disk. Hydration of the samples caused the resistance to increase slowly with time, but extrapolation to an initial value was easily made. No significant increase in resistance was found as a result of the carbon treatment. We must conclude that any reaction layer was very thin or quite permeable to aqueous solutions.

Ceramic Interaction with Sodium

Coloration by Sodium

Sample History : The coloration of BASE ceramics by exposure to sodium is well-known. We have studied this phenomenon by experiments on a type B tube used in a SHE cell on test for 1000 hours. In this particular test, a linear temperature gradient (in order to protect the seal) was established along the tube axis between isothermal regions maintained betwen 900° and 200°C by internal heaters. The tube was filled with liquid sodium and the outside surface, coated with a Mo electrode only in the 900°C region, was exposed to an evacuated space in equilibrium with liquid sodium at 200°C. The tube was cooled rapidly from the test temperature and then sectioned with a diamond wafering saw lubricated with kerosene. A thin section cut parallel to the tube axis exposed the wall in the gradient section, and the remaining piece was cut normal to the tube axis into ring sections of uniform length of 1.6 mm. The wall sections, on inspection, revealed a gray-black coloration darkest at the inner (sodium) surface and fading toward the outer (vacuum) surface. The apparent depth of color penetration into the wall increased with exposure temperature. Microscopic inspection revealed no evidence of chemical attack at the interior surface, or any unusual phases in the darkened regions.

Samples of type A were taken from isothermal cells held at 700°C (160 hrs), 800°C (1500 hrs) and 900°C (150 hrs). In every case the entire tube exterior was coated with a molybdenum electrode and exposed to sodium vapor in equilibrium with liquid at 200°C. The observed coloration in these samples was much less intense than in samples of type B. It was also noted that the interior tube walls, after extended contact with liquid sodium at temperatures above 700°C, were not wet by sodium near the melting point upon subsequent examination in an inert atmosphere.

Proceedures and Results : A number of analyses were performed on the type B samples to determine the nature of the coloration. Rings from the gradient section were placed in an alumina tube and baked in a 10^{-6} torr vacuum at 1000°C for 24 hours. On the inside of the tube, in a cooler region outside the furnace, a silvery metallic band was deposited which readily dissolved in water to make an alkaline solution. The baked rings appeared as white as the virgin ceramic stock. The samples were also weighed on a torsion microbalance before and after heating. Upon baking, the exposed samples suffered a net weight loss with respect to the control samples, as shown in Figure E2. Both baked and non-baked sample sets were immersed in $AgNO_3$ at 350°C for 48 hours to convert any neutral sodium component to silver by chemical reduction. The weight gains for the two sets are shown in Figure E3. The baked set was slightly darkened by this procedure but to a lesser degree than the non-baked set. Exchangeable silver was replaced by sodium in both

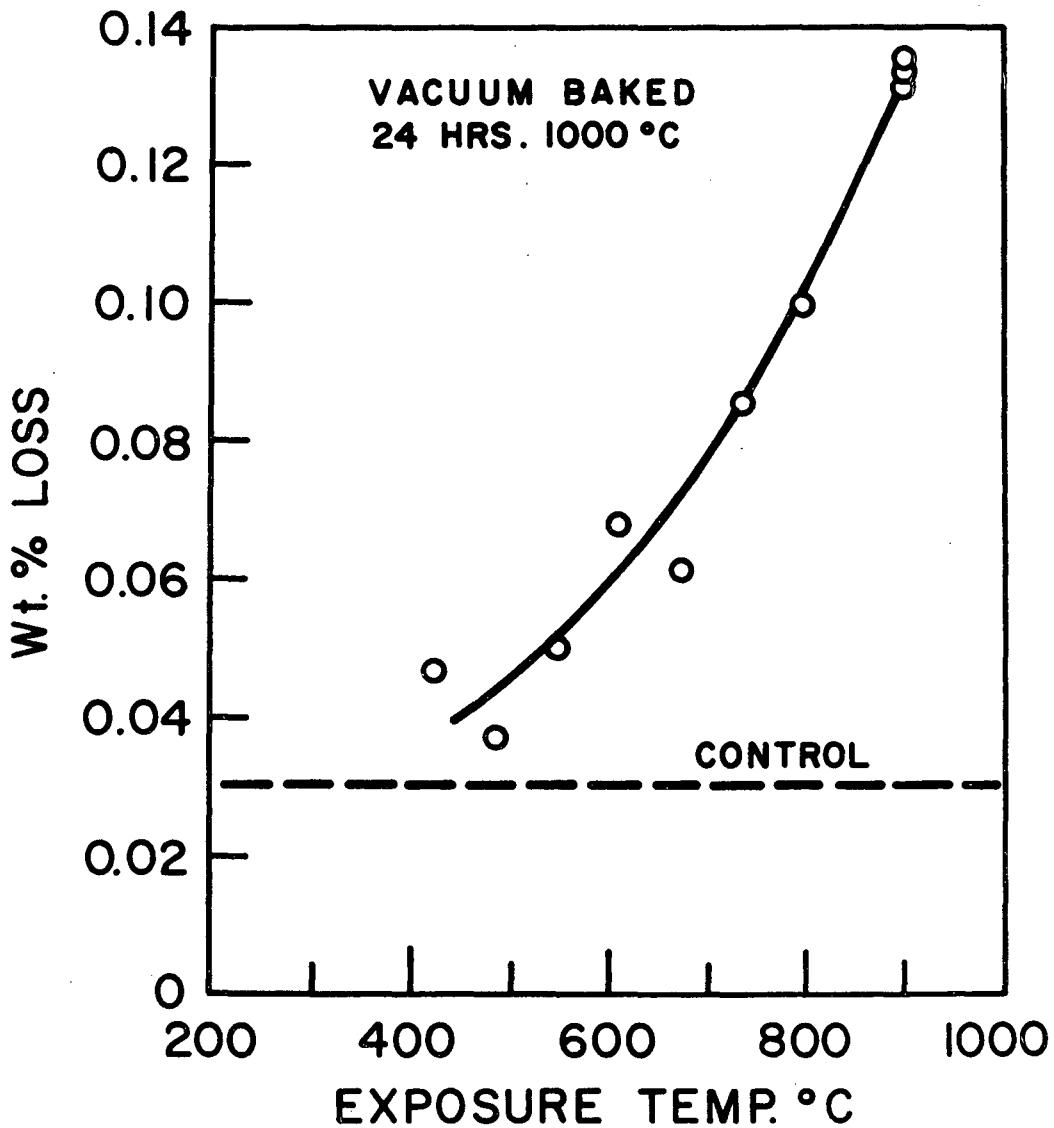

E2. Weight loss of sodium exposed and not exposed control samples vs. exposure temperature.

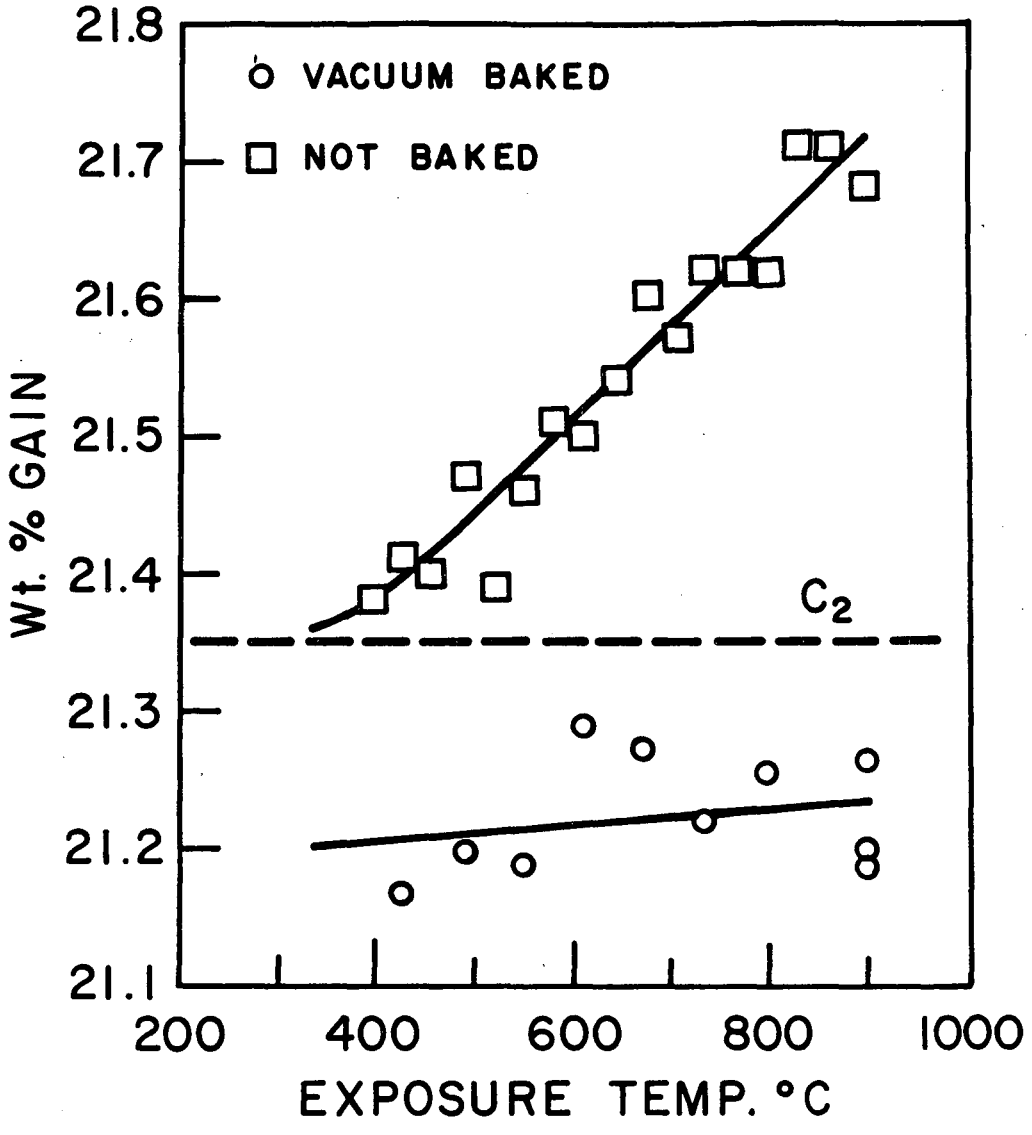

E3. Weight gain of sodium exposed samples after ion exchange in molten silver nitrate vs. exposure temperature.

sets by means of two successive 48-hour immersions in $NaNO_3$ saturated with NaCl at 350°C. The weight gains relative to the weights before silver exchange are shown in Figure E4. Also shown are the changes in the final sample weights when the double ion-exchange was carried out a second time on the non-baked set. The average loss, 0.03%, which is believed to result from mechanical attrition, was used to establish the net weight gain. A similar control procedure was not performed on the baked set. The double ion-exchange samples from both the gradient and the 900°C sections were analyzed for silver by electron micro- probe. The silver concentration profiles are shown in Figure E5. Within the resolution of the fully focussed beam (~ 5 μm) no large deviations from the average local silver concentration were found. In Figure E6 are compared the section-average concentrations of the neutral sodium component C_1 calculated using the four data sets and the formulae in Table E2. These expressions apply when the ion of the neutral sodium has mobility in the conducting planes and when only sodium and sodium oxide are expelled by the vacuum baking.

Thinned ring sections of non-exchanged material, wetted with a liquid of matching refractive index, were scanned with an optical microdensitometer. The excess optical density is compared with the microprobe results in Fig. E5, normalizing at the wall concentrations. The excess optical density of the double exchange samples (not shown) was three times larger at the inside wall, and it varied linearly across the section.

TABLE E2

Procedure	Sample	Measured	Calculated
Vacuum Bake	Control	Wt.% loss, P_o	$C_o=P_o/100(M_{Na_2O})$
''	Exposed	Wt.% loss, P_1	$C_1=(P_1-P_0)/100(M_{Na})$
$AgNO_3$ Exchange	Unexposed Non-Baked	Wt.% gain, P_2	$C_2=P_2/100(M_{Ag}-M_{Na})$
''	Exposed Non-Baked	Wt.% gain, P_3	$C_1=(P_3-P_2)/100(M_{Ag}-M_{Na})$
''	Exposed Baked	Wt.% gain, P_4	$P_4=(C_2-2C_o)(M_{Ag}-M_{Na})100/[1-C_1M_{Na}+C_oM_{Na_2O}]$
Double Exchange	Exposed Baked	Net Wt.% Gain, P_5	$C_1=P_5/100(M_{Ag}-M_{Na})$
Electron MicroProbe	Exposed Double Exchange	Av.Wt.% Ag, P_6	$C_1=P_6/[100M_{Ag}-P_6(M_{Ag}-M_{Na}]$

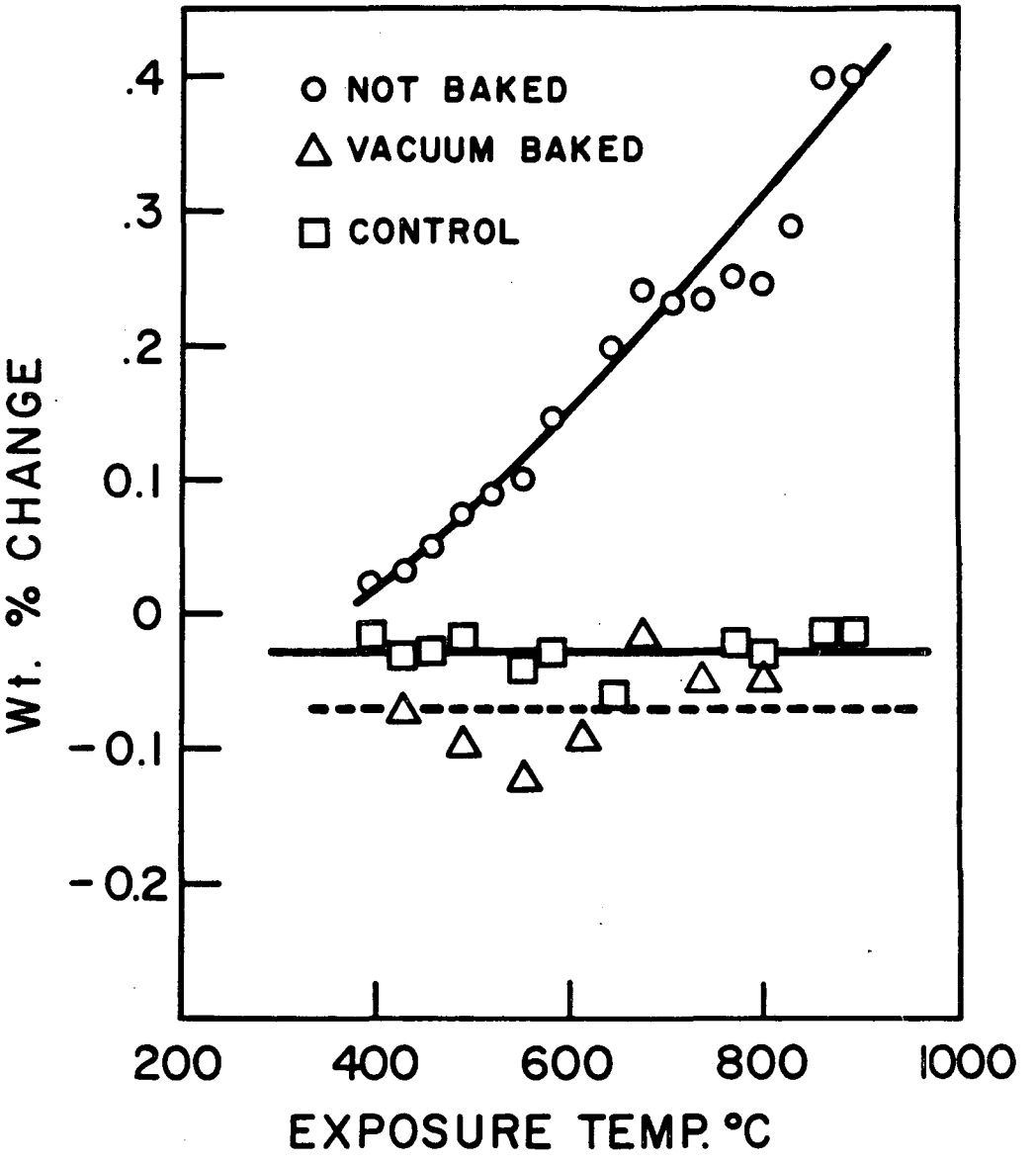

E4. Weight change of three sample sets after double ion exchange vs. exposure temperature.

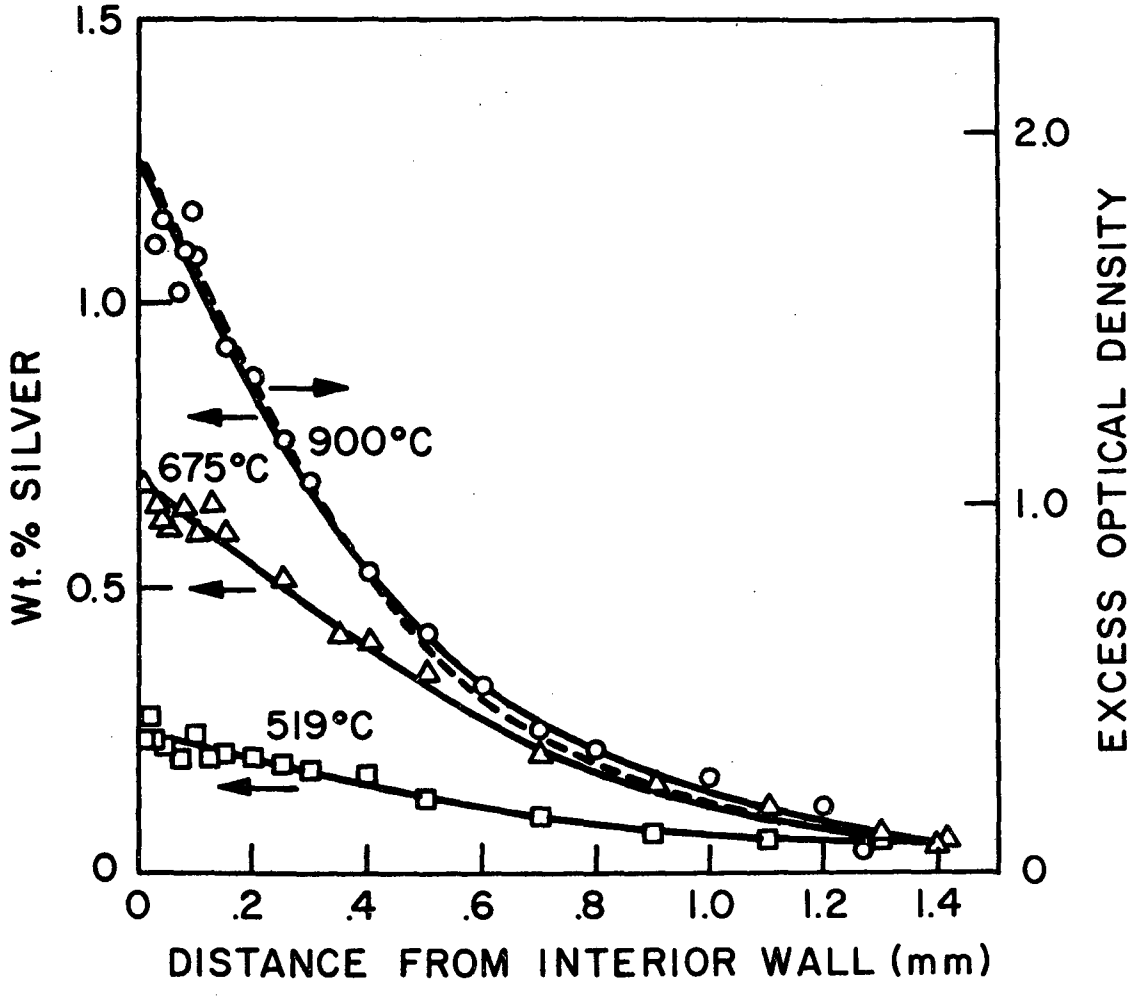

E5. Silver concentration by electron micro-probe and optical density of double exchanged samples vs. distance from the interior wall.

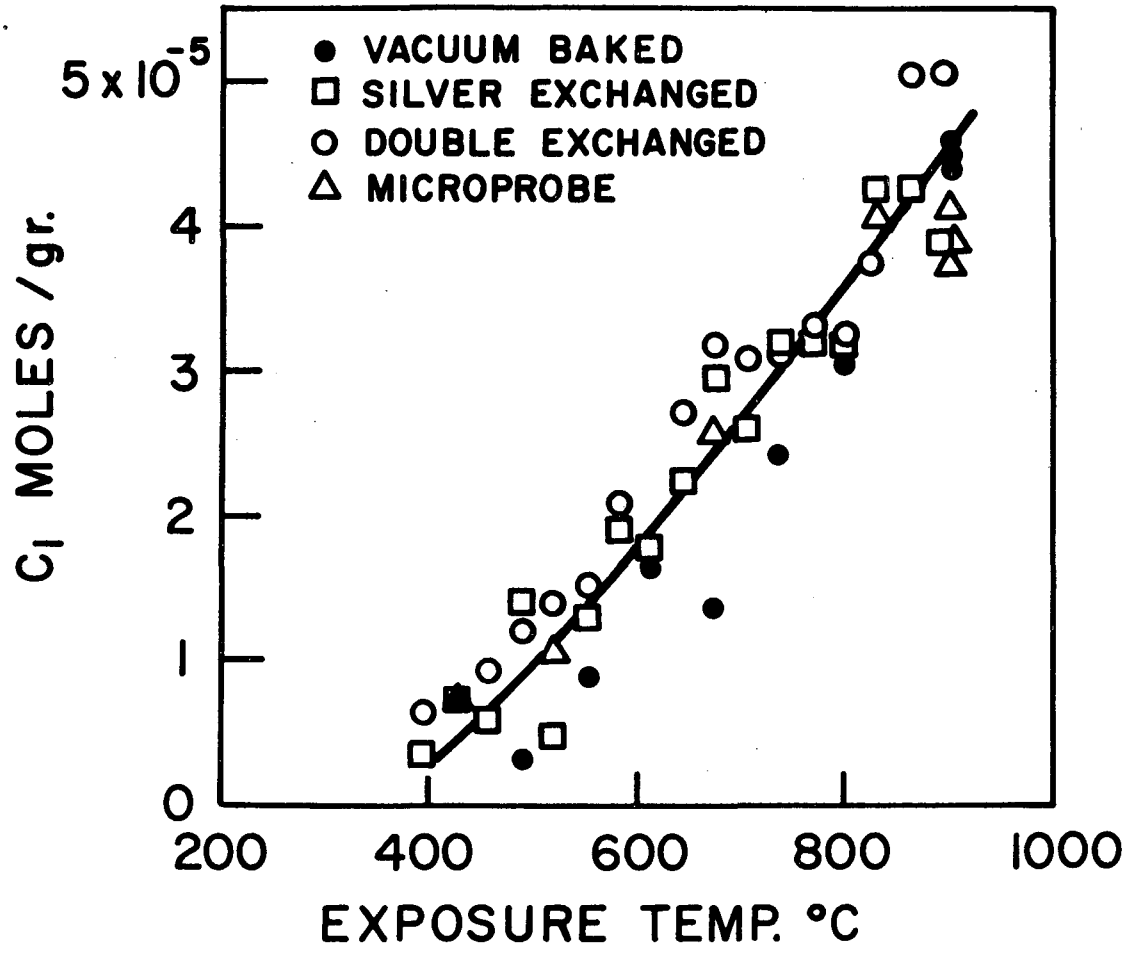

E6. The section-average neutral sodium concentration C_1, as calculated from four data sets by the formulae in Table E2 vs. exposure temperature.

X-ray diffraction analysis of material taken from the surfaces of a 900°C specimen indicated an increase of 0.07 % in the c-axis lattice parameter of the beta'' component at the inner wall relative to that at the outer wall. A sample exposed at 900°C was pulverized and examined by electron spin resonance (ESR) at room temperature. A broad signal with a g-factor near 2.0 was detected with a source concentration of 10^{18} spins/gram.

Sections from type A samples were also double ion exchanged and analyzed by electron microprobe. The concentrations of silver found in the 900°C sample are nearly coincident with the 519°C curve for the B sample in Fig. E5. In the 700° and 800° samples, the measured concentrations were very small (less than 0.2 wt %), and no systematic gradient could be inferred from them though such was evident visually.

Evidence From SHE Cell Tests

Operation of these ceramic electrolytes in SHE systems has generally revealed a step increase in cell impedance occurring on a time scale of 5 to 25 hours at temperatures above 800°C. This impedance step may be due to an increase in membrane resistivity, to an increase in charge transfer impedance or to permeability changes in the electrode leading to a sodium 'back pressure'. If chemical changes associated with the observed darkening cause an increase in the membrane resistivity, it is important to know whether it results primarily from effects in the bulk of the ceramic or at the sodium interface.

Cells which have suffered the step increase in impedance have had their electrodes removed and replaced numerous times. Old tubes with newly deposited electrodes exhibit initial cell performance that is essentially equivalent to that for cells with virgin electrolyte. This repeated restoration of initial cell performance implies that no permanent damage has been done either to the bulk of the electrolyte or to the BASE - sodium interface as a result of high-temperature testing. The initial cell performance is at a level approaching the theoretical limits (of order 1 watt/cm^2 at 900°C, interfacial resistance < 0.03 ohm cm^2).

One SHE cell test strongly points to a reaction of type A BASE with sodium in the vicinity of the positive electrode-electrolyte interface. With the object of defining the chemical state of an electrode, a SHE cell with an Mo electrode at 3 volts positive bias, was heated in 1 atm of hydrogen. These measures were intended to eliminate the possibility of mutual reaction between a sodium flux due to electronic conductivity, water flux desorbing from the ceramic during initial heating and the metal electrode. After 24 hrs at 900°C the bias was removed, the hydrogen pumped off, and the cell was loaded to short circuit. The electrode was found to be in the high impedance state. (With the cell at short circuit the sodium activity at the electrode is only slightly less than unity and this occurred at low currents such that the voltage drop across the electrolyte was small. Thus the major portion of the voltage drop occured at the electrode.) The electrode was subsequently lifted from the tube by pulling a fine mesh screen epoxied to the surface only within the perimeter of the electrode. The under surface of the electrode was then examined by SEM. Elemental analysis identified aluminum and molybdenum as major constituents, and x-ray diffraction analysis revealed a major amount of a

phase indexed as $MoAl_3$. The molybdenum electrode had been prepared by CVD from molybdenum hexacarbonyl, but under conditions explicitly chosen to minimize carbon content. Very small amounts of Mo_2C were found.

Non-SHE Cell Tests

Sodium aluminate has been observed on the interior surface of some BASE tubes tested in the normal SHE operating mode. This can occur either by the path indicated in Eq. 1 or by direct reaction with sodium oxide. The latter reaction is not expected to raise problems for operational SHE systems which should have only very small amounts of oxygen contamination. The possibility of sodium reaction with beta''-alumina has been examined experimentally by looking for the products of the possible reactions.

In these experiments a piece of high-purity copper foil was hermetically sealed inside a BASE tube filled with sodium. The BASE tube was supported and electrically isolated within a stainless steel bomb by three alpha-alumina ceramic insulators. The bomb was then heated and maintained at 800°C in a furnace for a period of 300 hours. In the event that the Na-β-alumina reaction occurs, the copper should act as a getter for the free aluminum reaction product, and X-ray analysis should then reveal its presence. The BASE tube was sealed by vacuum brazing a molybdenum cap holding the fill line to the open end using active-metal brazing filler material. In the first attempt a stainless steel bomb closed with copper-gasketed vacuum flanges was used. These leaked after prolonged high-temperature exposure and permitted oxygen entry to the test cell. The analysis performed following the heating cycle showed significant amounts of aluminum in the copper. The unintended presence of oxygen allowed for the generation of free aluminum by the reaction of sodium with the sodium aluminate; this confused the interpretation of the results. The experiment was therefore repeated with the bomb carefully welded shut, and the final closure made in a high-purity argon atmosphere to prevent oxygen contamination which could again raise the possibility of the Na_2O - β-alumina reaction.

Following the 300 hour heating period, the bomb and tube were opened, and the sodium was removed by reacting it with methanol. Substantial recrystallization of the OFHC copper was observed, but X-ray fluorescence analysis found no concentrations of aluminum above the background level present in a copper control sample. The sample was then sectioned and the edge profile examined using the electron microprobe system. No aluminum above the 0.05 wt percent level was detected. Within the limits imposed by the analysis there appears to be no evidence for the occurrence of the reaction given by Eq. 1. The sensitivity of this experiment could be improved by using a high-surface-area beta''-alumina powder. Such efforts may be warranted if other evidence for any of these decomposition reactions arises in SHE cell testing.

Discussion

Armstrong[10] has found no indication of substantial electrochemical breakdown of BASE at room temperature, even at positive potentials up to 11 volts, although a decomposition potential of 3 - 4 volts might be expected. We find no effect of decomposition on charge transfer at voltages up to 6 volts even at 900°C.

The results shown in Figs. E2-E6 strongly suggest that type B ceramic absorbs sodium at high temperature. That the metal component is responsible for the darkening may be inferred from the near coincidence of the optical density and silver concentration curves.

The concentration of unpaired electrons observed by ESR in the 900°C sample is a factor of 27 times lower than the neutral sodium concentrations obtained by gravimetric and electron microprobe analyses. This disparity could result from recombination in a homogeneous distribution of electrons and ions on cooling, but it could also imply that a large fraction of the neutral sodium was concentrated in pores. Measurements of the density of type B BASE allow for a pore-fraction less than 0.01%, a level which could just accommodate the neutral sodium observed. However, the absence of large excursions of the silver concentration in the microprobe scans and the observed non-wetting of type A BASE weigh strongly against this possibility.

In one model for the darkening process, absorption of both sodium ions and electrons into the conducting planes occurs at a rate governed by the diffusivity of electrons. The possible sites for electrons in these planes have been identified from ENDOR measurements of defects in X-irradiated sodium beta-alumina[11]. According to this model, there should be a quantitative relation between the temperature dependences of electronic conductivity, defect concentration, and coloration rates. Because of the very low mobility of sodium ions in the 'spinel' blocks of these crystals, and the requirement of local electroneutrality, this model also predicts a large anisotropy in the coloration rates.

A new mechanism to account for the propagation of color into beta- and beta''-alumina ceramics and crystals has been proposed in a recent article by De Jonghe and Beuchele[12]. They reject the sodium absorption model after finding approximately isotropic coloration at 250 - 400°C in single crystals, and they obtained poor agreement between the coloration rates and an activation energy for silver-substituted beta-alumina. They propose that the color center is an oxygen vacancy compensated by two electrons, and induced by sodium reduction of the BASE surface. Sodium oxide would be produced and the oxygen vacancies would diffuse rapidly through the 'spinel' blocks to account for the distribution of coloration. It would appear however that the presence of a major contribution from the De Jonghe-Beuchele model requires that the initial weight gain of silver-exchanged samples must be nearly independent of their oxygen vacancy concentration (color intensity), since the abstraction of neutral oxygen from the blocks should not affect the concentration of the sodium ions for which the silver substitutes. This is substantially at odds with the data shown in Fig. E3.

The concentration profiles in Fig. E4 are, in spite of their curvature, believed to represent the defect equilibrium state, at least above 500°C. The characteristic diffusion times for a sample of size h should be of order h^2/D, where D is the defect diffusivity. We have obtained estimates of D by correlating the concentrations observed in the present study with the electronic conductivities of beta''-alumina ceramic measured previously[1]. The

1000-hour test duration is to be compared to the characteristic diffusion times ranging from 0.1 hours at 900°C to 18 hours at 500°C. The non-linearity of the concentration curves is ascribed to a non-ideality in the defect solution, analogous to that in aqueous electrolyte solutions.

The finding of $MoAl_3$ in the low carbon electrode of a SHE cell tested at 900°C implies a reduction of BASE type A by sodium. It would appear unlikely that this could happen by direct reaction with sodium in the brief time at short circuit, even if allowance is made for the additional energy conferred by the reaction between aluminum and the molybdenum of the electrode. A simpler explanation is found in the model of De Jonghe and Beuchele according to which the sodium activity gradient across the BASE gives rise to a flux of oxygen vacancies. Sodium oxide (or sodium aluminate) is formed at the liquid sodium interface, and aluminum and sodium are liberated at the electrode. The model can be extended to allow for the formation of oxygen vacancies by reaction with aluminum to form aluminum oxide. The aluminum activity in the electrode should rise, the gradient of oxygen vacancies across the BASE diminish, and an approach to a steady state governed by the rate of evaporation of aluminum from the electrode alloy should occur. In the light of our other observations, this explanation requires that the layer of sodium oxide or sodium aluminate, formed at the sodium interface, not contribute significantly to the membrane resistivity. By whichever mechanism the reduction proceeds, the extra driving force arises from the reaction of aluminum with molybdenum. For $MoAl_3$ as a product in reaction (1) $-\Delta G$ would be greater by an estimated 3.0 kcal.

References

1. N. Weber, 'A Thermoelectric Device Based on Beta-Alumina Solid Electrolyte' Energy Conversion, 14, 1 (1974).

2. T.K. Hunt and N. Weber, 'The Sodium Heat Engine: A New Approach to Direct Heat-to-Electricity Conversion', Energy Technology IX, 498 (1982).

3. F.A. Elrefaie and W.W. Smeltzer, 'The Stability of β-A1203 (Na20-11A1203) in Oxygen Atmospheres', J. Electrochem. Soc., 128, 1443 (1981).

4. Alain Dubreuil, Martin Malenfant and A.D. Pelton, 'Thermodynamic Stability of Beta-Alumina', J. Electrochem. Soc., 128, 2006 (1981).

5. J.T. Kummer, 'β-Alumina Electrolytes', Progress in Solid State Chemistry Vol. 7, p. 146 (edited by J.O. Mcaldin), Pergamon Press, N.Y. (1972).

6. Thermodynamic data was obtained from: Alvin Glassner, 'The Thermochemical Properties of the Oxides, Fluorides and hlorides to 2500°K', ANL report No.5750 (NiO) : D.R. Stull and H. Prophet et al. JANAF Thermochemical Tables, Second Edition NSRDS - NBS 37 (Al_2O_3, Na_2O, Na): Richard H. Schumm, 'Thermodynamic Properties of Solid Alkali-Aluminosilicates at Elevated Temperatures', Report 1981, NBSIR -81-2343 ($NaAlO_2$).

7. Terry Cole, Neill Weber and T.K. Hunt, 'Electrical Resistivity of Beta-Alumina Solid Electrolytes', Proceedings of the International Conf. on Fast Ion Transport in Solids, p. 277 (1979).

8. Ceramatec Inc., 163 West 1700 South, Salt Lake City, Utah 84115.

9. These samples were kindly provided by Dr. I. Wynn-Jones.

10. R.D. Armstrong, R.A. Burnham and P.M. Willis, 'The Breakdown of β-Alumina at Positive and Negative Potentials', J. Electroanal. Chem., 67, 111 (1976).

11. R. Barklie, J.R. Nicklas and J.M. Spaeth, 'ENDOR Measurements of Defects in Sodium β-Alumina I', J. Phys., 13, 1745 (1980).

12. L. C. De Jonghe and A. Beuchele, 'Chemical Colouration of Sodium Beta-Aluminas', J. Mat. Sci., 17, 885 (1982).

F. ELECTRODE PREPARATIONS BASED ON PHASE STUDIES IN THE SYSTEM Na_2O-Al_2O_3-MoO_x

These studies were undertaken in an attempt to find improved electrodes for SHE applications, making use of past experience with Mo film electrodes and recent phase studies in the system Na_2O-Al_2O_3-MoO_x. Based on observations of experimental SHE cells and on a review of the chemical literature, we have proposed that under certain conditions, the behavior of molybdenum electrodes is explained by the appearance and disappearance of a molten salt phase, essentially Na_2MoO_4 in the porous metal film electrodes. A bronze phase $Na_2Mo_3O_6$, which is known to be a good electronic conductor, may also play a role. There is some evidence that the degradation of film electrodes above about 800°C, i.e. loss of electrochemical performance, is accompanied by a loss of adhesion of the electrode to the ceramic electrolyte substrate. This correlation suggests that the loss of performance may result from a loss of physical contact or a partial separation of the electrode from the electrolyte. The fact that liquid metal (tin alloy) electrodes saturated with Mo do not degrade in the same manner is consistent with this postulate. The results of current interrupt experiments, however, when interpreted in terms of reasonable models for the electrical response of a cell, suggest that degradation occurs by a loss of neutral sodium permeability in the electrode, and not from impaired charge transfer processes at the interface as might be expected if physical separation of the two phases occurred.

Whatever the origin of the degradation, there is good reason to try an extended area or porous electrode. This is a standard recourse of electrochemists when faced with an electrode performance that is limited by charge or mass transfer. The precedent for this approach can be found in accounts of fuel-cell electrode development, especially those dealing with high-temperature cells using zirconia electrolyte.[1]

Certain general considerations will govern the design of a porous electrode for the SHE. What is wanted is a three phase structure, one phase is the pores, and a second the beta''-alumina, a unique electrolyte for this application. The third phase must be an electronic conductor, may be a mixed conductor and may be liquid or solid. It must be continuous, and it would seem desirable to have all three phases continuous and interpenetrating. Of the solid electronic conductors, Mo must be considered a prime candidate for the same reasons it was selected as a film electrode material, namely, inertness to sodium, low vapor pressure and appropriate thermal expansivity.

With a porous three-dimensional electrode, there will be trade-offs between the interfacial area and permeability so that in general there will be an optimum thickness for fixed values of the other variables. The sheet resistance is important and should be kept low, and in any case must be properly matched to the bus and current collection system. By comparison with a planar metal film electrode, a porous electrode may have a greater thermo-mechanical stability of the metal/ceramic interface by virtue of the inherent curvature at the phase boundary. In contemplating ways of making such an electrode, an important constraint is that it is difficult to co-sinter a mixture of base metal and beta''-alumina. At temperatures for which beta''-alumina sinters at reasonable rates ($T > 1560°C$), loss of soda and formation of alpha-alumina occurs at the low oxygen partial pressures needed to prevent

metal oxidation. If co-sintering is to be employed, it becomes necessary to find unconventional methods for achieving a sintered beta''-alumina structure at temperatures below 1200°C in reducing atmospheres. Alternatively a porous beta''-alumina layer or structure obtained by sintering above 1560°C could be impregnated with a metal in a separate process below 1200°C. Sintering of beta''-alumina at low temperatures is not trivial. In this connection Kummer has pointed out that oxide additives of calcium, sodium, and lanthanum are known to inhibit sintering and reduction in area of gamma-alumina catalyst supports. The fact that these oxides react with Al_2O_3 to form beta-alumina, or closely related structures, is suspiciously consistent with the weak tendency of beta-alumina to sinter. Liquid-phase sintering with fluxes based on NaF- $3AlF_3$ (cryolite) or B_2O_3 may be possible, but there is a danger of producing electrically resistive or sodium-reducible phases unless the flux is expelled or converted in some way after performing its function.

Other forms of Al_2O_3 such as the alpha-phase are more prone to sinter[2], and there is evidence that certain additives perform as sintering aids. For example, MoO_3 is a potent agent for loss of surface area in gamma-alumina substrates because it promotes the conversion to alpha-alumina at low temperatures. The formation and decomposition of $Al_2(MoO_4)_3$ was suggested as a possible mechanism. It has been observed that alpha-alumina reacts with $NaAlO_2$ or Na_2O vapor to form beta''-alumina beginning at about 1100°C.

Porous Electrode Preparations

1) Electrodes were prepared by spraying a milled acetone slurry of Mo or MoO_3, beta''-alumina and a small amount of NaCl-NaF in eutectic proportions (35 mol% NaF). The slurry was sprayed on a rotating beta''-alumina tube, and the coated tube was then heated at 800-1100°C in dry hydrogen. The halide eutectic was added as a flux to promote bonding of the beta''-alumina particles to each other and to the dense beta''-alumina substrate. The halides were expected to be lost eventually by volatilization. The proportions of Mo or MoO_3 and electrolyte were chosen to have metal and electrolyte volumes in the proportion 60/40. In some cases the formulations with MoO_3 were heated above 800°C in air to melt and distribute MoO_3 before reduction to Mo metal.

The electrodes prepared by this procedure performed quite well in DTCs (DTC-Z). At 900°C the maximum power deteriorated more slowly and reached an apparent asymptotic value of nearly 0.5 W/cm^2. The process control was not carefully worked out and there was significant variation of sheet resistance from one preparation to the next. The electrode coatings were also softer than desired and relatively susceptible to bruising in subsequent sealing and mounting operations. When the tubes that were to be coated were attached to a Mo thimble by an active metal braze, either Ti-Ni or Ti-Cu-Ni, flowing hydrogen could not be used below about 600-700°C without causing embrittlement and damage to the ceramic-metal seal.

Several sintering runs were made successfully using argon below 700°C and hydrogen at higher temperatures. Usually the tube was pre-wrapped with Mo wire (10 mil) for current collection, and frequently the 1/8 inch copper bus wires were also mounted on the molybdenum wire before spraying and heat treating. This was done to promote bonding of the electrode to the bus system and to minimize handling after applying the electrode coat.

Examination of a few electrodes by XRD revealed the presence of substantial amounts of alpha-alumina. It had been assumed that beta''-alumina is unreactive toward MoO_3 and to treatment in dry hydrogen at 800-1100°C. From later phase studies it was learned that MoO_3 and sodium molybdates, which are less basic than Na_2MoO_4, react readily with beta''-alumina at low temperatures to form alpha-alumina or the ternary compounds Na_2O-Al_2O_3-$4MoO_3$ and $5Na_2O$-Al_2O_3-$8MoO_3$. When these compositions are heated in a reducing atmosphere, the reverse reaction to reform beta''-alumina does not occur below 1200°C. This partly explains why alpha-alumina formed in some of these electrodes. The formation of alpha-alumina is also promoted by the use of dry rather than wet hydrogen in the reduction step.

The formation of alpha-alumina may not be totally undesireable since this phase should tend to inhibit sintering of the Mo phase, and thus perhaps reduce the potential loss of sodium permeability contributed by the mechanical impedance of the film.

2) Beta''-alumina powder prepared from Na_2CO_3, $LiNO_3$ and Linde C Al_2O_3 and reacted at 1200°C was sprayed as an acetone slurry on sintered beta''-alumina electrolyte tubes. After the methacrylate binder was burned off at 800°C in air, the tube was encapsulated in a platinum tube and pulled through a zone sintering furnace with a hot zone at 1580°C. This procedure resulted in a hard porous beta''-alumina layer 50-100 microns thick. These tubes were immersed in a saturated solution of ammonium dimolybdate. The vessel holding the solution was evacuated and then vented to the atmosphere in order to impregnate the pores with solution. The tube was next immersed in isopropanol to precipitate the molybdenum salt by solvent exchange, and then dried in a vacuum oven at 120°C. The metal deposit obtained by repeating the impregnation procedure three times, followed by reduction in hydrogen at 800°C, had acceptably low sheet resistance. Electrodes prepared in this way delivered good power when tested for several weeks in a recirculating cell at temperatures up to 900°C. Because the test cell had other, inherent power limitations, the full potential of the electrode could not be measured, but comparisons with previous electrodes were favorable. A test in a less limited cell was also very encouraging, but tests above 600°C were not possible.

This procedure appears to be useful, but requires firing tubes at 1580°C where encapsulation is required and warping of the substrate tubes is possible. It was observed that the ammonium dimolybdate solutions can age and lose concentration by precipitation. In one series of preparations it was noted that the porous electrode coating, after prolonged immersion in the aqueous solution, became soft and erodable. The degree to which $NH_4^+ - Na^+$ ion exchange takes place in the aqueous solution was not studied. The tendency of such exchange to occur ought to be suppressed by the addition of a sodium salt to the solution.

This impregnation procedure has also been used on porous beta''-alumina structures that are deposited by the flame-spraying of beta''-alumina powders using the methods described in section D. Plasma-spray coatings of beta''-alumina have also been described in the patent literature[3] but have not yet been tried by us.

3) The following method of fabricating a porous electrode is based partly on phase studies in the system Na_2O-Al_2O_3-MoO_x. The method makes use of the fact that, while the beta-aluminas are difficult to sinter below 1200°C, alpha-Al_2O_3 does sinter to some extent. In the system Na_2O-Al_2O_3- MoO_3 it is found that at 800°C, alpha-Al_2O_3 is in equilibrium with the liquid formed by additions of sodium molybdates to Al_2O_3. This is true for compositions ranging from MoO_3 to Na_2MoO_4. The liquid in equilibrium with alpha- and beta-alumina is close to Na_2MoO_4 as one might expect from the thermochemical properties of Na_2MoO_4 and $Na_2Mo_2O_7$. The results of this study of the phases of the system Na_2O-Al_2O_3-MoO_x are shown in the phase diagram in Figure 1.

If sodium molybdates are added to colloidal aluminas (eg. Degussa, Alon), and the mixture held at 800°C in air, the liquid phase (containing several mole % Al_2O_3) appears to promote sintering of the alumina particles to each other and to the beta''-alumina substrate. If the atmosphere is switched to wet hydrogen after firing in air, reduction of the molybdates proceeds. The Na_2O component is free to react with Al_2O_3, and after heating for several minutes at 1200°C the product is beta''-alumina and Mo metal. If the ratio Na_2O/Al_2O_3 exceeds that for beta''-alumina, $NaAlO_2$ can form. The vapor pressure of Na over $NaAlO_2$ and beta-alumina is about a factor of 10 greater than that over the beta-alpha equilibrium and so excess soda tends to be swept away in the gas phase. Indeed, even at 1200°C in wet hydrogen, beta- alumina will slowly lose Na_2O and firings at this temperature should be of short duration. Loss of Na_2O by firing in dry hydrogen, as was used previously, is very substantial at temperatures above 700°C.

The calculated sodium concentrations in the gas phase (equivalent pressure) as a function of the water/hydrogen ratio are presented in figure F2. The sheet resistance and other properties should be a function of the relative amounts of Mo and Al_2O_3. When the molybdate is Na_2O-$2MoO_3$ and the alumina is Degussa Alon, low sheet resistance electrodes are obtained by applying an acetone slurry of both the pure salt (no alumina) in the molar proportions Na_2O- $2MoO_3/0.86Al_2O_3$. The latter ratio corresponds to 1.6 cm^3 of beta-alumina per cm^3 of Mo.

The proportions of salt and alumina should be such that all of the alumina gets converted to beta''-alumina. The salt compositions Na_2O-$4MoO_3$, Na_2O- $3MoO_3$, Na_2-$2MoO_3$ and Na_2O-MoO_3 have all been tried in a limited number of experiments. With the exception of Na_2MoO_4, all of these salts react with beta''-alumina to form alpha-alumina at 800°C. This reaction may roughen or otherwise create a porous layer on the substrate electrolyte tube. Firing the electrode mixture in air for up to 1/2 hour appears to work. Longer times of over an hour with the pure salts gave unsatisfactory results. This may happen from loss of molten salt by draining or by volatilization. A poor electrode film was obtained with pure Na_2MoO_4 in one trial using conditions satisfactory for Na_2O-$2MoO_3$ and Na_2O-$4MoO_3$.

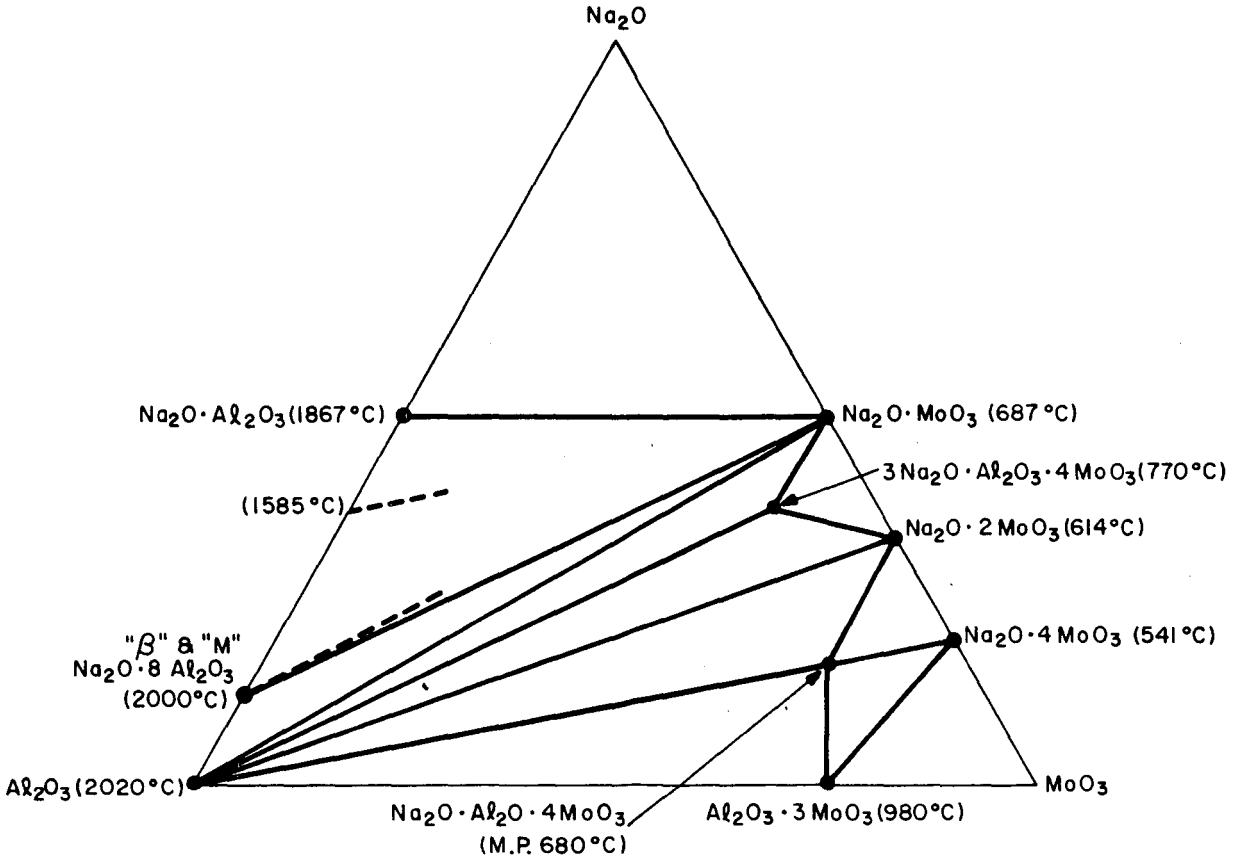

F1. Phase diagram for Na_2O - MoO_3 - Al_2O_3 showing the variety of low melting compounds possible in this system.

The conversion of the alpha-alumina/sodium polymolybdate salts to beta''-alumina and Mo takes place by heating to 1200°C in wet hydrogen[4].

The bronze $Na_2Mo_3O_6$ is not stable at this temperature but is present at 700°C in wet hydrogen. Many of these electrode preparations gave tough films with low sheet resistance. None has been tested in a SHE cell as yet.

ANALYSIS

We calculated the concentration of sodium atoms in the vapor phase over both the beta-alumina - alpha alumina and beta-alumina - sodium aluminate equilibria in wet hydrogen. The concentrations are calculated as functions of the water/hydrogen ratio at three temperatures. These calculations serve to guide the choice of conditions for the reduction of metal oxides or for preventing metal oxidation in a system which also contains beta-alumina. The calculations are based on recent thermodynamic data for beta-alumina. The corresponding data for beta''-alumina are not currently available, but significant differences in the results are not expected.

Four equations describe the major interactions in the systems of interest.

$$2Na(g) + 1/2\ O_2(g) \longrightarrow Na_2O \qquad (1)$$

$$Na(g) + H_2O(g) \longrightarrow NaOH(g) + 1/2\ H_2(g) \qquad (2)$$

$$H_2(g) + 1/2\ O_2(g) \longrightarrow H_2O(g) \qquad (3)$$

$$2NaOH(g) \longrightarrow H_2Na_2O_2 \qquad (4)$$

Expressing the equilibrium constants for these reactions in terms of the standard change in Gibbs Free Energy, and solving for ln(P(Na)) and $\ln(P(H_2Na_2O_2))$, we get

$$\ln P(Na) = -1/2RT(\Delta G_3^\circ - \Delta G_3^\circ) - 1/2\ln(P(H_2O)/P(H_2))$$

$$\ln(P(NaOH) = -1/RT(2\Delta G_2^\circ+\Delta G_3^\circ/2- \Delta G_1^\circ/2)+\ln(P(H_2O)/2P(H_2))+1/2\ln P(H_2)$$

$$\ln(P(H_2Na_2O_2)) = -1/RT(2\Delta G_2^\circ+\Delta G^\circ{}_3-\Delta G^\circ{}_1+\Delta G^\circ{}_4+\ln(P(H_2O)/P(H_2))+\ln P(H_2)$$

The quantity P_{total} defined by

$$P_{total} = P(Na) + P(NaOH) + 2\ P(H_2Na_2O_2)$$

is a measure of sodium concentration in the vapor phase.

If the cover gas is obtained at one atmosphere pressure by bubbling hydrogen through water then we may assume that

$$P(H_2) + P(H_2O) = 1 \quad \text{and that} \quad P(H_2) = 1/(1 + P(H_2O)/P(H_2))$$

Values of the Gibbs free energies of formation of the various species are given in Table F1. Also shown in the table are the sodium oxide activities for the beta-alumina - alpha-alumina and beta-alumina - sodium aluminate equilibria. The activity in the latter equilibrium is calculated from the former by adding a term obtained from EMF measurements on the cell

air-Pt-$NaAlO_2$/beta-alumina /beta-alumina/alpha-alumina-beta-alumina-Pt-air

The changes in the standard free energy for the four reactions involving the gaseous species are given in Table F2. In Table F3 are listed the values of $\log(P_{total})$ as a function of $P(H_2O)/P(H_2)$ for three temperatures. These data are shown plotted in Figure F2. This figure includes representative curves appropriate for each equilibrium defining the phase fields of a metal and its lowest oxide, in this case Mo and MoO_2.

TABLE F1

ΔG_f^o (kCal)

T (K)	$Na_2O(c)$	RTln a	Na(g)	$H_2O(g)$	NaOH(g)	H_2	$Na_2O_2(g)$-MoO_2
600	-80.41	-65.23	11.757	-51.156	-51.929	-134.25	
800	-73.64	-61.94	7.593	-48.646	-51.696	-126.097	
1000	-67.062	-58.64	3.529	-46.046	-51.294	-117.737	
1200	-59.832	-55.34		-43.371	-50.314	-108.344	-89.707
1400	-46.217	-52.05		-40.663	-45.774	-91.940	-81.841
1600	-32.975	-48.76		-37.927	-41.210	-75.588	-74.147

For the beta-alumina - alpha-alumina equilibrium,

$$\ln a(Na_2O) = -37,800/T + 8.29 \pm 4.6 \ .$$

For the beta-alumina - sodium aluminate equilibrium,

$$\ln a'(Na_2O) = \ln a(Na_2O) + 2\,fV/RT$$

where f is the Faraday and the cell voltage V is given by

$$V \text{ (millivolts)} = 0.242\ T\ (K) - 95.8 \ .$$

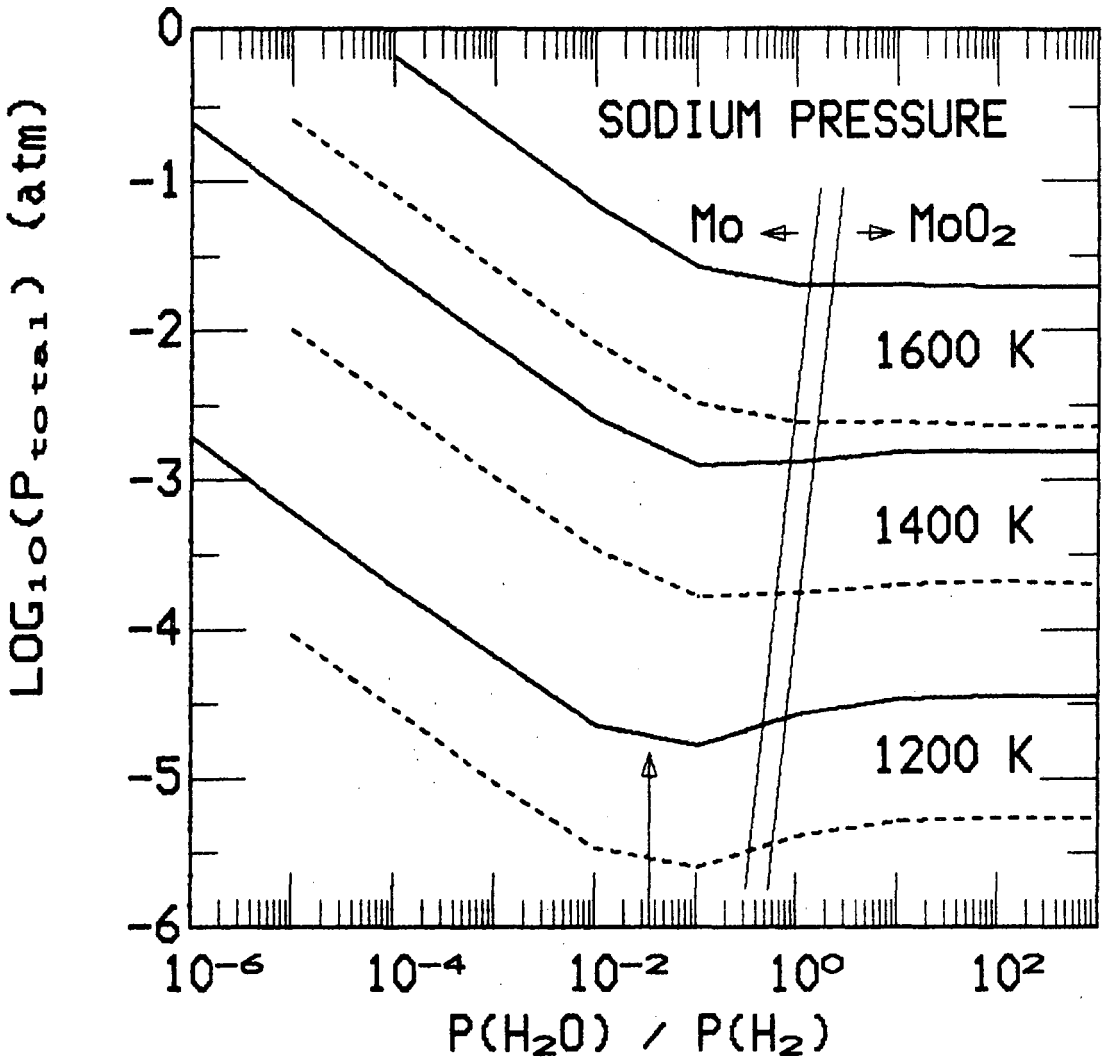

F2. Plots of total sodium pressure as a function of water/hydrogen ratio and temperature. The solid lines represent the beta-alumina/sodium aluminate equilibrium and the dashed lines represent the beta-alumina/alpha alumina equilibrium.

TABLE F2

T (K)	ΔG^{o}_{1}	ΔG^{o}_{2}	ΔG^{o}_{3}	ΔG^{o}_{4}	ΔG^{o}_{1}*	ΔG^{o}_{2}*	ΔG^{o}_{3}*	ΔG^{o}_{4}*
600	-167.56	-12.53	-51.156	-30.392				
800	-156.77	-10.643	-48.646	-22.705				
1000	-132.76	-8.783	-46.040	-15.149				
1200	-115.17	-6.943	-43.371	-7.716	-106.16	-6.943	-43.371	-7.716
1400	-98.27	-5.111	-40.663	-0.392	-87.02	-5.111	-40.663	-0.392
1600	-83.32	-3.283	-37.927	+6.832	-69.83	-3.283	-37.927	+6.832

TABLE F3

$\log_{10}(P_{total})$

$P(H_2O)/P(H_2)$	B-A	B-$NaAlO_2$	B-A	B-$NaAlO_2$	B-A	B-$NaAlO_2$
	1200 K		1400 K		1600 K	
10^{-6}		-2.72		-0.618		0.821
10^{-5}	-4.04		-2.00		-0.60	
10^{-4}	-4.54	-3.72	-2.50	-1.62	-1.10	-.179
10^{-3}	-5.03		-2.99		-1.60	
10^{-2}	-5.47	-4.65	-3.47	-2.59	-2.09	-1.17
10^{-1}	-5.60	-4.78	-3.79	-2.91	-2.50	-1.58
1	-5.39	-4.57	-3.76	-2.88	-2.62	-1.70
10	-5.29	-4.47	-3.70	-2.82	-2.62	-1.70
10^{2}	-5.27	-4.45	-3.69	-2.82	-2.64	-1.72
10^{3}	-5.27	-4.45	-3.70	-2.82	-2.65	-1.72

References

1. T.L. Markin, R.J. Bones and R.M. Dell, Superionic Conductors, G.D. Mahan and W.L. Roth, editors Plenum Press, New York, N.Y. (1976)

2. Masato Kumagain and Gary L. Messing, 'Enhanced Densification of Boehmite Sol Gels by Alpha-Alumina Seeding', J. Am. Ceram. Soc., 67, 705 (1984).

3. Jpn Kokai Tokkyo Koho JP 58,109,165 [83,109,165] (C1B05D1/10), US Appl. 331,107, 16 Dec. 1981. 4pp, (29 Jun. 1983).

4. James D. Hodge, 'Powder Processing and Crystallization of Beta and Beta''-Alumina', Bull. Amer. Ceram. Soc., 62, 244 (1983).

G. CONCLUSIONS

Each of the tasks that were proposed at the outset of the contract period has been addressed. The specific accomplishments made during the contract period have been summarized briefly and measured against the project goals in section B of this report. In this section we extend that summary somewhat, with emphasis on the conclusions that can now be drawn and discuss some of the directions in which we believe further research is desirable.

Electrode Performance :

Substantial progress has been made in achieving an understanding of the behaviour of refractory metal electrodes for the Sodium Heat Engine. It has been shown that the impedance of SHE cells utilizing these electrodes can approach the lower limit imposed by the resistance of the electrolyte. We now believe that this nearly ideal initial performance observed for molybdenum film electrodes can be accounted for by the presence of a molten sodium ion-conducting salt, both at the electrode-electrolyte interface and at grain boundaries and pore surfaces within the electrode volume. The presence of the salt at the interface and within the pores and grain boundaries of the electrode film can provide an ion-conducting medium that combines a high sodium carrier concentration with reasonable mobility. The high carrier concentration in the electrode can lead to a large exchange current and a small effective interfacial impedance. The presence of this medium allows one to understand the excellent initial performance of these electrodes and also suggests simple explanations for a substantial number of observations associated with the behaviour of such electrodes. Among such observations are : 1) extremely low (0.03 ohm cm^2) interfacial impedance between the electrode and electrolyte 2) a rapid increase in the impedance of these electrodes after periods of 10's to 100's of hours at open circuit at 800 - 900°C 3) nearly complete rejuvenation of such electrodes upon exposure to oxygen at high temperatures 4) output impedance which falls with time after the onset of current loading (referred to as 'training'). Physical analysis of molybdenum film electrodes has verified the expected presence of sodium molybdate. Sodium molybdate with a melting point near 680°C should be capable of serving as the conduit for sodium to and through the permeable electrode.

In this model the increase in cell impedance is expected to occur when evaporation or decomposition of the sodium molybdate reduces the effective ionic-electronic conductor interfacial area and shuts down the mixed conductor transport mechanism. This mechanism is extremely effective for carrying neutral sodium through the permeable electrode and dispersing it upon the outer electrode surface from which it then evaporates. This shut-down leads to a 'back pressure' and the resulting increase in sodium activity at the electrode-electrolyte interface required by the overall sodium flux leads to a significant reduction in SHE output voltage and the observed increase in the effective electrode impedance. The rejuvenation of degraded molybdenum electrodes after treatment with oxygen at high temperature can then be readily understood in terms of the regeneration of the molybdate compounds. The 'training' phenomenon can be understood as resulting from an increase in the sodium-ion carrier concentration of the sodium-molybdenum-oxygen compounds beyond stochiometry when the sodium activity is raised due to the passage of current. While it has not yet been observed, the current-related increase in

sodium activity may also tend to retard somewhat the decomposition of the molten-salt compounds. It should also be noted that the vapor pressure of sodium molybdate at SHE operating temperatures implies an evaporation rate of the order of a few microns in 10's of hours, matching rather well with the period over which the electrode impedance is observed to rise.

BASE Stability :

The effective stability of sodium beta''- alumina in contact with liquid sodium at temperatures up to 900°C has been verified by several methods. No evidence of significant reduction of the bulk ionic conductivity or important increase in the electronic conductivity of BASE has been seen in SHE service. Chemical and x-ray analyses of the BASE surface in direct contact with the hot sodium show no evidence of chemical attack or unusual phases after 1000 hours of operation at 900°C, although a slight expansion of the C-axis (0.07%) was observed. The commonly observed dark, gray-black coloration acquired by BASE material in contact with hot liquid sodium has been investigated by several analytical approaches, including optical densitometry and electron microprobe analysis. The apparent depth of penetration appears to increase with increasing temperature. The results from the tests are consistent and indicate that the coloration correlates very well with the presence of neutral sodium incorporated into the bulk material. The absorption/coloration effect is observed to be smaller in pure beta'' than in mixed beta/beta'' material by nearly a factor of 4.

The reduction of the output power of molybdenum SHE electrodes with time has been shown to be consistent with the changes due to loss of mixed conductor sodium-molybdenum-oxygen compounds at the BASE-electrode interface and within the electrode. No evidence of changes in the material properties important to SHE performance has been observed in the bulk of the BASE material.

Novel Electrode Materials :

A number of new electrode materials were investigated for use in SHE systems. Among these, liquid tin and liquid tin/zirconium alloy electrodes have proved capable of extended high-performance lifetimes that are apparently limited only by the rate of electrode material loss due to evaporation at the SHE operating temperatures. Following the discovery of the liquid-phase interfacial compositions in the molybdenum/BASE system in the presence of sodium, titanium nitride electrodes were investigated, in part because they can serve as examples of a clean solid electrode-solid electrolyte system. Sputtered TiN electrodes have proven to be capable of rather good performance at the 0.5 w/cm^2 level and also appear to have better than average endurance, though long term stability has not yet been demonstrated.

The use of mixed ionic-electronic conductors as SHE electrodes offers both an extended interfacial area and enhanced resistance to sintering or grain growth mechanisms which might cause a loss of sodium permeability. The phase diagram of the Al_2O_3-MoO_3-Na_2O system was investigated to provide information which could then direct fabrication of porous ceramic electrode coatings. These coatings could then be subsequently impregnated with metals under conditions consistent with the successful assembly of practical SHE systems. In this effort, electrodes were produced by coating commercial BASE

tubes with a thin porous layer of beta''- alumina and then impregnating the layer with molybdenum metal deposited in the pores from solution. Some tests of such electrodes have shown durable performance (up to the testing limit of about 500 hours with minimal output reduction) at output levels as high as 0.5 w/cm^2.

In the course of this work it was discovered that beta''-alumina and beta''- alumina/metal composites could be deposited by flame-spraying in an oxygen-acetylene torch system without undergoing severe decomposition of the beta''- alumina. While an exhaustive study of this system could not be undertaken, a substantial series of electrodes deposited in this way were tested in small SHE cells and they achieved modest output power levels. While this approach appears to hold considerable promise both for performance and ease of fabrication, flame-sprayed mixed-conductor electrodes do not appear to be the best choice for application in SHE systems at this time.

Directions :

The deposition of beta''-alumina by flame-spraying appears to offer great promise for electrode deposition and for the formation of electrolyte bodies in thin and/or complicated shapes. Further exploration of this system should be undertaken in order to pursue the advantages it may yield for sodium/sulfur battery systems, as well as for improvements in SHE operation and economies of production of SHE systems. The TiN system has shown promise, and longer term testing of this electrode material is clearly warranted. A considerable sensitivity to the details of the sputtering operation became evident toward the end of the program as the sputtering apparatus was put into a closed loop, computer controlled mode of operation. The investigation of a wider range of sputtering parameter values may now prove rewarding. A variety of new electrode materials has been investigated, but the spectrum of analogs to the molybdate system is still largely unexplored, as are possible approaches to the stabilization of liquid metal films in contact with BASE.

LAWRENCE BERKELEY LABORATORY
TECHNICAL INFORMATION DEPARTMENT
UNIVERSITY OF CALIFORNIA
BERKELEY, CALIFORNIA 94720